On Power Quality and Protection

by

Fan Wang

Technical Report No. 372L

Submitted to the School of Electrical and Computer Engineering
Chalmers University of Technology
in Partial Fulfillment of the Requirement for
The Degree of Licentiate of Engineering

Department of Electric Power Engineering
Chalmers University of Technology
Göteborg, Sweden
March, 2001

CHALMERS UNIVERSITY OF TECHNOLOGY
Department of Electric Power Engineering
S-412 96 Göteborg, Sweden

Chalmers Bibliotek, Reposervice
Göteborg, 2001

Abstract

This project combines knowledge from the power quality field and the protection field. The concept of power quality is extended to the terminals of the protective relay. Disturbances in voltage and/or current, not due to a fault in the zone-to-be-protected, may lead to an incorrect trip of the relay. This phenomenon has been known for a long time, and has its consequences in both the threshold setting of relays and the testing of relays. Future generations of protection relays are expected to be faster, and thus more sensitive to disturbances. This project aims at using power quality data and knowledge for the testing of future relays and protection algorithms.

A study was made on the different disturbances that occur in the power system and the way in which they affect protection equipment. Information was obtained from: power quality monitoring surveys, power quality and power system literature; measurements performed in our laboratory. Potential impact was assessed from the transients and non-fundamental frequency components of voltage and current.

From the study, it is observed that the relay performance characteristics will be changed due to the existence of power system disturbances. The changes include the variation of setting limits of relays, as almost all the relays are designed to operate under fundamental frequency conditions. Depending on the types of disturbance, as well as the relay operation philosophies, such a variation can be in two opposite directions, either reducing the relay security margin or weakening the relay dependability. The sampling window size of the relay, which stands for the speed of relay decision-making, also plays a key role in determining the severity of the impact.

A number of methods were developed for quantifying the potential impact of measured disturbances on the protection. The quantification of the disturbance impact on protective relays can be made in two different ways. The setting-based quantification indicates the potential risk that the relay protection zones could be falsely reached due to the disturbance. The design-based quantification illustrates the severity of impact on relay output performance due to unwanted components in the disturbance signal.

The quantification diagrams provide intuitive information on the details of the disturbance. By developing criteria on the impact diagrams, the disturbances can be classified according to their impact severity and duration, based on which databases can be set up for relay testing.

Keywords: power quality, power system disturbance, power system protection, digital protective relays, protection algorithms, distance protection, overcurrent protection.

Acknowledgement

The work presented in this book was implemented at the Department of Electric Power Engineering, Chalmers University of Technology. It was funded by Energimyndigheten, Elforsk and ABB Automation Products.

The author is greatly indebted to his supervisor and examiner, Professor Math H. J. Bollen, for his serious supervision and precious comments that guide the author carry out the research smoothly. Also benefit the author a lot in the research is his creative thinking in simplifying complicated problems.

Special thanks to the members of the steering group, Murari Mohan Saha (ABB Automation Products AB), Helge Seljeseth (SINTEF Energy Research), Christian Roxenius (Göteborg Energi Nät AB) and Robert Olofsson (Unipower AB), for their valuable suggestions on research work throughout the duration of this project.

Also thanks to SINTEF Energy Research, Göteborg Energi Nät AB (GENAB), Scottish Power and Swedish Transmission Research Institute (STRI), for providing large amount of field measurement data, which are crucial in analysis study in this project.

The author is very grateful to his family, for their understanding, care and selfless support.

Finally the author wishes to thank the staff at the Department of Electric Power Engineering, including his colleagues and all the others, who in one way or the other, have contributed to the successful completion of this project.

List of Relevant Publications

I **Wang**, **F.**; **Bollen**, **M. H. J.**, "Evaluating the effect of measured power disturbances on protective relay operation", *Proceeding of International Conference on Electric Utility Deregulation and Restructuring, and Power Technologies 2000 (DRPT 2000)*, London, 2000, page(s): 232-237

II **Wang**, **F.**; **Bollen**, **M. H. J.**, "Disturbance database setup for protective relay testing", *Proceedings of 9th International Conference on Harmonics and Quality of Power (ICHQP)*, Orlando, 2000, Vol. 3, page(s): 1059-1064

III **Wang**, **F.**; **Bollen**, **M. H. J.**, "Measurement of 182 Hz interharmonics and their impact on relay operation", *Proceedings of 9th International Conference on Harmonics and Quality of Power (ICHQP)*, Orlando, 2000, Vol. 1, page(s): 55-60

IV **Wang**, **F.**; **Bollen**, **M. H. J.**, "Quantifying the potential impacts of disturbances on power system protection", Accepted by *Seventh International Conference on Developments in Power System Protection*, Amsterdam, April 2001.

Table of Contents

Chapter 1 Introduction

The research in this project, as indicated by the title of this work, is related to *power quality*. According to the understandings accepted by most people, the term power quality refers to a wide variety of electromagnetic phenomena that exist in power systems. From the viewpoint of theoretical research, it is the appearance of phenomena and the reason behind these phenomena that matters. From the viewpoint of practical application however, the focus of study is on the role these phenomena play in the whole system. Simply speaking, the theoretical research tells *what* the phenomena are and *why* they are generated, while the application research tells *how* these phenomena affect the power system. As these phenomena will more or less interfere with the normal operation of power systems, a derogatory term *power system disturbance* is adopted in application research.

A power system disturbance is actually an electromagnetic disturbance which means, according to the definition in IEC 161 standard, *any electromagnetic phenomenon which may degrade the performance of a device, equipment or system, or adversely affect living or inert matter* [1]. It may be noise, an unwanted signal or a change in the propagation medium itself. Such phenomena have been around since power systems have been put into service, but these phenomena have become more frequent with the system and load activities increasing. The presence of a power system disturbance may affect any component in the system. The protective relays, which play a vital role in power system security, also are not immune from power system disturbances. It is therefore important to assess the severity of the effect of power system disturbances on the protection.

1.1 Background of Power System Disturbance Effect on Relays

Power system disturbances may have detrimental effects on operation relays. They may cause relay operating when the relay should not operate, or make that the relay fails to operate when it is supposed to operate. The relay operation characteristics may shift with the presence of the disturbance, which means the operation time of the relay may deviate from the intended one. Modern technology has created a new generation of digital relays, with increased immunity against these disturbances. The same modern technology also enables the use of novel protection algorithms based on completely different principles than the existing ones. These algorithms are potentially much faster and reliable, but their immunity from disturbances is unknown. During the design stage of a relay it is difficult to predict all the possible disturbances that a relay may encounter when it is installed in a practical system. It is therefore necessary to collect the disturbance data from practical measurements and carry out disturbance analysis. The analysis results show the power quality environment that a relay is facing. This information is fed back to relay manufacturers for relay testing so as to improve the relay characteristics in the future design, as well as to the power system administrator for locating the disturbance sources.

1.2 Existing Research for Disturbance Effect on Relays

At present, already some research studies are carried out on the effect of disturbances on protective relays. These studies are mainly carried out in the following directions:

- Influence of a certain type of disturbance (e.g. harmonics, transient) on a certain type of relay [2] [3]

- Performance evaluation of a certain type of relay using field data [4]
- Algorithm improvement or development for increasing the immunity of a certain type of relay against certain disturbances [5] [6]

These studies are mainly focused on individual cases. In practice, a certain type of disturbance might be harmful to one type of relay while having no impact on another one. Other types of disturbance might have almost the same effect on the performance of relay. It is also possible that a relay algorithm suitable in dealing with some disturbances might turn out to be very susceptible to other disturbances. To make the evaluation applicable to all cases, it is necessary to set up a general approach, including an overall assessment of the disturbances, shortlist the available disturbance data and store them in well-classified databases.

1.3 Objective of the Project

The aim of this project is the creation of a set of general procedure for the testing of protection relays and algorithms. By applying these procedures, disturbance database can be set up. Such a database will consist mainly of voltages and currents recorded in the power system during actual disturbances.

Simply speaking, the disturbance data are obtained at the user-terminal in the viewpoint of relays, and then ranked and designated for different applications in the future.

1.4 Chapter Outline

Chapter 2 introduces the main terminology in the study. The accurate definitions of the terms adopted in this project, as well as their sources, are listed. To illustrate these concepts, the disturbance phenomena are depicted with some typical diagrams.

Chapter 3 discusses the potential impact of power system disturbances on protection. The disturbances are classified into events and variations, based on which further sub-classification is made according to their various sources. The impact in each particular case of event and variation is studied.

Chapter 4 describes in details the principles of digital protective relays in power systems. A clear understanding of this helps one find out how the disturbances affect the operation of relays and how severe the effect is.

Techniques for quantifying the severity of disturbances in power systems are proposed in chapter 5. Two approaches are developed for different purposes. The methods, which provide intuitive assessment of disturbance impact on relay operations, form the basis for criteria used in disturbance database setup.

Using the approaches developed in chapter 5, various case studies are carried out in chapter 6 to evaluate the impact of some typical disturbances on relay operation. Comparison among the cases tells the quantified difference of their impact severity.

Chapter 7 gives the summary and generalization of the work implemented in this project. The direction and prospects of further research work are discussed and proposed.

In Appendix, power system disturbances are studied in an overall view. Simulation models and measurement results are used to uncover the reasons behind these disturbances. Detailed explanation is given for each case, in a way from source to phenomena.

Chapter 2 Main Terminology in the Study

To precisely describe the power system disturbance phenomena, some well-defined technical terms are adopted. Based on independent research and studies by different institutions, various technical standard systems exist, among which IEC and IEEE standards are the most commonly used ones in the world. These two standard systems, which reflect the viewpoints of Europe and America respectively, show much similarity in most of the definitions and requirements, while some discrepancies do exist due to different experiences and interpretations on phenomena, as well as different philosophies in solving these problems. As the research in this project is based on the power grids in Europe, IEC standards are adopted. For those terms (marked with *) that are not available in IEC standards but exist in IEEE standards, the definitions in IEEE standards are borrowed.

2.1 Definitions and Sources

Transient Pertaining to or designating a phenomenon or a quantity which varies between two consecutive steady states during a time short compared with the time-scale of interest (IEC 161-02-01). A transient can be a unidirectional impulse of either polarity or a damped oscillatory wave with the first peak occurring in either polarity.

Dip (Sag) A sudden reduction of the voltage at a point in an electrical system followed by voltage recovery after a short period of time from a few cycles to a few seconds (IEC 161-08-10).

Swell An increase in RMS voltage or current at the power frequency for duration from 0.5 cycles to 1 min. Typical values are 1.1 to 1.8 pu (IEEE 1159).

Undervoltage A voltage of a value falling below the lowest rated value (IEC 151-03-21).

Overvoltage A voltage of a value exceeding the highest rated value (IEC 151-03-19).

Waveform Distortion Any unintentional and generally undesired change in the form of a signal (IEC 702-07-43). The main waveform distortions are harmonics, interharmonics and DC components.

Voltage Fluctuation A series of voltage changes or a cyclic variation of the voltage envelop (IEC 161-08-05). Voltage fluctuation may cause the luminance or spectral distribution of a light source to fluctuate with time, thus inducing the impression of unsteadiness of visual sensation of human eyes. This direct sequence is defined as voltage flicker (IEC 161-08-13).

Voltage Unbalance In a polyphase system, a condition in which the RMS values of the phase voltages or the phase angles between consecutive phases are not all equal (IEC 161-08-09).

2.2 Illustration of Disturbance Phenomena

The following diagrams demonstrate the waveforms of electrical parameters during disturbances. Most of them come from practical measurements. For

those that are not available from the collected disturbance data, diagrams from technical standards and other reference materials are adopted.

Transient The waveform shown in Fig. 2.2.1 was obtained in a distribution system. The transient in current waveform was due to synchronized capacitor switching in a 10 kV system.

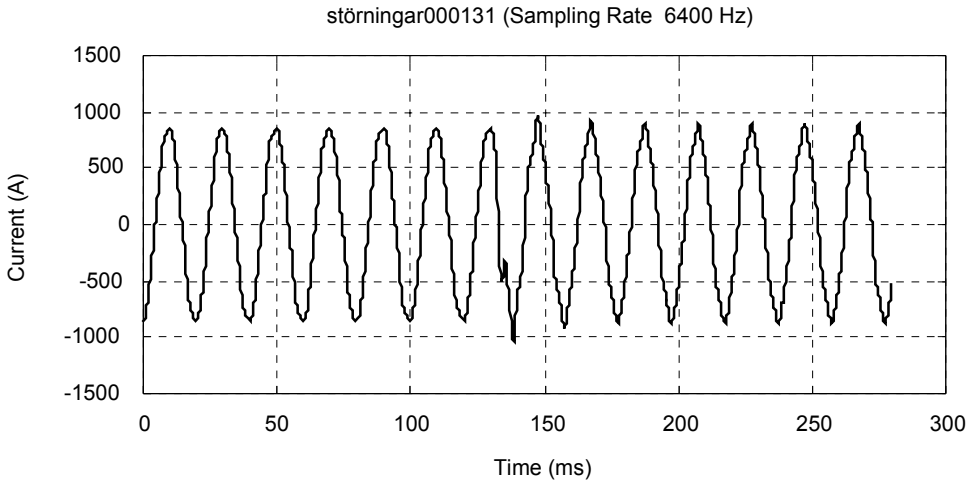

Figure 2.2.1 Transient due to synchronized capacitor switching

Dip (Sag) An example of a voltage dip is shown in Fig. 2.2.2. This event was captured at the Department of Electric Power Engineering, Chalmers, at 400 V. This phenomenon was due to a two-phase-to-ground fault in a 400 kV system. The fault was cleared about 5 cycles (100 ms) later.

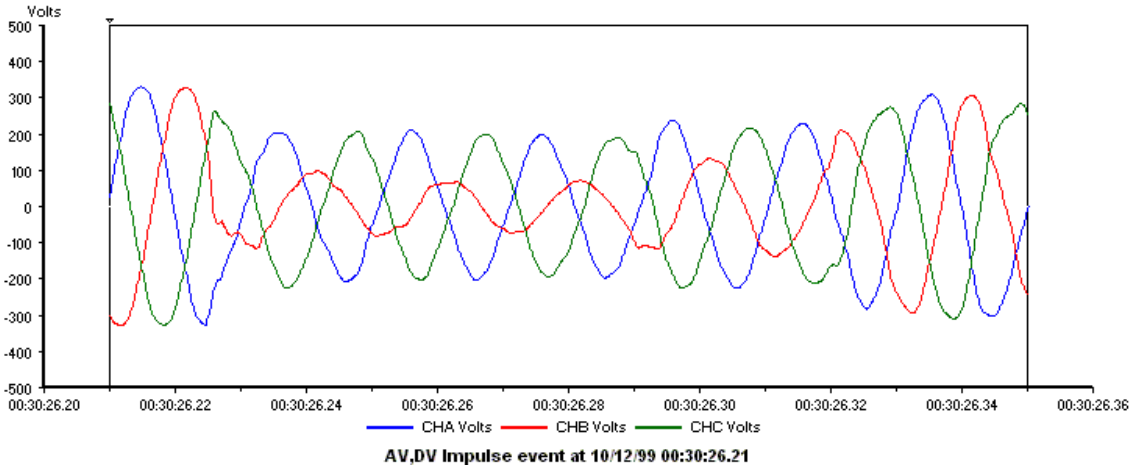

Figure 2.2.2 Voltage dip due to system fault

Waveform Distortion According to the definition, waveform distortion reflects undesired changes in the waveform. This change is obtained by referring the actual signal to the fundamental (50 Hz sinusoidal) component in the signal. Fig. 2.2.3 shows such a case. This waveform was measured in a commercial area in Gothenburg. It was due to the operation of a large lighting load in a nearby theatre, at half load.

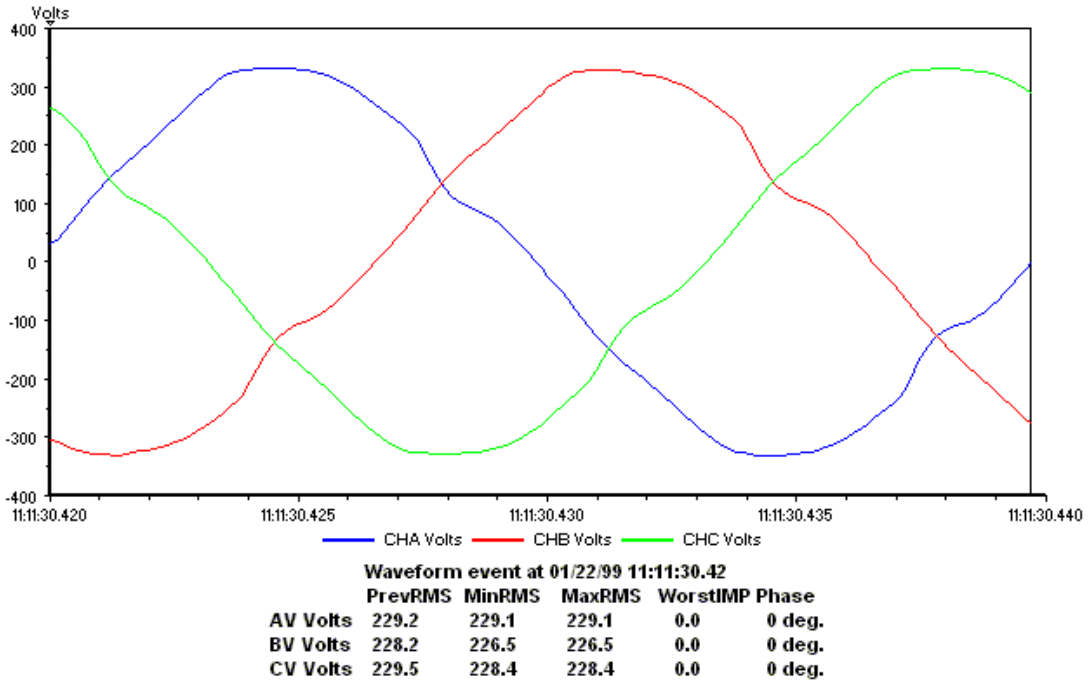

Figure 2.2.3 Waveform distortion due to non-linear loads

Voltage Fluctuation Fig. 2.2.4 shows an example of voltage fluctuation. This was measured near an arc-furnace plant at 10 kV. As the arc-furnace is an intermittent load, its power consumption keeps on changing. The fluctuations in current cause irregular voltage magnitude fluctuations. The figure shows the case in one phase. The situation in the other 2 phases is similar.

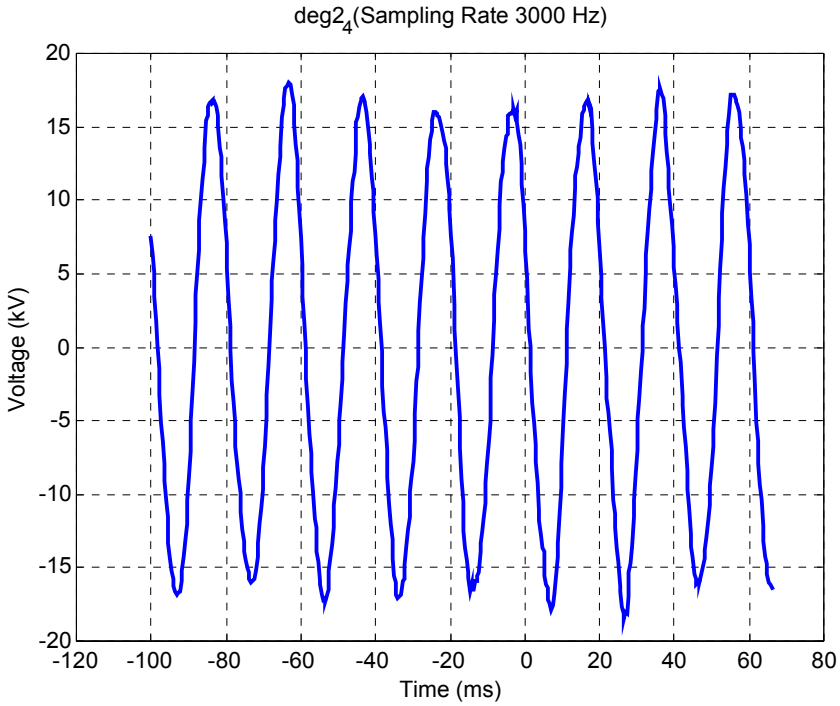

Figure 2.2.4 Voltage fluctuation due to intermittent loads

Voltage Unbalance There is always some voltage unbalance in polyphase systems. The voltages on three phases cannot be exactly equal. Fig. 2.2.5 shows a case measured in Norway. From the diagram it is obvious that one phase (the one shown through a dashed line) has a lower voltage magnitude compared with the other two phases.

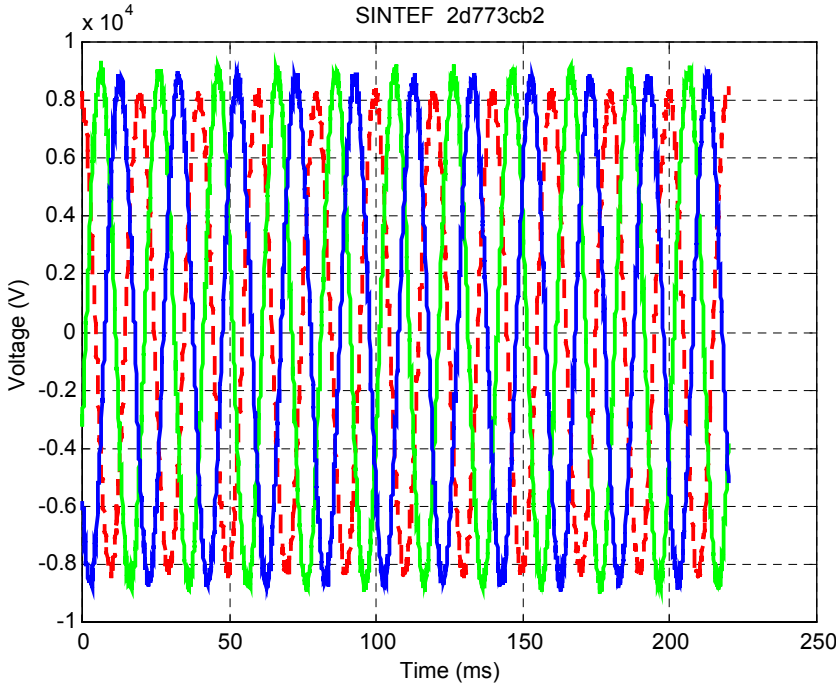

Figure 2.2.5 Voltage unbalance

Chapter 3 Potential Impact of Power System Disturbances on Protection

Power system disturbances can be divided into two categories: events and variations [7].

An event means a dynamic change of status. Normally it involves switching on/off of system components, operation of automatic devices, or external influence. A variation refers to the disturbance due to non-linear components in the system, or external influence. Variations are steady state phenomena.

Table 3.1 shows the main sources of both events and variations in power systems.

Table 3.1 Sources of events and variations in power systems

System		Sources of Events	Sources of Variations
A	Generation	Generation Unit Switching	Nonlinear Generation
	Transmission	Line/Cable Switching	HVDC
	Distribution	Transformer Switching	Transformer
	Load	Motor Switching	Nonlinear Load Intermittent Load Unbalanced Load
	Regulator	Capacitor Switching	SVC
B	Automatic Device	Tap Changer	—
C	Unpredictable External Effect	Lightning Short Circuit & Earth Faults	GIC Radio-interference

In the table, A stands for switching or static operation of system components, B stands for operation of automatic devices and C stands for external influences.

3.1 How to Assess the Disturbance Impact on Protection

The potential impact of a disturbance on the protection will be assessed from voltage and current simulation results (in some cases from measurements of typical events). Note that we are in this chapter not yet assessing the impact of a specific event on a specific protection relay. Instead we are assessing the potential impact of different types of disturbances on different types of protection relays.

We will distinguish between dynamic and static effects of the disturbance. *Static effects* are changes in voltage and current, either in the fundamental or in the harmonic component. These changes potentially lead to mal-trip of any of the more classical protection types. A drop in fundamental voltage may lead to tripping of an undervoltage relay; a rise in harmonic current may lead to tripping of an overload relay; a drop in the apparent impedance (ratio of fundamental voltage and current), may lead to tripping of a distance relay. Also note that a potential trip does not at all imply a likely trip. As an example, any rise in fundamental current will be presented below as a potential risk for an overcurrent relay, where obviously the risk is very small as long as the current does not significantly exceed the rated current.

Dynamic effects are short-duration, typically sub-cycle, changes in voltage and current that potentially endanger the operation of (future) high-speed protection algorithms. This impact will be more difficult of assess, as novel protection algorithms can be of any type. Phenomena or potential concern

are: a short-duration rise or drop in voltage or current; a non-fundamental-frequency component in voltage or current.

Points of discussion are long-duration transients, e.g. due to motor starting. These are strictly speaking dynamic effects but of such a long duration that they may seriously affect the operation of the classical protection types. We will refer to these as *semi-static effects*, which are in fact dynamic effects with long time-constant.

The following sections discuss the possible impacts on protection by various disturbances. The various disturbances are described in more detail in Appendix.

3.2 Impact on Protection by Events due to Component Switching

1. Generation unit switching

The main *static effect* of the switching of a generator unit, is the rise in fundamental current. This could potentially lead to tripping of overcurrent relays, but the stationary current will normally not exceed the rated current so that the risk is small.

A more serious *semi-static* effect is the inrush current of induction generators. The current could significantly exceed the rated current and endanger the operation of overcurrent, undervoltage and impedance-type relays. The transformer-inrush current with large generator energizing could lead to tripping of the transformer differential protection. These two cases are typically considered in the protection setting.

Dynamic effects include the dc component in current when connecting a synchronous machine. Also the harmonic distortion due to the energizing of the generator transformer is of potential concern. For induction generators, the energizing of a power-factor correction capacitor together with the generator could lead to a high-frequency transient.

2. Switching of unloaded line or cable

The *static effects* of unloaded line or cable switching are small. The cable or line takes only capacitive current during unloaded operation. Normally line or cable switching only slightly increases or decreases the current magnitude elsewhere in the system, depending on the pre-event current.

The *dynamic effects* on the other hand are much bigger. Line and cable energizing leads to a severe transient in both voltage and current at the sending end (the terminal from which the line or cable is being energized). Travelling waves originate at the sending end, propagate to the receiving end, and are reflected back to the sending end. After a number of reflections, the travelling waves become part of the electromagnetic oscillation between the (mainly capacitive) line or cable and the (mainly inductive) rest of the system. These transients can propagate to other parts of the system and potentially endanger the operation of high-speed protection algorithms. The propagation of energizing transients through the system very much depends on the system configuration. Line and cable de-energizing do not cause significant transients.

3. Switching of loaded line or cable

The switching of loaded lines or cables can be considered as a combination of switching of an unloaded line or cable and the switching of load. The resulting static, semi-static and dynamic effects are therefore a combination of the effects of these two phenomena.

The *static effects* are mainly due to the load: a change in fundamental current; a minor change in fundamental voltage for large load only. The energizing of a heavily loaded line or cable may endanger the operation of overcurrent, undervoltage, and impedance relays.

Semi-static effects include inrush currents or transformer or motor load, and may cause mal-trips again for overcurrent, undervoltage, and impedance relays.

The *dynamic effects* are due to the energizing transients of the cable or line. See switching of unloaded line or cable for details.

De-energizing of loaded lines or cables does not lead to any significant static, semi-static of dynamic effects.

4. Transformer switching

The *static effects* are most severe for a loaded transformer. The switching of a loaded transformer gives a change in fundamental current. The switching of a large loaded transformer even gives a change in fundamental voltage. Overcurrent and undervoltage relays are potentially affected.

Switching of unloaded transformers does not significantly affect the steady-state voltages and currents.

Semi-dynamic effects are related to the inrush current of the transformer and possible also to the inrush current of the load behind the transformer. The latter will be discussed under load switching. The inrush current to a transformer contains a significant amount of harmonic components, and has decay time constants up to several seconds. Although even harmonics not necessarily dominate the spectrum, they are specific for transformer energizing. The even harmonics, rarely present in other situations, propagate to lower voltage levels where they could interact with load. It is shown [8] that even harmonics lead to a dc current for single-phase rectifiers. This could in turn lead to saturation of current transformers at unexpected places in the system. Also, the voltage dip due to the energizing of a transformer could lead to saturation, and thus increased currents, for other transformers [9].

5. Motor starting

The main effect of motor starting is of a *semi-dynamic* character. The starting of a large induction motor leads to an inrush current, which is typically 5 to 6 times the normal operating current. This large current may be present for several seconds, thus putting a severe strain on overcurrent protection. Also undervoltage protection is potentially affected. As motor load is only present at lower voltage levels, distance protection (only present at higher voltage levels) is not affected by it.

A *dynamic effect* is formed by the transients due to the switching of a power-factor correction capacitor with the motor load. This capacitor limits the

voltage drop due to the starting of the motor, but its switching could cause a high-frequency transient. This transient is discussed in the section on capacitor switching.

The *static effect* of motor starting is an increase in fundamental current, but the increase is small compared to the inrush current and therefore normally not of concern.

6. Capacitor switching

The *static effect* of capacitor switching is small: a change in the reactive part of the current. In some cases, capacitor de-energizing leads to an increase in current magnitude. This potentially endangers the operation of overcurrent protection.

The *dynamic effect* of capacitor energizing is a severe oscillation in voltage and current, with frequencies from 300 to about 1000 Hz. This transient can propagate through the system, especially when other capacitors are present. The most severe case is back-to-back transformer energizing. This leads to a very severe high-frequency transient, which is normally confined to the system between the two capacitors. Like with normal capacitor energizing, the resulting voltage transient may propagate to capacitors located elsewhere in the system.

The initial drop in voltage may affect high-speed undervoltage protection; the associated rise in current (for locations upstream of the capacitor location) may affect high-speed overcurrent protection; the overvoltage due to the electromagnetic oscillation may affect high-speed overvoltage protection. In fact, mal-trip of undervoltage protection has been reported for static-transfer

switches and mal-trip of dc bus overvoltage protection is the main concern of adjustable-speed drives during capacitor energizing transients.

The *dynamic effect* of capacitor de-energizing is small.

3.3 Impact on Protection by Events due to Automatic Device

1. Tap changer

The main *static effect* of tap changer operation is the change in fundamental voltage. As the rise in voltage is limited, the effect on relay protection is very small.

3.4 Impact on Protection by Events due to External Influences

1. Lightning

Lightning does not have any *static effect*; the phenomenon is completely over after a few milliseconds. A short-circuit or earth fault due to a lightning stroke does lead to a fundamental overcurrent and undervoltage, but only for a limited duration.

The *dynamic effect* of the lightning stroke is the high overvoltage and the large overcurrent during a very short duration, typically only a few tens of microseconds. High-speed overvoltage protection is potentially affected by this. Note that the most severe lightning currents lead to insulation breakdown and thus to a fault. Only the less severe lightning strokes lead to overvoltages that get the chance to propagate through the system.

2. Short-circuits and earth faults

This is the normal event for which protection is supposed to operate. Faults outside of the zone-to-be-protected could lead to mal-trip of any type of relay. This typically only affects relays close to the fault location, where the fault currents are high. The study of nearby faults is part of the normal testing procedure for protection relays, and therefore of lesser importance for the research forming the basis of this thesis.

A special *semi-dynamic effect* that is worth mentioning here is the inrush current after fault clearing. Transformers, induction motors, and generators, take a high inrush current when the voltage recovers. This could lead to tripping of overcurrent relays at places far away from the fault location, especially at lower voltage levels where the load effects are more severe.

A related *dynamic effect* is due to the inrush current of capacitor banks and rectifier load upon voltage recovery. This could lead to mal-operation of high-speed overcurrent protection, again especially at lower voltage levels.

3.5 Impact on Protection by Variations due to Component Operation

1. Nonlinear generation

Some types of generation can cause severe current distortion, which could affect the operation of some relay types. These generation types are currently only present at lower voltage levels, so that the harmonic distortion is contained to a small area of the system.

2. HVDC

HVDC converter stations generate harmonics of, typically, order 11, 13, 23 and 25. These higher order harmonics, if not properly filtered at the origin, could propagate to other parts of the system. Local resonance may lead to high harmonic currents or voltage at other transmission substations or at lower voltage levels.

3. Transformer

The magnetizing current of a transformer (even in normal operation) contains large harmonic components. But in most cases these cannot be distinguished from the harmonic components due to non-linear load. An exception is the zero-sequence third harmonic component for transformers with grounded neutral point. This current could interfere with earth-fault protection.

4. Nonlinear load

This is the main source of harmonic distortion at most locations in the system. The non-sinusoidal currents may interfere with the operation of overcurrent protection. Especially certain types of solid-state relays are sensitive to harmonic current distortion.

Harmonic voltage distortion is normally too low to affect any relay. An exception occurs due to harmonic resonance, where the harmonic current through a capacitor can become significant and lead to mal-operation of the capacitor protection. Note that this is not necessarily a protection mal-operation, as the large current could otherwise lead to damage to the capacitors.

Future high-speed protection algorithms, sensitive to higher frequencies, could show mal-trips close to capacitor banks during harmonic resonance states.

5. Intermittent load

Interharmonic voltage and current components lead to an error in the extraction of the fundamental component. This could lead to protection mal-operation.

The changes in load lead to changes in fundamental voltage and current, which could potentially endanger the operation of undervoltage, overvoltage, overcurrent, and impedance relays.

6. Unbalanced load

Unbalanced load leads to a negative-sequence component in voltage and current. This can interfere with the operation of any relay that uses negative-sequence components.

7. SVC

SVC (Static Var Compensator) is used for fast dynamic compensation of reactive power. It operates to maintain voltage stability at the control point, and to improve power factor. Overall, it has positive rather than negative impact on protection. But the harmonic currents produced by the SVC could potentially interfere with protection.

3.6 Impact on Protection by Variations due to External Influences

1. Geomagnetic induction

The effect of the geomagnetic current itself is small. It is not the magnitude of this current but its frequency that is of concern. The very low frequency (a period of about 5 minutes) drives power transformers into saturation. The resulting large magnetizing current leads to inadvertent tripping of various relays.

2. Radio interference

The magnitude of radio-interference signals is much too small to affect any protection relay. It's also unlikely that future generations of relays will use any of these frequencies in the decision making.

Chapter 4 Principles of Digital Protective Relays in Power System

Protective relays are the devices that detect faults or abnormal operating conditions in power systems. In the history of protective relay development, electromechanical relays formed the first generation, followed by static relays and digital relays.

In electromechanical relays, the actuating force is created by electromagnetic interaction due to input electrical parameters. These relays contain mechanical parts such as spring, dashpot, induction disc etc. If the torque generated by the input overcomes the torque generated by the pre-stored energy in the spring, the moving part of the relay will act and cause the output signal. Electromechanical relays are in general reliable and have low requirements on operation environment. They are still in wide application today.

However, the shortcomings of these relays are also obvious: problems of maintenance, slow in action, high power consumption for auxiliary mechanisms and worst of all, incapability of implementing complex characteristics. With the advent of integrated circuits and static circuits, a new generation of devices called static relays was developed. Compared with electromechanical relays, static relays are faster, more accurate and can realize more complex functions. They require much less power consumption and little maintenance. In practical applications static relays, also called solid-state relays, are mainly applied in protection for transmission level systems.

But there are some other weak points in static relays. Since static relays consist of many electronic components, the overall reliability can be affected by individual components, and these electronic components are sensitive to ambient temperature. Even worse is that static relays are vulnerable to voltage transients, which might cause mal-operation. Although various approaches were explored for the amelioration of the situation, the real solution was not available until the early 70's, when relays based on computer could provide performance at least as good as conventional relays. The relays of the 3rd generation are called digital relays, numeric relays, or microprocessor relays alternatively.

The main advantages of digital relays over conventional relays are their reliability, functional flexibility, self-checking and somewhat self-adaptability. They are able to implement more complex function, be more accurate and be immune from physical environment effects. Although they are relatively costly, the benefits in enhancing system security and reliability by adopting these relays can make their application worthwhile. At present, their application is mainly in transmission system protection as well as for generation unit protection. The rapid growth in computer and communication industries will alleviate their price disadvantage and explore new horizons for their wider application.

In this project, digital relays are adopted to study the power disturbance impact on protective devices.

4.1 Structure of Digital Relays

A digital relay consists of the following main parts:

- Processor
- Analog input system
- Digital output system
- Independent power supply

Fig. 4.1.1 shows the block diagram of a digital relay [10].

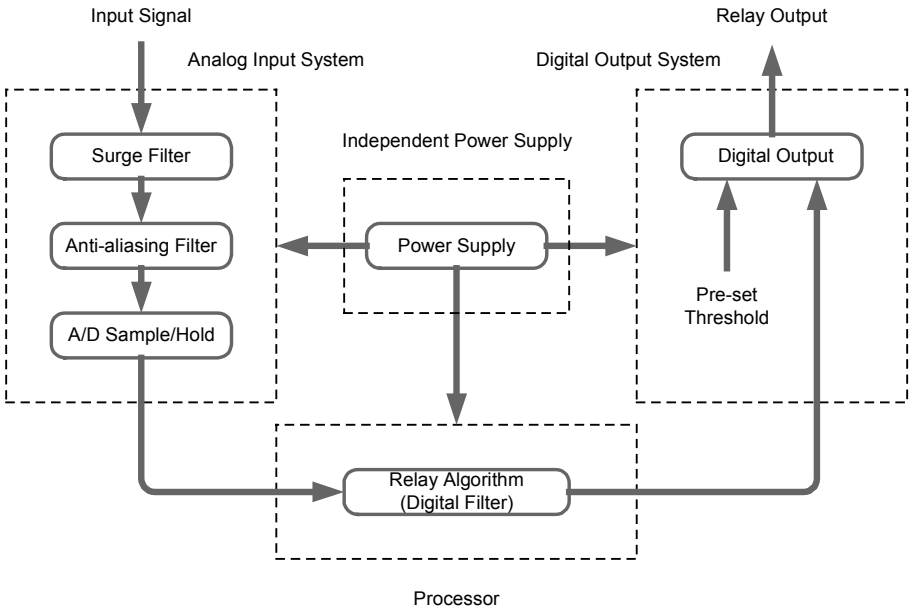

Figure 4.1.1 Block diagram of digital relay

The main difference in principle between digital relays and conventional relays is in the way of input signal processing. The input signals, which come from CTs or PTs, are analog signals. They are directly imposed to the electromagnetic winding or electronic circuits in conventional (electro-mechanical and static) relays. In the case of digital relays, the input signals are converted into digital signals in the analog input system before being processed by processor. In the analog input system, a surge filter is used to suppress the large inrush in the input signals, for the safety of the digital relay.

An anti-aliasing filter is used to avoid possible errors in reconstructing the input signal, which is carried out after the A/D Sample/Hold section. Any signal sampled at a frequency of N*50 Hz (or N*60 Hz in North America) can exhibit aliasing when reconstructed, if the signal contains harmonic components of order N±1, 2N±1, …, xN±1. An anti-aliasing filter has to cut off all signal components above the Nyquist rate of N/2, i.e. the cut-off frequency for anti-aliasing filter should be set not higher than (N/2)*50 Hz. In practice however, such a filter cannot remove all out of band frequencies, so the cut-off frequency for the anti-aliasing filter is typically set at about (N/3)*50 Hz.

The A/D sample and hold circuit is adopted to convert the input signal from analog to digital. To scan the whole signal, a data window of limited length is applied to acquire information on part of the signal. Within the section of the signal that is scanned by the data window, a limited number of points of the waveform are sampled. With the window moving forward, more samples are obtained at different snapshots of time. In Fig. 4.1.2, it is illustrated that the input signal is frozen by the data window to achieve simultaneous sampling at each moment, when the oldest sample point is discarded and the newest one is embedded. These samples are held until the next sampling moment. The sampling window length, sampling number in the window as well as the shape of the sampling window are dependent on the relay algorithm stored in the processor.

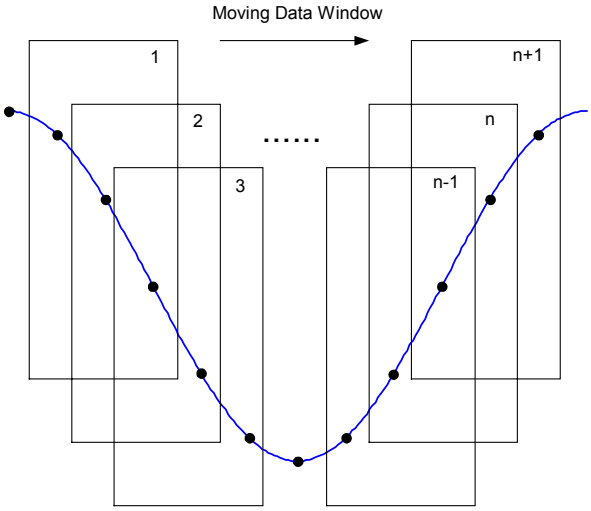

Figure 4.1.2 Data window for sampling

The relay algorithm stored in the processor is the core of the digital relay. It determines the way to reconstruct the input signal based on the digital samples from the A/D converter. As the input signal may contain unwanted components such as harmonics, interharmonics and DC, the algorithm is designed to remove them as much as possible. The algorithm functions as a digital filter to extract the fundamental component of the input signal, based on which the relay operation is carried out. With different algorithm principles, the shape of data window varies. The rectangular window, as shown in Fig. 4.1.2, is only one option. The length of the data window is dependent on the required decision speed of the algorithm. The number of sampling points in the data window is determined by the sampling frequency set in the algorithm.

In digital output system, the reconstructed signal from the digital filter is compared with the pre-set threshold. The decision on whether the relay should operate is made according to this comparison.

4.2 Digital Filters for One-Element Relay

A "One-element relay" is a relay that operates on only one input signal. Many relays, which have either voltage or current as their inputs, are one-element relays. The philosophy of digital filters for such relays is to remove the unwanted components as much as possible so as to extract the fundamental component from the input signals.

Several filters are available for this purpose. The most common ones are Fourier, Walsh, and Kalman filters.

4.2.1 Fourier filter

The main concept of the Fourier filter is that any signal can be regarded as a combination of periodic components, provided that it meets the Dirichlet conditions, i.e. finite discontinuous points, limited extremes and limited integration value within any period.

The deductions of Fourier filter is based on the assumption that measurement errors have constant covariance and are independent from sample to sample.

An input signal to be sampled can be written as

$$y(t) = \sum_{n=1}^{N} Y_n s_n(t) + \varepsilon(t) \qquad (4.1)$$

where the coefficients Y_n are unknown while the signals $s_n(t)$ are pre-selected as follows [11]:

$$\left.\begin{aligned} s_1(t) &= \cos \omega_0 t \\ s_2(t) &= \sin \omega_0 t \end{aligned}\right\} \quad \text{fundamental component}$$

$$\left.\begin{aligned} s_3(t) &= \cos 2\omega_0 t \\ s_4(t) &= \sin 2\omega_0 t \end{aligned}\right\} \quad \text{second harmonics}$$

…

$$\left.\begin{aligned} s_{N-1}(t) &= \cos\frac{N}{2}\omega_0 t \\ s_N(t) &= \sin\frac{N}{2}\omega_0 t \end{aligned}\right\} \quad \frac{N}{2}\text{th harmonics}$$

N/2 is the highest harmonic order contained in the signal, assuming N is an even number. ε(t) stands for the noise in the measurement.

The choice of $s_n(t)$ above is in accordance with the form of the Discrete Fourier Transform. The component at a certain harmonic order n is split into two orthogonal terms, sin $n\omega_0 t$ and cos $n\omega_0 t$. Equation (4.1) can be expressed in matrix form as follows:

$$\begin{bmatrix} y_1 \\ y_2 \\ \vdots \\ y_K \end{bmatrix} = \begin{bmatrix} s_1(\Delta t) & s_2(\Delta t) & \cdots & s_N(\Delta t) \\ s_1(2\Delta t) & s_2(2\Delta t) & \cdots & s_N(2\Delta t) \\ \vdots & & & \vdots \\ s_1(K\Delta t) & s_2(K\Delta t) & \cdots & s_N(K\Delta t) \end{bmatrix} \begin{bmatrix} Y_1 \\ Y_2 \\ \vdots \\ Y_N \end{bmatrix} + \begin{bmatrix} \varepsilon_1 \\ \varepsilon_2 \\ \vdots \\ \varepsilon_K \end{bmatrix}$$

or

$$y = S\,Y + \varepsilon \tag{4.2}$$

where K is the sample number in one cycle, and Δt represents the time interval between two neighboring sample points. To estimate all N parameters, $K \geq N$ is required. If the error vector ε is assumed to have zero mean, and a covariance matrix

$$E\{\varepsilon\,\varepsilon^T\} = W \tag{4.3}$$

then the solution to Eqn.(4.2) using least square technique yields

$$\hat{Y} = (S^T W^{-1} S)^{-1} S^T W^{-1} y \tag{4.4}$$

With the assumption that the errors are uncorrelated and independent from sample to sample and have a constant covariance, W is a multiple of a unit matrix. Therefore the least square solution (when $\varepsilon^T W^{-1} \varepsilon$ is minimized) is

$$\hat{Y} = (S^T S)^{-1} S^T y \tag{4.5}$$

Substituting the orthogonal expressions of sine and cosine terms in (4.5), the ij^{th} entry of the matrix $S^T S$ is

$$(S^T S)_{ij} = \sum_{k=1}^{K} s_i(k\Delta t) s_j(k\Delta t) \tag{4.6}$$

$$= \begin{cases} K/2 & ; \quad i = j \\ 0 & ; \quad i \neq j \end{cases}$$

The fundamental frequency components are given by

$$\hat{Y}_c = \frac{2}{K} \sum_{k=1}^{K} y_k \cos(k\theta) \tag{4.7}$$

$$\hat{Y}_s = \frac{2}{K} \sum_{k=1}^{K} y_k \sin(k\theta) \tag{4.8}$$

where $\theta = 2\pi/K$. The output magnitude of such Fourier filter can be calculated by

$$|Y| = \sqrt{\left(\hat{Y}_c\right)^2 + \left(\hat{Y}_s\right)^2} \tag{4.9}$$

Note that the results for fundamental frequency, in Eqns. 4.7 and 4.8, are independent of the number of parameters N. The fundamental component obtained from the Fourier filter, is the optimal solution in the least square sense, under the assumption that the noise samples are uncorrelated.

4.2.2 Walsh filter

The Walsh filter is based on Walsh functions: a set of orthogonal signals on the interval [0, 1] which only take on the values ±1. Compared with Fourier functions which deal with complex numbers, Walsh functions deal only with two integer numbers.

The Walsh function is defined in the following way [11]:

$$W_k(t) = \prod_{r=0}^{p-1} \mathrm{sgn}(\cos(k-1)_r 2^r \pi t) \qquad (0 \le t < 1) \qquad (4.10)$$

where k Walsh function number, positive integer

In binary system $(k)_2 = \sum_{r=0}^{p-1} k_r 2^r$

p total digits of (k-1) in binary expression

sgn sign function (only sign of the result is taken)

For example, $W_6(t)$ can be deduced as follows:

$$6-1 = 5 = 1\times 2^2 + 0\times 2^1 + 1\times 2^0$$

so $(k-1)_2=1$ $(k-1)_1=0$ $(k-1)_0=1$

Since there is 3 digits in binary expression, p=3

Therefore

$$\begin{aligned} W_6(t) &= \prod_{r=0}^{2} \mathrm{sgn}(\cos(k-1)_r 2^r \pi t) \\ &= \mathrm{sgn}(\cos(k-1)_2 2^2 \pi t)\cdot \mathrm{sgn}(\cos(k-1)_1 2^1 \pi t)\cdot \mathrm{sgn}(\cos(k-1)_0 2^0 \pi t) \\ &= \mathrm{sgn}(\cos 4\pi t)\cdot \mathrm{sgn}(\cos \pi t) \end{aligned} \qquad (4.11)$$

The following diagram shows the waveforms of the first 8 Walsh functions.

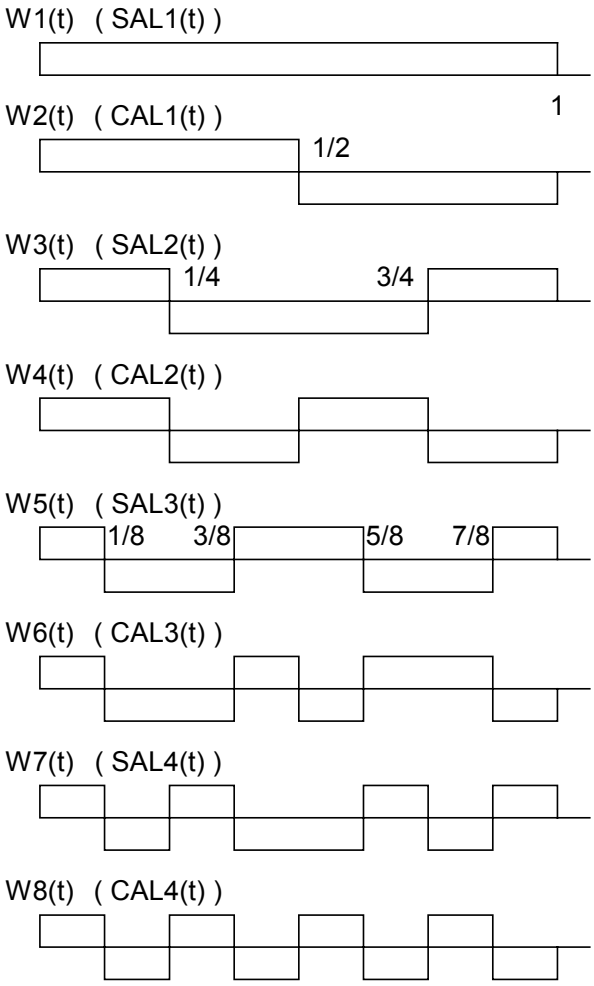

Figure 4.2.2.1 The first 8 Walsh functions

For the convenience of comparing the Walsh function with trigonometrical functions, Walsh function can be further classified as

$$W_k(t) = \begin{cases} sal_m(t) & \text{when} \quad k = 2m-1, \quad m = 1,2,3\cdots \\ cal_m(t) & \text{when} \quad k = 2m, \quad m = 1,2,3\cdots \end{cases} \tag{4.12}$$

Similarly as in Eqn. (4.1), any periodic signal function can be expanded as a series of Walsh functions plus a noise term:

$$y(t) = \sum_{n=1}^{N} Y_n W_n(t) + \varepsilon(t) \tag{4.13}$$

The functions $sal_m(t)$ and $cal_m(t)$ in Eqn. (4.12) correspond to $\sin(m\omega t)$ and $\cos(m\omega t)$ in the Fourier filter algorithm.

In the same way as for Eqn (4.6), we obtain

$$\left(S^T S\right)^{-1} = \frac{1}{K} \cdot \mathbf{I} \tag{4.14}$$

with I the unit matrix and K the number of samples per cycle. The coefficients for fundamental component in Walsh series can be deduced as

$$\hat{Y}_{cal} = \frac{1}{K} \sum_{k=1}^{K} y_k cal_1(k\theta) \tag{4.15}$$

$$\hat{Y}_{sal} = \frac{1}{K} \sum_{k=1}^{K} y_k sal_1(k\theta) \tag{4.16}$$

where $\theta = 1/K$.

Similarly, the output magnitude of the Walsh filter can be calculated by

$$|Y| = \sqrt{\left(\hat{Y}_{cal}\right)^2 + \left(\hat{Y}_{sal}\right)^2} \tag{4.17}$$

The expression for the Walsh filter is quite similar to that of the Fourier filter, but the amount of computational programming is much less. However, for any smooth continuous waveform, the Walsh filter requires the calculation of more coefficient terms to obtain the same accuracy in estimation. Its simplicity in programming is counterbalanced by the need for a large number of terms. Its frequency response is indistinguishable from the full-cycle Fourier filter if a sufficient number of Walsh coefficients are used [11].

4.2.3 Kalman filter

The Kalman filter is designed for dynamic system estimation. Its application is justified only when

a. An initial status estimation is available

b. The covariance of white noise cannot be assumed constant

As shown in section 4.2.1, the deduction of the Fourier filter does not hold if the noise covariance is not constant, and neither does the Walsh filter. In such a situation, the Kalman filter is a possible solution.

In Kalman filtering, a studied system is described by the following equations [11]:

$$x_{k+1} = \varphi_k x_k + \Gamma_k w_k \tag{4.18}$$

$$z_k = H_k x_k + \varepsilon_k \tag{4.19}$$

where

	x_k, x_{k+1}	state vector for sample k, sample k+1
	k	evolution number
	φ_k	state transition
	Γ_k	state noise transition
	w_k	state noise vector
	z_k	measurement result vector
	H_k	measurement
	ε_k	measurement error vector

Consider a pure sinusoidal signal in the form

$$y(t) = Y_c \cos(\omega t) + Y_s \sin(\omega t)$$

and sampled at equal intervals $t_k = k\frac{\psi}{\omega}$, then the state can be taken as

$$x_k = \begin{pmatrix} Y_c \\ Y_s \end{pmatrix} \qquad \text{for all values of k}$$

so the matrices φ_k and H_k are

$$\varphi_k = \begin{pmatrix} 1 & 0 \\ 0 & 1 \end{pmatrix} \qquad H_k = \begin{pmatrix} \cos(k\psi) & \sin(k\psi) \end{pmatrix}$$

For a non-stationary, distorted signal a certain model order is chosen. The simplest form is to assume that the signal consists of a time-varying fundamental component. All other components in the measurement are considered as noise. A more advanced model also includes a certain number of harmonic components. The Eqns. 4.18 and 4.19 remain the same but the order of the various vectors and matrices increases.

Having chosen the model, the aim of the Kalman filtering process becomes the estimation of the state vector as a function of time from a known initial state. The basic step in this is the estimation of the state vector xk+1 from the history $x_1, x_2, \ldots, x_{k-1}, x_k$.

The following assumptions about state noise, measurement noise and state are made to be able to estimate the state vector:

- w_k and ε_k are assumed to be independent of each other and uncorrelated from sample to sample
- w_k and ε_k are assumed to have zero means, which implies that their variances $Var(w_k)=Q_k$ and $Var(\varepsilon_k)=R_k$ are positive definite
- The initial state x_0 is assumed to be independent of w_k and ε_k and with a known mean and covariance matrix $P_{0|0}$

The state estimate $\hat{x}_{k+1}$ is obtained from the previous estimate $\hat{x}_k$ and the new measurement z_{k+1}:

$$\hat{x}_{k+1} = \varphi_k \hat{x}_k + K_{k+1}\left[z_{k+1} - H_{k+1}\varphi_k \hat{x}_k \right] \tag{4.20}$$

In the above equation, $\varphi_k \hat{x}_k$ is the predicted state and $H_{k+1}\varphi_k \hat{x}_k$ is the predicted measurement. It is clear that the state estimate at time k+1 equals to

the predicted state for time k+1 (based on the estimate at time k) plus some correction. The correction is based on the difference between actual measurement and estimated measurement for time k+1.

The correction matrix K is computed as

$$K_{k+1} = P(k+1|k)H_{k+1}^T\left[H_{k+1}P(k+1|k)H_{k+1}^T + R_{k+1}\right]^{-1} \quad (4.21)$$

where

$$P(k+1|k) = \varphi_k P(k|k)\varphi_k^T + \Gamma_k Q_k \Gamma_k^T \quad (4.22)$$

$$P(k+1|k+1) = \left[I - K_{k+1}H_{k+1}\right]P(k+1|k) \quad (4.23)$$

In Eqns. 4.22 and 4.23, P(k|k) is the covariance of the estimation error at time k, while P(k+1|k) is the covariance matrix of the prediction for time k+1 based on P(k|k).

The Kalman filtering process can be depicted by the following flow diagram [12]:

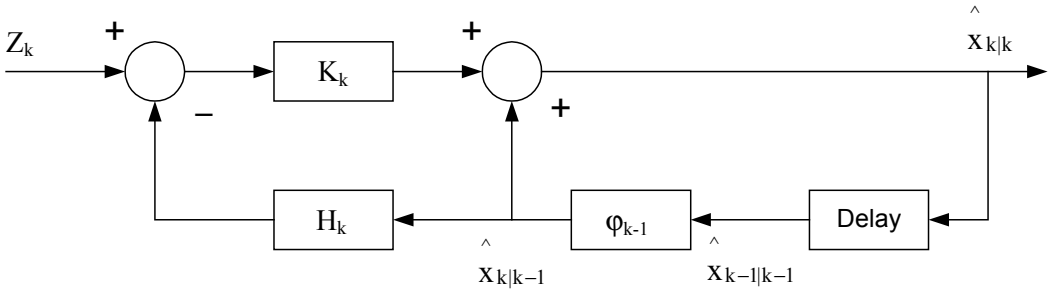

Figure 4.2.3.1 Kalman filtering process

If there is no initial information and the measurement error has a constant covariance, the Kalman filter estimate becomes a combination of discrete Fourier transform terms. This means that the Kalman filter will yield a result with an accuracy comparable to the case of Fourier filter, but involving

considerably more computation. In this case, Kalman filter actually is much less efficient than the Fourier filter.

Among the three kinds of digital filter mentioned above, the Fourier filter has a much wider application in practice than the other two filters. In this project, the Fourier filter for one-element relay is studied.

4.3 Digital Filters for Dual-Element Relay

A dual-element relay here refers to a relay that requires two input parameters. Relays such as distance relays, power factor relays and directional relays are dual-element relays. In this project, only the distance relay that requires both voltage and current inputs is studied.

There are two main algorithms for dual-element relays: Fourier algorithm and differential equation algorithm. Also some travelling wave based algorithms have been proposed for this purpose.

4.3.1 Fourier algorithm

The principles of the Fourier algorithm are similar to those for the Fourier filter as discussed in section 4.2. The input signals, both voltage and current, are split into two orthogonal components by using the Fourier filter. Starting from these components, the real part and imaginary part of the apparent impedance are calculated as follows:

$$Z = \frac{U}{I} = \frac{U_c + jU_s}{I_c + jI_s} \tag{4.24}$$

so

$$R = \frac{U_c I_c + U_s I_s}{I_c^2 + I_s^2} \tag{4.25}$$

$$X = \frac{U_s I_c - U_c I_s}{I_c^2 + I_s^2} \tag{4.26}$$

where U_c, U_s, I_c, I_s are the orthogonal components of voltage and current respectively.

Normally the Fourier filter is used to obtain the fundamental complex voltage and current, U and I respectively. But they can equally well be obtained by any other method, like Walsh filters or Kalman filters.

4.3.2 Differential equation algorithm

Unlike Fourier algorithm which is based on the description of the waveform, differential equation algorithm is based on a system model. The studied line is modeled as an R-L series connection by the following differential equation:

$$RI(t) + L\frac{dI(t)}{dt} = U(t) \tag{4.27}$$

Supposing voltage and current signals are sampled at the equal-distant instants $k\Delta t$, $(k+1)\Delta t$, $(k+2)\Delta t$, the integration of Eqn. (4.27) can be expressed as:

$$\int_{k\Delta t}^{(k+1)\Delta t} U(t)dt = R\int_{k\Delta t}^{(k+1)\Delta t} I(t)dt + L[I_{k+1} - I_k] \tag{4.28}$$

$$\int_{(k+1)\Delta t}^{(k+2)\Delta t} U(t)dt = R\int_{(k+1)\Delta t}^{(k+2)\Delta t} I(t)dt + L[I_{k+2} - I_{k+1}] \tag{4.29}$$

where $I_k = I(k\Delta t)$, etc.

The above two equations can be approximated using trapezoidal rule as follows:

$$\int_{k\Delta t}^{(k+1)\Delta t} U(t)dt = \frac{\Delta t}{2}\left[U_{k+1} + U_k\right] \tag{4.30}$$

where $U_k = U(k\Delta t)$, etc.

Eqns. (4.28) and (4.29) can be written as a matrix equation:

$$\begin{bmatrix} \frac{\Delta t}{2}(I_{k+1} + I_k) & (I_{k+1} - I_k) \\ \frac{\Delta t}{2}(I_{k+2} + I_{k+1}) & (I_{k+2} - I_{k+1}) \end{bmatrix} \begin{bmatrix} R \\ L \end{bmatrix} = \begin{bmatrix} \frac{\Delta t}{2}(U_{k+1} + U_k) \\ \frac{\Delta t}{2}(U_{k+2} + U_{k+1}) \end{bmatrix} \tag{4.31}$$

from which the estimates of R and L are calculated as follows:

$$R = \left[\frac{(U_{k+1} + U_k)(I_{k+2} - I_{k+1}) - (U_{k+2} + U_{k+1})(I_{k+1} - I_k)}{(I_{k+1} + I_k)(I_{k+2} - I_{k+1}) - (I_{k+2} + I_{k+1})(I_{k+1} - I_k)}\right] \tag{4.32}$$

$$L = \frac{\Delta t}{2}\left[\frac{(I_{k+1} + I_k)(V_{k+2} + V_{k+1}) - (I_{k+2} + I_{k+1})(U_{k+1} + U_k)}{(I_{k+1} + I_k)(I_{k+2} - I_{k+1}) - (I_{k+2} + I_{k+1})(I_{k+1} - I_k)}\right] \tag{4.33}$$

Compared with the Fourier algorithm, the differential equation algorithm is faster and more suitable for transient conditions. However, the approximation of the line as an ideal R-L loop somewhat affects the accuracy of this algorithm. Both of them have application in line relaying.

The differential-impedance-based algorithm can be further extended by adding the shunt capacitance of the line to the model. Expression (4.27) would become more complicated but the solution would still be possible. Alternatively, information from more samples could be used, extending the number of equations in (4.27). Resistance and inductance could be estimated by using a least square method.

4.3.3 Travelling wave based algorithm

Travelling wave based algorithms make use of the characteristics of travelling waves along the transmission lines for calculating impedance. There are several types of algorithms in this category, such as correlation technique by Vitins et al.[13] [14], Kohlas' algorithm [15], Christopoulos' algorithm [16] etc. In this section, Kohlas' algorithm is introduced.

The assumptions for Kohlas' algorithm are:

- The line is considered to have frequency independent R, L and C
- When there is no fault on the line the voltage variation along the line is zero.

The algorithm uses the travelling wave equations of the line as a model relating voltages and currents.

$$-\frac{\partial U}{\partial z} = RI + L\frac{\partial I}{\partial t}$$

$$-\frac{\partial I}{\partial z} = C\frac{\partial U}{\partial t}$$

By using these equations an expression is obtained for the voltages at any point along the line as a function of time. Input to this expression are the voltages and currents measured at the line terminal over a certain measurement window T. The fault location is detected as the place where the voltage is closest to zero.

The fault detection function by Kohlas' algorithm is as follows:

$$G(z) = \frac{d^2}{dz^2}\left[\frac{1}{T - 2z/c}\int_{z/c}^{T-z/c} U^2(z,t)dt\right] \qquad (4.34)$$

where c propagation velocity of travelling wave

T measurement window length

U voltage, is a function of distance and time

z distance away from the measurement terminal of the line

When a fault occurs at point z, its voltage remains zero during the travelling wave propagation period. However, the voltage variation at this point is higher than the others. So Eqn. 4.34 will show up a very sharp maximum in G(z).

Kohlas' algorithm develops complicated expressions for voltages and currents along the line. However, according to later research [17], the resistance R of a line has little effect on the accuracy of final results. By assigning R=0, the expressions become much simpler. It is also found that the following detection function can yield results with satisfying accuracy:

$$F(z) = \frac{1}{T - 2z/c} \int_{z/c}^{T-z/c} U^2(z,t)dt \qquad (4.35)$$

The fault is located at the point z, which shows up a minimum of F(z). Compared with the previously mentioned 2 algorithms, this technique demonstrates a completely new approach in dealing with distance protection. Experiments have shown that it makes a fairly good discrimination between internal faults and external faults [18].

However, such a technique has the following weakpoints:

- Faults close to one of the line terminals are not detected
- Most of the phase-to-phase faults are not detected
- The calculation needs a lot of computation time

Therefore compared with Fourier algorithm and differential equation algorithm, this technique remains to be improved before it can be adopted in practice.

4.4 Trade-off Between Speed and Accuracy

From the analysis of previous sections, it is clear that the digital filters based on Fourier principles are quite popular in practical application. The Fourier filter uses moving a sampling window to scan the input signal. The decision-making time of the relay is dependent on the length of the sampling window.

In normal case, a 1-cycle (also called full-cycle) sampling window is adopted, which means that the decision-making time will be at least 20 ms. The frequency response of 1-cycle Fourier filter is shown in Fig. 4.4.1.

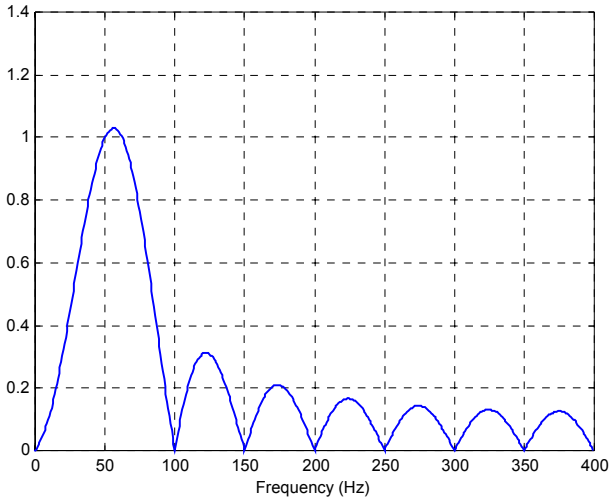

Figure 4.4.1 Frequency response of 1-cycle Fourier filter

From Fig. 4.4.1 it is obvious that the 1-cycle Fourier filter has a good performance in rejecting all integer orders of harmonics as well as the DC component.

Sometimes a faster relay algorithm is needed. In such a condition, a half-cycle Fourier filter is often adopted. Compared with the 1-cycle filter, its decision-making time is reduced to 10 ms, which facilitates fast detection of changes in input signal. Its frequency response is shown in Fig. 4.4.2.

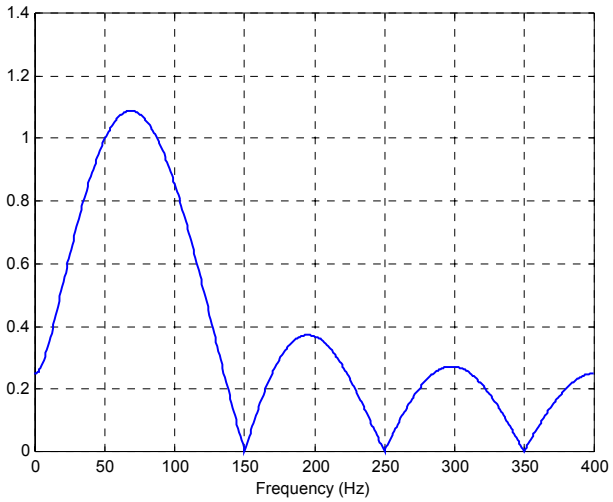

Figure 4.4.2 Frequency response of half-cycle Fourier filter

However, by checking Fig. 4.4.2 against Fig. 4.4.1, it can be concluded that the half-cycle filter loses its immunity from the even harmonics and DC component. The output signal after filtering may still contain these unwanted components. In other words, half-cycle filters improve the speed of the relay at the cost of accuracy.

In case when interharmonics are presented (e. g. ½ or 1/3 fundamental frequency components), a longer sampling window is required so as to remove these components. Longer sampling windows, on the other hand, lead to longer decision-making times.

Therefore, there is always a trade-off between relay speed and accuracy. It is impossible and unnecessary to seek the optimal balance point between these two factors for all the cases, as the proper choice of sampling window length is dependent on system structure, operation mode and even economic factors.

The comparison among cases of different window lengths is illustrated in chapter 6.

4.5 Generic Protection Algorithms

Among the one-element relays, the overcurrent relay is a typical example, while among the dual-element relays the distance relay is more representative. Meanwhile, these 2 types of relay are the most widely used ones in power systems.

Whatever the input measurement parameters are, they only stand for signals in the viewpoint of relays. Although the relay principles may more or less differ from each, they have some characteristics in common. For the convenience of the case studies in later chapters, generic protection algorithms for these two types of relay are introduced.

Fig. 4.5.1 shows the operation principle for overcurrent relays. The input signal is compared with a pre-set threshold continuously. Whenever the threshold is exceeded, a counter is started to calculate the duration that the signal is kept above the threshold. If the duration is longer than a pre-set time delay, the relay sends out a tripping signal. This pre-set time delay is for relay decision-making. If the input signal falls below the threshold before its duration reaches the pre-set time delay, the counter will be reset and a new round of comparison is started. The tripping zone is the plane above the threshold line, while the rest is the non-tripping zone.

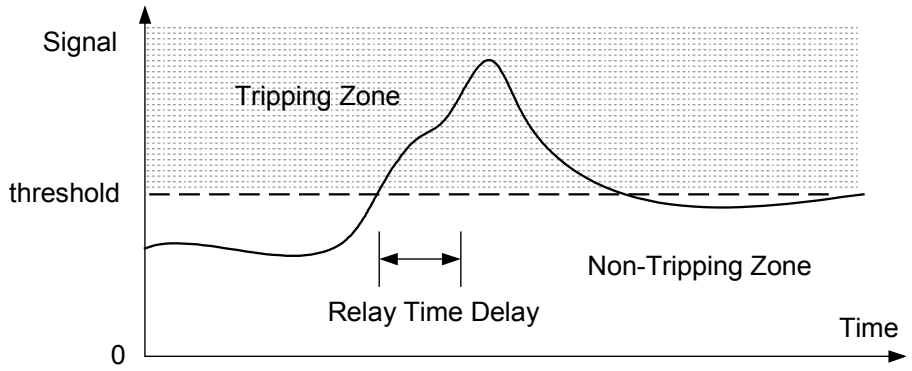

Figure 4.5.1 Operation principle of overcurrent relay

The operation principle of overvoltage relays is quite similar to that of overcurrent relays. The input signals in these 2 cases are for different parameters. But in the viewpoint of relay algorithm, this does not make difference. The operation principle for undervoltage relays is opposite to that of overvoltage relays. Instead of counting the signal variation that exceeds the pre-set threshold, its algorithm calculates the duration that the input signal drops below a certain pre-set threshold.

The operation principle of the generic distance relay is shown in Fig. 4.5.2. It is a mho distance relay. Its tripping zone is the inside of the circle that passes through the origin of the coordinate system. X-axis and Y-axis in this coordinate system stand for resistance R and reactance X, respectively. The diameter line that starts from the origin is at an angle θ with the x-axis. This angle is the same as that of the impedance of the protected line. Any point on this plane corresponds to certain impedance seen from the relay installation place. Whenever the impedance measured by a relay is inside the circle for longer than a pre-set duration, the relay will generate a trip signal. The tripping zone is the area covered by this characteristic circle, while the outside region is the non-tripping zone.

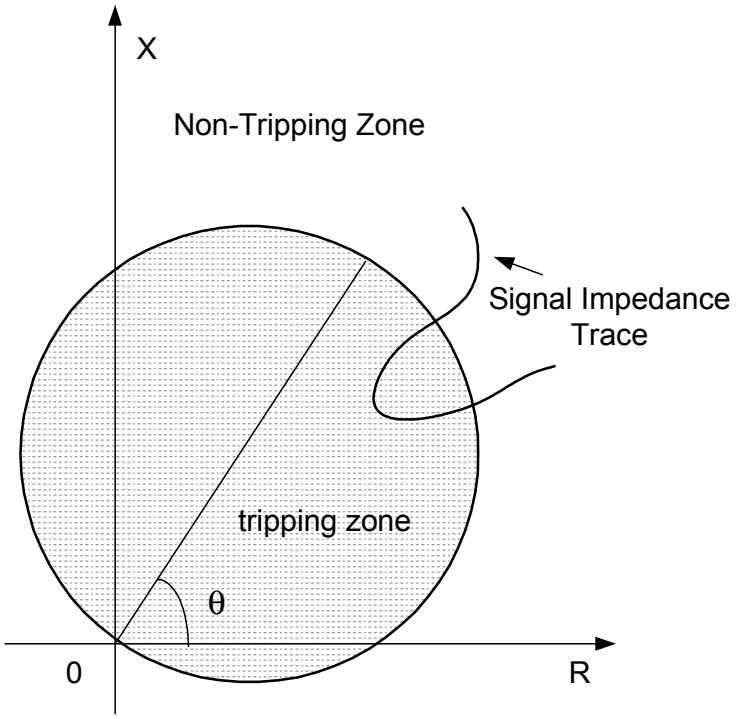

Figure 4.5.2 Operation principle of distance relay

Chapter 5 Quantification of Disturbances in Power Systems

As mentioned in previous chapters, the presence of disturbances may affect the operation of protective relays which, as a direct consequence, endangers the reliability of power systems.

A disturbance may cause relay mal-trip or fail-to-trip, depending on the particular case. If the disturbance that causes relay mal-trip is due to a fault, it will lead to the loss of the faulted as well as the non-faulted component. For other disturbances, several relays may react in the same way. The loss of multiple components in a transmission system may trigger a large-scale blackout. The risk of a mal-trip due to a disturbance is minimized during the design process of a relay (mainly through the use of filters) and by a conservative choice of threshold and time delay settings. All this typically leads to an increase of the fault-clearing time and greater risk of fail-to-trip. Actually, generating a tripping signal too late (e. g. exceeding the critical fault-clearing time in angular stability) is also considered as a fail-to-trip event. To make an accurate trade-off between fail-to-trip, fault-clearing time and mal-trip, a detailed knowledge is needed of voltage and current disturbances at the relay terminals. Assessment of disturbance impact on relays can in no doubt facilitate the choice of proper relay parameters.

5.1 Two Ways of Quantification

To assess the disturbance impact on relays, relay testing under the disturbance condition is necessary. Normally, protective relays are tested using a set of synthetic disturbances. But these disturbances, which are in fact

simulated signals, cannot completely take the place of practically measured disturbances. The use of measured disturbances will form an important and necessary complement to this.

In normal case, disturbance data are obtained from digital fault recorders or power quality monitors installed on site. However, studying the recorded disturbance cases shows that only a small portion contains severe disturbances. Some first pruning is needed, based on the potential impact of a disturbance on a certain relay type.

A measured disturbance may or may not lead to relay mal-trip when imposed on a studied relay, depending on the severity of the disturbance, the relay algorithm and the relay setting. The output of relay can be in 2 status only: trip or non-trip. However, these two conditions are not enough to describe the difference on impact severity in various cases. A disturbance might not lead to relay mal-trip as a final result, but make the relay characteristics shifted near the critical boundary of mal-trip, which is also potentially risky. Also possible is that a disturbance that causes no mal-trip for a certain type of relay may lead to mal-trip for another relay type, due to the trade-off between relay speed and security as mentioned in the previous chapter. It is inappropriate to discard altogether a signal leading to such “almost trip”, only because it gives a non-trip relay output status. Assessment of impact severity is crucial in ranking the potential risk of measured disturbances, for various relay types.

It is difficult to intuitively tell the potential risk of disturbances by checking their waveforms. A quantification technique is adopted to demonstrate the nuances by means of a disturbance factor. While the voltage and current

waveforms of various voltage disturbances appear quite similar, the disturbance factors might be different.

The assessment of disturbance impact can be made in two ways. A disturbance may cause the measured parameter to falsely enter the relay tripping zone, leading to a mal-trip. The approach based on this effect is referred to as "setting-based quantification" in this project. Disturbances will affect the relay operation in another way as well. A digital relay can be seen as a filter that extracts the desired component from the measured voltages and/or currents. The presence of a disturbance will produce an error in extracting the desired component. This approach is referred to as "design-based quantification".

In practical applications, most relays are designed to operate under fundamental frequency, i.e. 50 Hz. Some special relays, e.g. relay for generator stator ground fault, work under harmonic frequency. It is therefore assumed that in this work that the desired component is the fundamental component while the unwanted components are harmonics, interharmonics, dc, transients etc.

5.2 Setting-Based Disturbance Quantification

In practical installation, the main concerns are whether the disturbances may trigger the relay protection by falsely entering the protection tripping region. A disturbance studied in this project means a voltage and/or current signal with a short-term transient, or a long-term distortion, or both. The practically measured disturbance signals have limited duration, from several cycles to more than ten cycles. To evaluate the disturbance impact, it is necessary to study the possible impact region for disturbances.

5.2.1 Disturbance impact factor

Figs. 5.2.1.1-5.2.1.3 give two examples of such disturbances, for overcurrent relay and impedance relay respectively. In both cases, the generic protection algorithms as introduced in chapter 4 are applied.

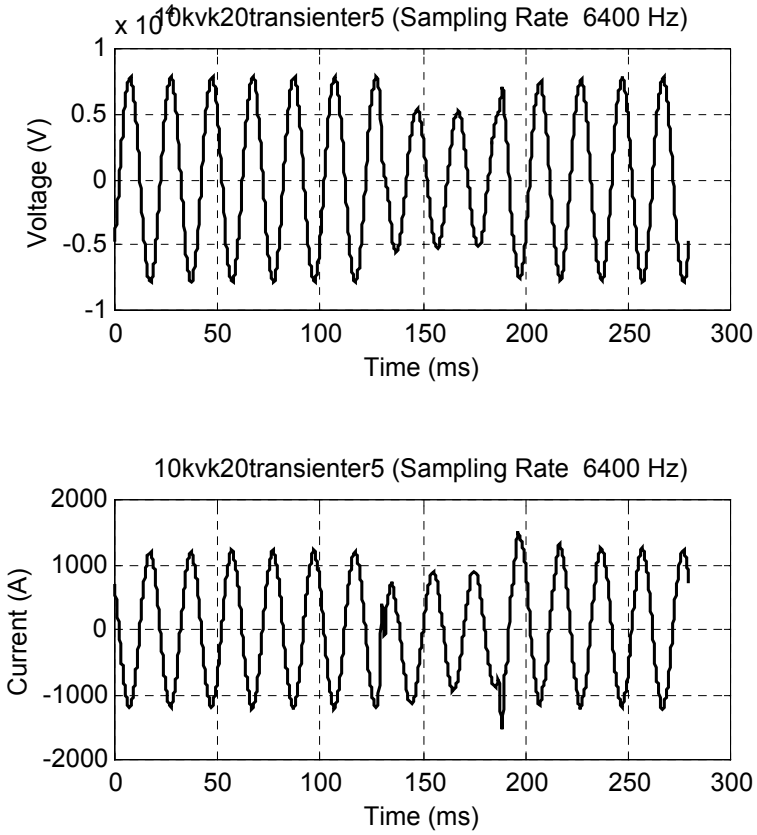

Figure 5.2.1.1 Disturbance signals

Fig. 5.2.1.1 shows the recording of a voltage dip: both voltage (top) and current (bottom) are shown. The sag lasts for 3 cycles before the voltage recovers. With the voltage drop the current decreases accordingly. At the moments of dip starting and ending, transient disturbances are observed on both voltage and current waveforms, especially on the current waveform.

The response by an overcurrent relay to this disturbance is shown in Fig. 5.2.1.2. The dashed curve gives the measured current, as in the bottom plot in Fig. 5.2.1.1. The output curve (the solid curve) is obtained by applying the

Fourier algorithm filter, as described in section 4.2.1 to the current waveform. A sampling window length of 1 cycle has been used. The diagram demonstrates that such a relay (filter) can remove the spikes on the waveform of the input signal. However the output (the solid envelope line in the figure) shows transient characteristics at the beginning and end of the dip period. The output of the filter shows an undercurrent followed by an overcurrent. As the sampling window is of 1 cycle length, the output within 1 cycle after any sudden change or transient in the signal is inaccurate.

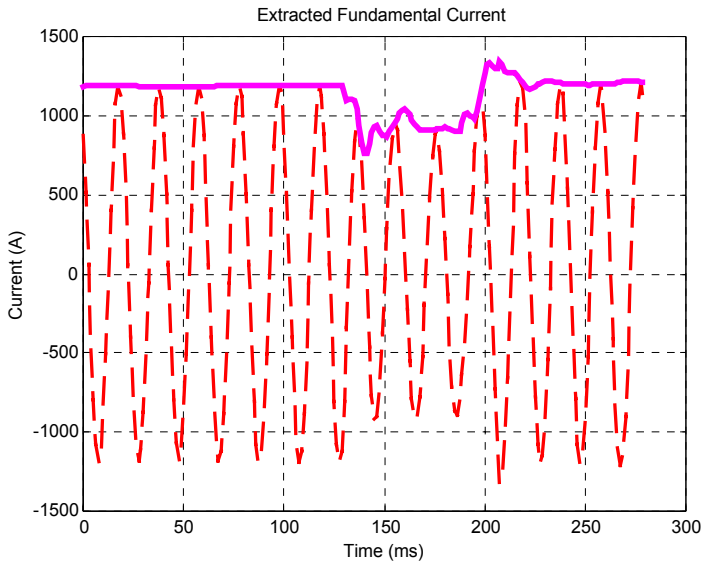

Figure 5.2.1.2 Disturbance impact on overcurrent relay setting

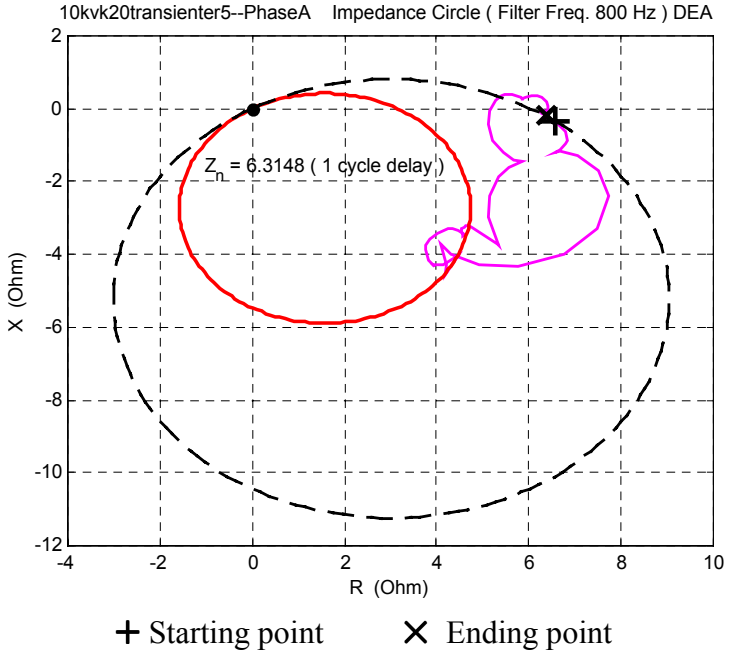

Figure 5.2.1.3 Disturbance impact on impedance relay setting

In Fig. 5.2.1.3, the apparent impedance observed by the relay filter moves around the R-X plane during the disturbance before it returns to a place near the original starting point. The impedance trace is obtained by applying the differential equation algorithm as described in section 4.3.2 of chapter 4. The setting of this relay is based on the MHO principle with the impedance angle being 60 degrees, which is a generic value for MV system lines.

The status at both the beginning and the end of the measurement window are considered stable for at least one cycle; the variation in the signal in between determines the impact on relay operation. The severity of the disturbance is given relative to a steady state value. Either the pre-disturbance or the post-disturbance value is used, whichever one is more severe. Two examples are given in Figs. 5.2.1.4 and 5.2.1.5.

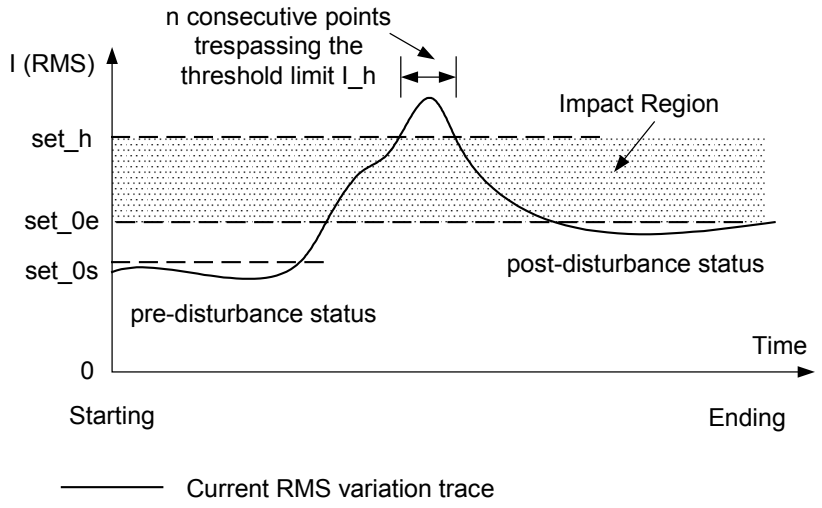

Figure 5.2.1.4 Impact region for overcurrent relay

In Fig. 5.2.1.4, a relay filter output is shown as a curve. During a certain part of the disturbance, the relay filter output exceeds the pre-disturbance and post-disturbance levels. As described in the generic overcurrent algorithm in chapter 4, a time delay is adopted for verifying the decision. In digital relaying, such a time delay means a certain number of consecutive points that are above the pre-set threshold. By moving a line parallel to the time axis up

and down, a certain threshold level can always be located, above which there are just a predefined number of consecutive points. Such a threshold level is named set_h, which represents the highest possible limit that relay filter output can trespass and keep for a pre-defined duration. The current levels of pre-disturbance and post-disturbance are defined as set_0s and set_0e respectively.

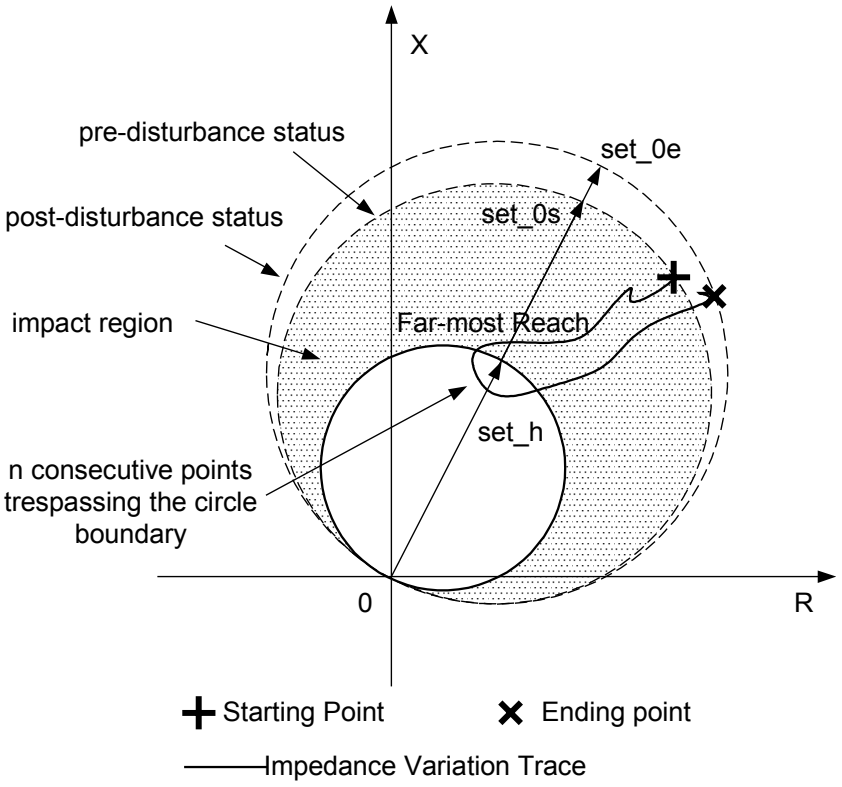

Figure 5.2.1.5 Impact region for impedance relay

In Fig. 5.2.1.5, the relay output is shown as an impedance moving trace. Similarly as in Fig. 5.2.1.4, a setting region can be located inside which a pre-defined number of consecutive points fall during the disturbance. The diameter of such a region (as MHO setting region is a circle, see the last section in chapter 4) is defined as set_h. The diameters of the two imaginary circles, on which the pre-disturbance and post-disturbance status points locate, are defined as set_0s and set_0e respectively.

To quantify the severity of an impact, a disturbance factor D is introduced. Let set_0 = max (set_0s, set_0e), or set_0=min (set_0s, set_0e), depending on the type of protection, then the disturbance factor is defined as:

$$D = | (set\_h-set\_0)/set\_h | \quad (5.1)$$

Fig. 5.2.1.4 shows an impact region starting from the post-disturbance value. In Fig. 5.2.1.5, the impact region is counted from the pre-disturbance point because it is closer to the setting region compared with the post-disturbance point.

5.2.2 Disturbance impact on various types of relay setting zone

Overvoltage, undervoltage, overload, overcurrent and impedance relays are the main force in feeder/line protections. Whenever a disturbance occurs, it is necessary to know its potential impact on various protections. For an overall evaluation of the disturbance, the impact region of the following relays are studied:

- Overvoltage (V ↑)
- Undervoltage (V ↓)
- Overcurrent (I ↑)
- Impedance (Z ↓)

The generic algorithms (see the last section of chapter 4) are adopted for these 4 types of relay. Table 5.2.2.1 lists the possible disturbances and their impacts on the setting zones of various relay protections. As in practice more than one factor can contribute to disturbances, their impacts on various relays might not be exactly as shown in the table. Anyhow, this table provides a rough assessment on the possible sequences of disturbances on relays.

Table 5.2.2.1 Disturbances and corresponding impact

V ↑	V ↓	I ↑	Z ↓	Disturbance type
✓	✓	✖	✓	Voltage transient
✖	✖	✓	✓	Current transient
✓	✖	✖	✖	Voltage swell
✖	✓	✓	✓	Voltage sag
✓	✓	✖	✓	Voltage fluctuation
✖	✓	✓	✓	Short-time overload
✓ potential impact			✖ minor or no impact	

Collecting all the quantified impact information together gives an overall estimation of the disturbance effect on the infringement of relay setting region. An example of such an illustrative diagram is shown in Fig. 5.2.2.1.

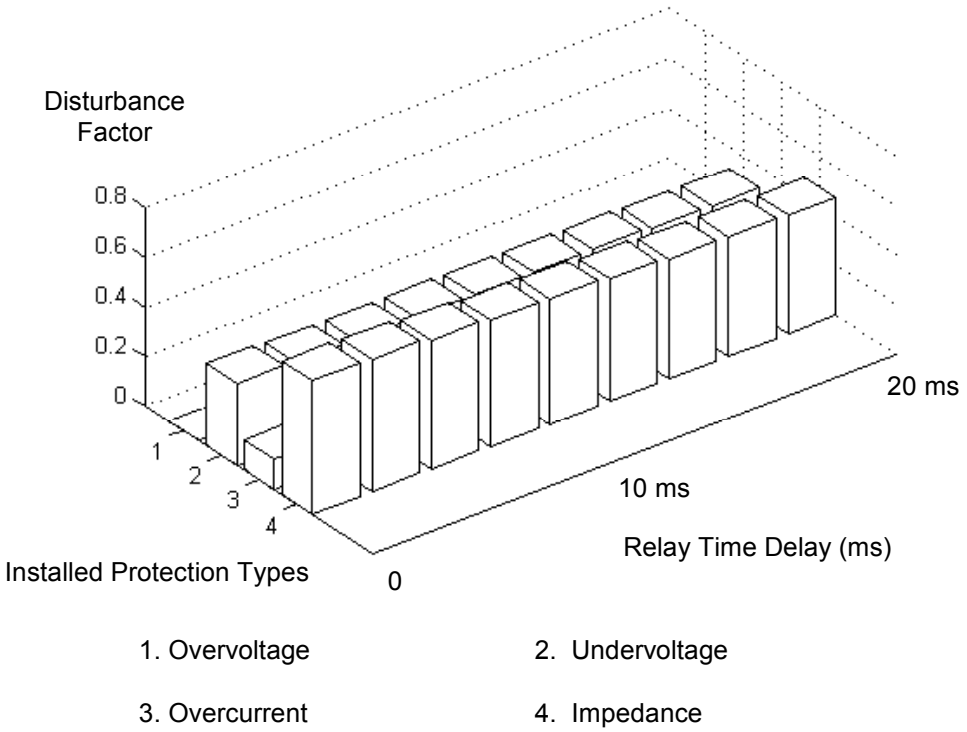

Figure 5.2.2.1 Disturbance impact on various relays

In the diagram, the duration of a disturbance and the severity of its impact on a certain type of relay are displayed. It provides an intuitive estimation of the possible impact due to the input disturbance signal. A diagram in which all the values are on the plane of D=0 (disturbance factor is zero) implies that the studied disturbance has no effect on relays. It is useful in determining the safety margin of relay setting. Disturbance signals can be quantified and ranked based on the information in this diagram, depending on the particular emphasis of a protection scheme.

5.3 Design-Based Disturbance Quantification

An important part of the design of digital relays involves the extraction of the fundamental component by a digital filter. Whatever the cause of the disturbance, it is just regarded by a digital filter as a (group of) input signals that contain not only the fundamental component, but also the other unwanted ones. Among the unwanted components, some can easily be removed while others can appear in the filter output. The design-based quantification aims at shortlisting the signals containing difficult-to-remove components. The following section describes the way to assess the impact of these components on relay output characteristics.

5.3.1 Disturbance impact factor

The window size and shape significantly affect the filter output. This is shown in Fig. 5.3.1.1 where the amplitude of the fundamental component is plotted for cosine/sine windows of different size, together with the (time-domain) disturbance factor.

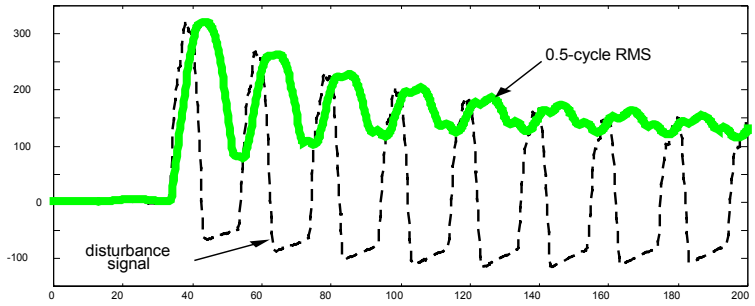

(a)

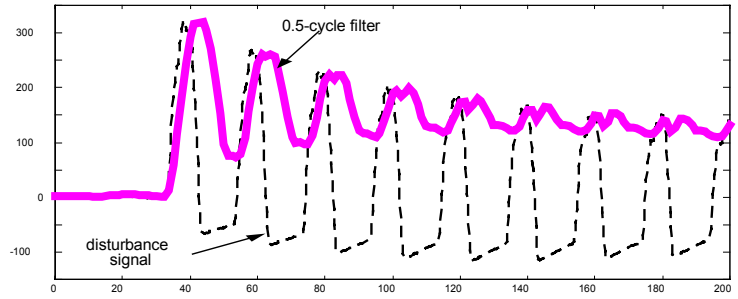

(b)

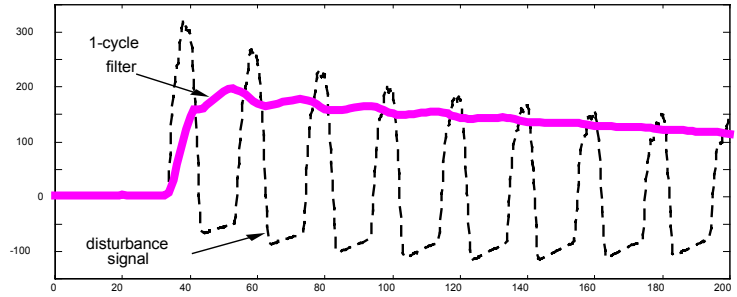

(c)

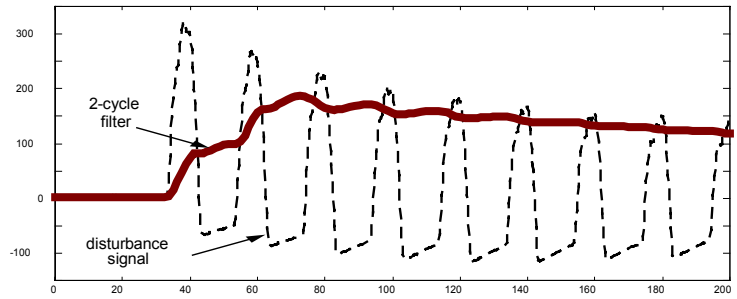

(d)

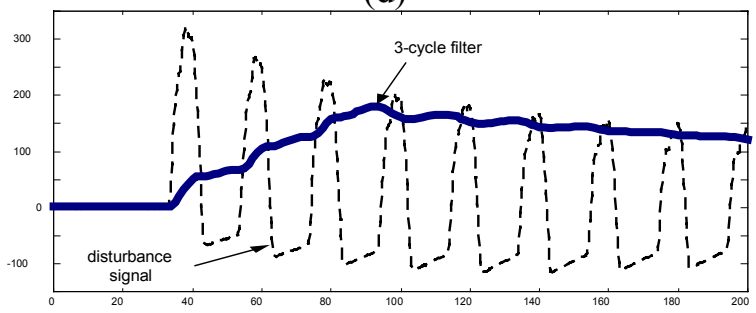

(e)

Figure 5.3.1.1 Outputs of filtered signal by different filters

Accordingly, Eqns. 4.7 and 4.8 are rewritten as:

$$\hat{Y}_c = \frac{2}{mK}\sum_{k=1}^{mK} y_k \cos(k\theta) \tag{5.2}$$

$$\hat{Y}_s = \frac{2}{mK}\sum_{k=1}^{mK} y_k \sin(k\theta) \tag{5.3}$$

where $\theta = 2\pi/K$, m is the multiple size of the window, K is the number of sampling point per cycle.

Plots (b), (c), (d) and (e) in Fig. 5.3.1.1 are obtained by applying Fourier filters with window lengths 0.5, 1, 2 and 3 cycles respectively. Plot (a) is obtained by calculating the RMS (root-mean-square) value over a 0.5-cycle window. The plots show a strong oscillation for a half-cycle window, but only minor oscillations for longer window lengths. Extending the window length from one to three cycles doesn't further reduce the oscillations. Note that these conclusions only apply to this specific signal and may not necessarily hold generally.

Corresponding to relay output characteristics, different filters may yield different results. An example is shown in Fig. 5.3.1.2, where the output characteristics of both 1-cycle Fourier filter and another filter (0.5-cycle Fourier filter) with different sampling window size are compared.

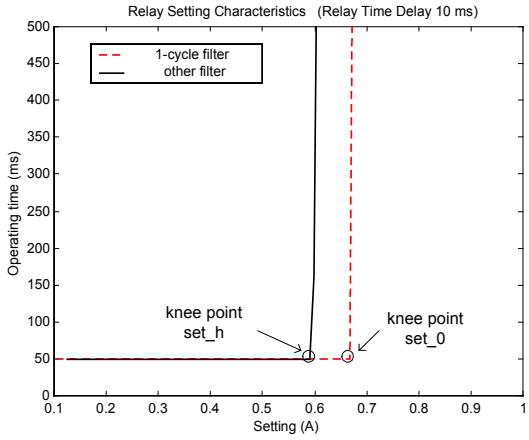

Figure 5.3.1.2 Shift of relay setting characteristics

In the figure, the knee point corresponds to the setting limit. It means a relay which, equipped with a certain type of filter and a certain time delay for decision-making, will not operate if the actual setting is greater than this limit. From the figure it can be observed that the type of relay filter may affect the output performance obviously.

Most relays are designed to operate under fundamental frequency. If the fundamental component is available, the impact of a disturbance on relay performance can then be evaluated by checking the setting limit shift due to the disturbance. However, the large number of possible events and system configurations give an almost unlimited amount of combinations of signal components. It is not possible to design a filter that in all cases extract the exact value of the fundamental component. There is thus no reference to which the output of a given filter can be compared.

There is however an indirect way to evaluate the impact of a given disturbance — by comparing the filter outputs by different relay filters. If all the filters yield similar setting limits, then it can be safely assured that the unwanted components in the input signal are not of much concern. They can either be of small magnitude or easily removed by all of the filters. If there is significant shift in setting limits among different filters, it means there is something in the input signal that may seriously affect relay performance.

Let the setting of 1-cycle filter be the reference value set_0 and the setting of another filter be set_h, the disturbance factor D, which has a somewhat different meaning from the one introduced in section 5.2.1, is defined through the following expression:

D = | (set_h-set_0)/set_h | (5.4)

where set_h and set_0 are defined as above.

This expression is the same in form as Eqn. 5.1.

5.3.2 Disturbance impact on various types of relay filters

The window length determines the frequency response of the filter. Table 5.3.2.1 shows the capability of different filters in removing various unwanted components.

Table 5.3.2.1 Capability of filter in removing disturbances

	RMS (0.5-cycle)	0.5-cycle	1-cycle	2-cycle	3-cycle
Transients					
Odd harmonics		✓	✓	✓	✓
Even harmonics			✓	✓	✓
DC			✓	✓	✓
1/2 interharmonics				✓	
1/3 interharmonics					✓

Whenever there is a transient, no filter can work hundred percent correctly. Depending on the window size, a filter will not yield correct output in less than 1 sampling window time, which means there is no way for a filter to extract the exact fundamental component.

The last two phenomena in the table, 1/2 interharmonics[1] and 1/3 interharmonics[2], occur in some special cases. Reference [19] reports the

1 A 1/2 interharmonic is an interharmonic with a frequency equal to a multiple of half the fundamental frequency, e. g. 25 Hz, 175 Hz.

2 A 1/3 interharmonic is an interharmonic with a frequency equal to a multiple of one third of the fundamental frequency, e. g. 56.7 z, 183.3 Hz

existence of 25 Hz and 125 Hz interharmonics (50 Hz system) due to DC arc furnace. During one of the measurements that were part of this research project, series of 1/3 interharmonics were observed [20].

From table 5.3.2.1, it is clear that normally a longer sampling window gives a more accurate output. However, more cycles for sampling also means more time for decision-making. So this is again the before mentioned trade-off between time and accuracy.

Similar to the approach in section 5.2.2, another kind of illustrative diagram is adopted to evaluate the disturbance severity. An example is shown in Fig. 5.3.2.1.

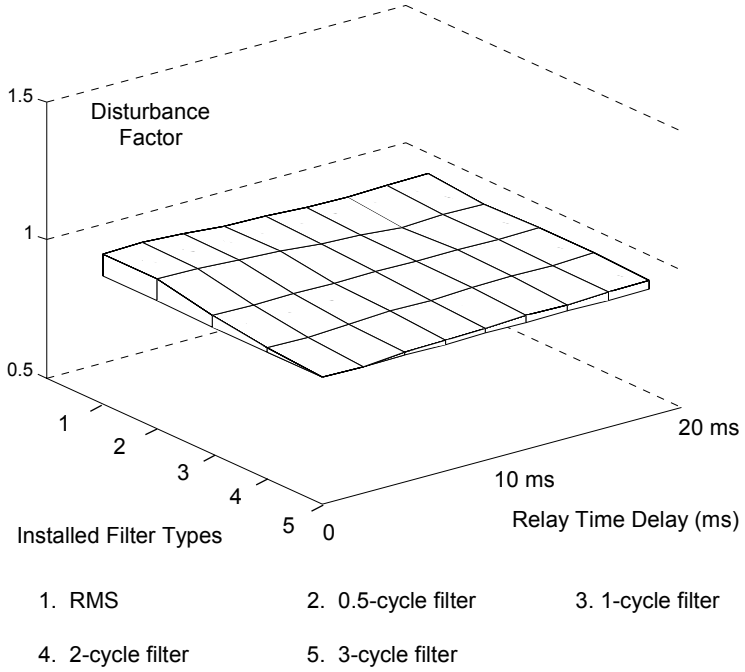

Figure 5.3.2.1 Disturbance impact in cases of different relay filters

In this diagram, the variation of impact severity is around 1.0. All the disturbance factor values form a surface. A surface closer to the plane of Z=1.0 means less unwanted components or variations. The greater the curvature at certain points, the more severe the impact is.

Chapter 6 Case Studies and Simulation Results

In this chapter, a number of measured disturbances are applied to an ordinary digital relay to demonstrate the disturbance impact severity. All the relays in the study use a sampling frequency of 800 Hz (16 samples per cycle).

The case studies are carried out for both setting-based quantification and design-based quantification. Under each of the two conditions, several typical disturbances are tested. Their disturbance impacts are illustrated in such diagrams as proposed in Chapter 5. The diagrams are interpreted and discussed. The implied conclusions behind these diagrams are drawn.

A comparison among various case studies is made in the last section. Further development of the disturbance impact criterion is discussed.

6.1 Setting-based Evaluation of Disturbance Impact

In this section, 5 typical disturbances as defined in Chapter 2 are used to test the setting-based quantification technique.

Case 1 Current Transient

This is a disturbance signal measured in a 10 kV system. A transient occurs at a certain moment and later diminishes. Besides, there is also harmonic distortion in the current waveform. The voltage and current waveforms are shown in Fig. 6.1.1.

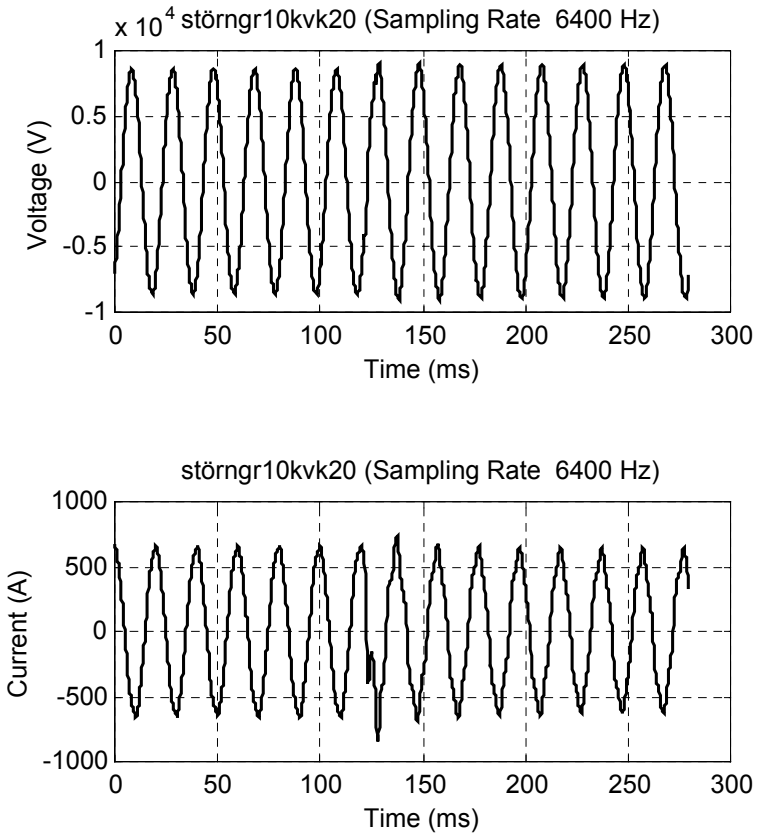

Figure 6.1.1 Current transient disturbance (Sweden)

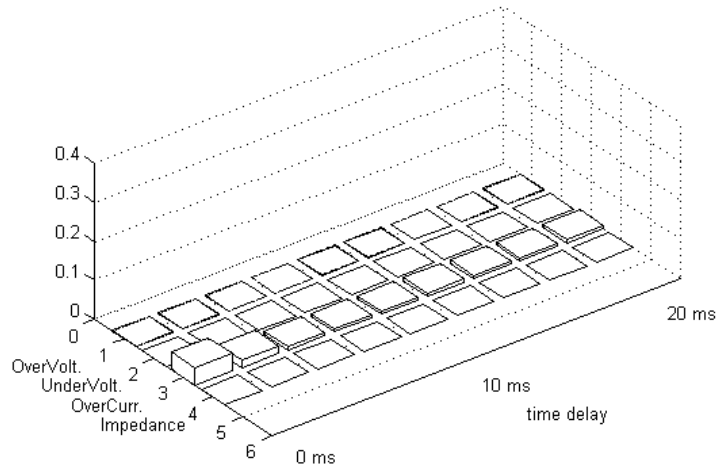

Figure 6.1.2 Impact on relay setting zone by current transient

From Fig. 6.1.1, it is observed that the transient lasts for about a quarter cycle (5 ms). Its impact on relay setting zone is shown in Fig. 6.1.2. This transient has little impact on any type of protective relay.

Case 2 Voltage Transient

Fig. 6.1.3 shows a transient voltage increase again measured in a 10 kV system. There is a large voltage overshoot when the voltage approaches its peak. Such a transient lasts for about 2 cycles before it attenuates.

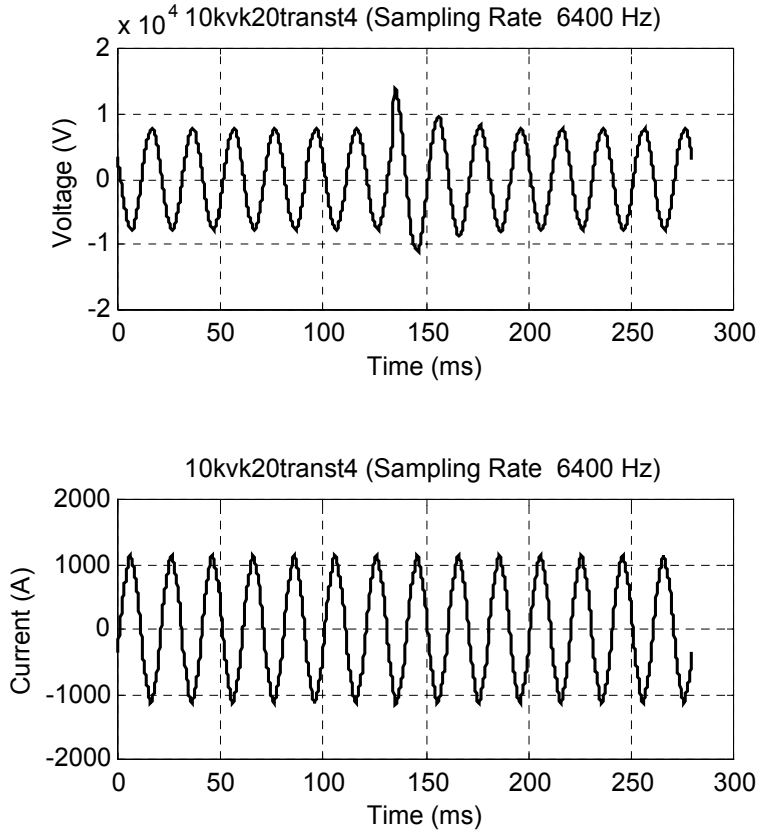

Figure 6.1.3 Voltage transient disturbance (Sweden)

The transient can have considerable impact on overvoltage relay operation. As illustrated in Fig. 6.1.4, the impact does not diminish within 1 cycle, making the risk of overvoltage relay tripping if the time delay is 20 ms or less.

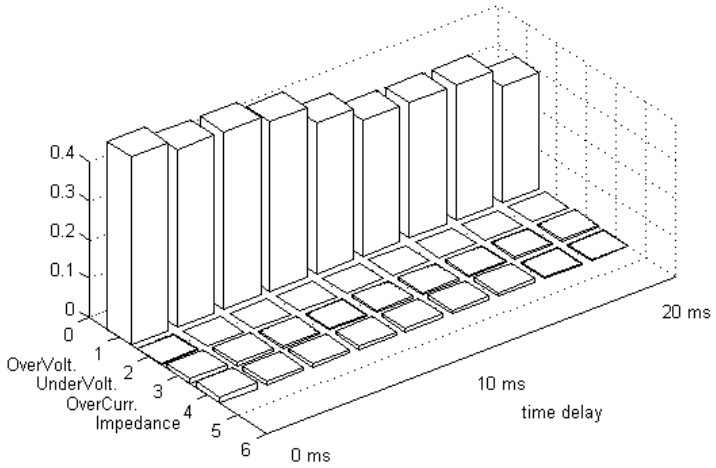

Figure 6.1.4 Impact of voltage transient on relay setting zone

Case 3 Current Inrush Transient

The transient in this case is due to component switching in a LV system.

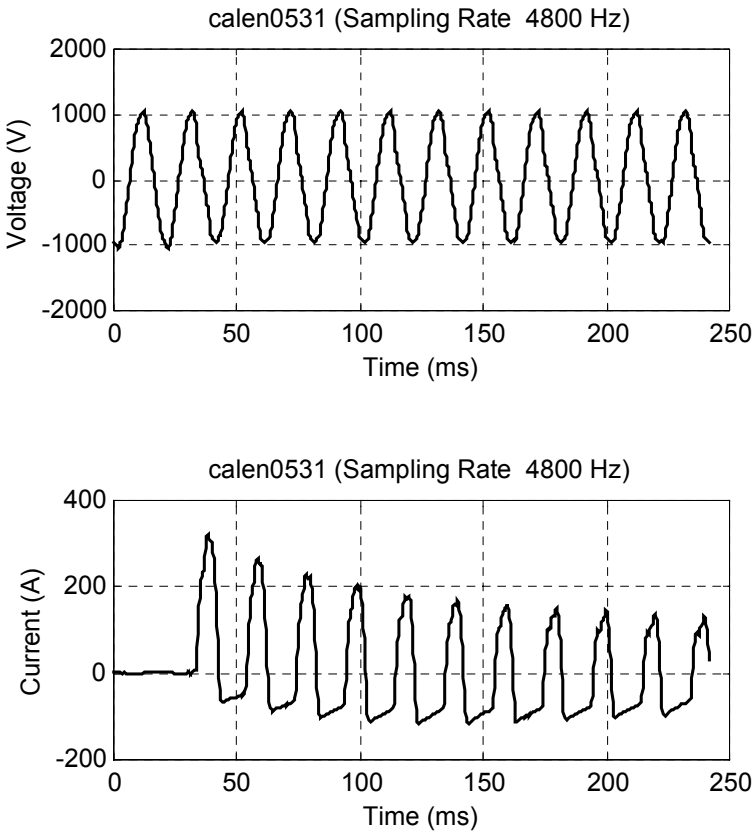

Figure 6.1.5 Inrush current transient (Scotland)

The transient generated in this situation contains both odd and even harmonics, which attenuate after some time. The attenuation period is so long that the transient does threaten the operation of some relays. From Fig. 6.1.6, it is demonstrated that both overcurrent relay and impedance relay are potentially affected.

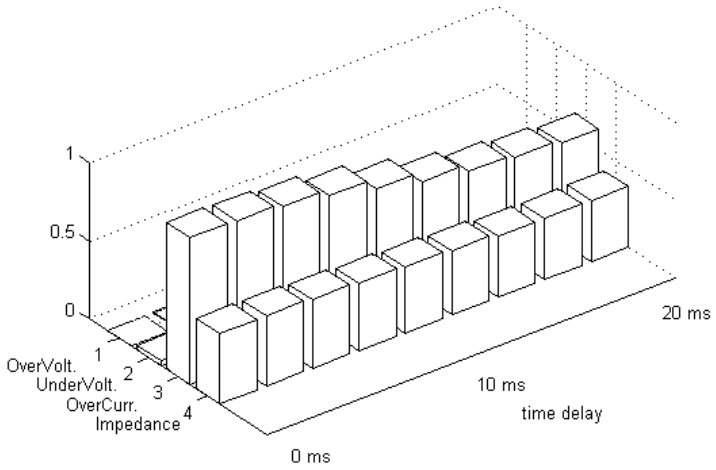

Figure 6.1.6 Impact of inrush current on relay setting zone

Due to the high overcurrent, the disturbance has considerable impact on overcurrent relay s. The impact on impedance relays can be depicted with the help of impedance trace diagram, as shown in Fig. 6.1.7.

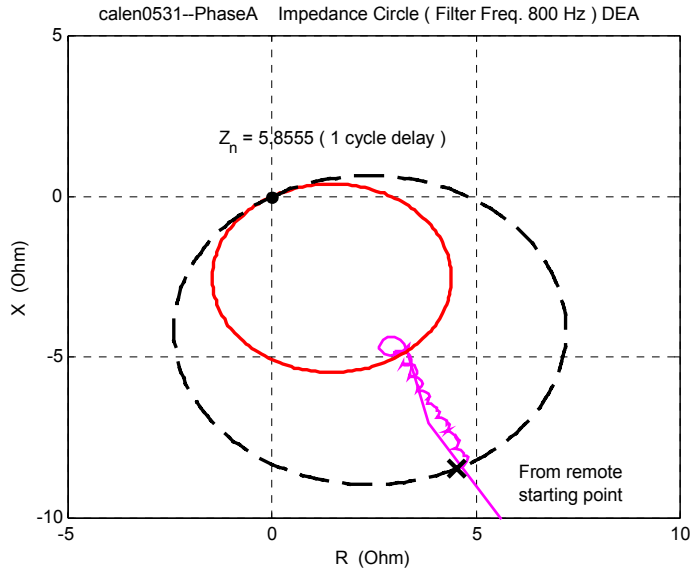

Figure 6.1.7 Impedance variation trace of inrush transient

The imaginary circle in Fig. 6.1.7 represents, as explained in chapter 5, the stable status (in this case the post-disturbance status). The solid line circle in this figure stands for the far most reach of the impact during the disturbance.

Case 4 Voltage Dip

When there is a voltage dip in the system, the load current on a particular feeder can experience either a short time increase or decrease, depending on the type of the attached load and the location of the monitor. Fig. 6.1.8 shows an example of decrease in both voltage and current simultaneously.

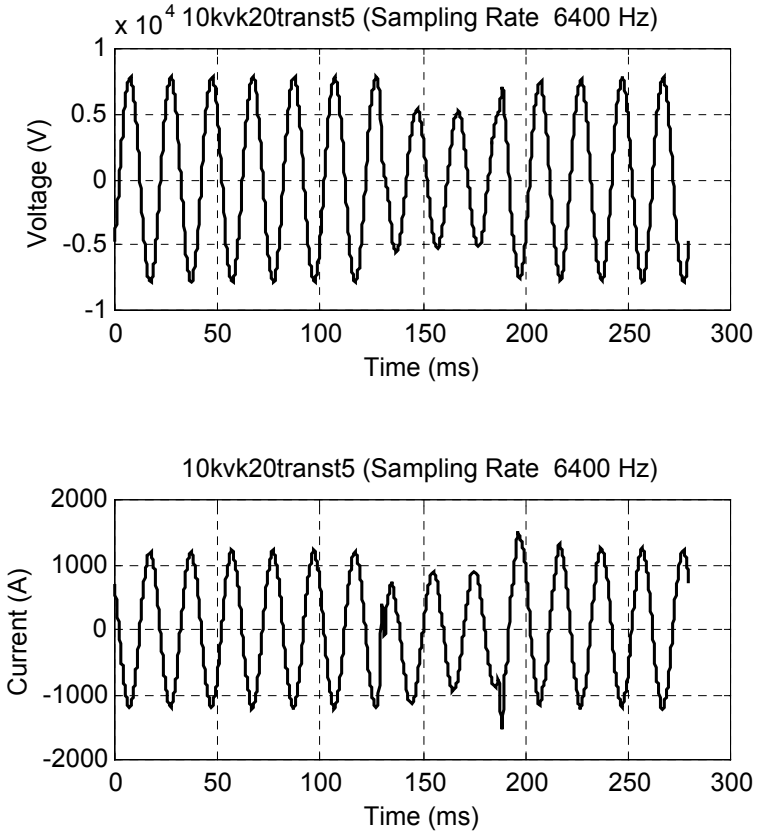

Figure 6.1.8 Voltage dip disturbance (Sweden)

In this case, three types of relay are affected, as demonstrated in Fig. 6.1.9. The impedance relay is affected the most, followed by undervoltage and overcurrent relays. Fig. 6.1.10 shows the impedance variation trace. During

the dip, the impedance trace moves towards the origin, which means the relay setting zone could be infringed. The risk of tripping for an undervoltage relay remains as long as the dip lasts. The current overshoot at the end of dip is relatively slight; thus having less impact on overcurrent relays when compared with the other two types.

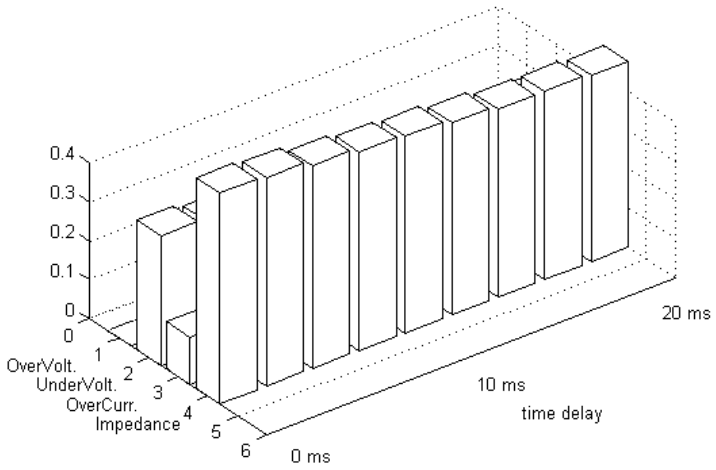

Figure 6.1.9 Impact of voltage dip on relay setting zone

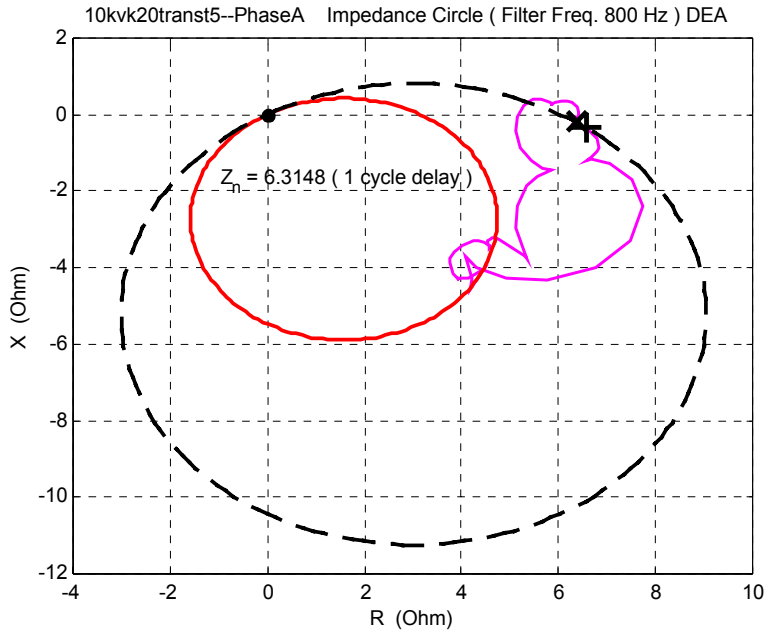

Figure 6.1.10 Impedance variation trace of voltage dip

Case 5 Voltage fluctuation

Fig. 6.1.11 shows a typical case of voltage fluctuation. Its impact on all types of relay is shown in Fig. 6.1.12. Such voltage fluctuation might affect all the relays except overcurrent relay. From the impact diagram, it is obvious that the detrimental impact is more severe at lower time delay, and negligible if the time delay is more than one half cycle. This means it only cause problem to the relays faster than 0.01s. Besides, the impact severity is not as great as in the previous cases. All these are dependent on the frequency and magnitude of voltage fluctuation.

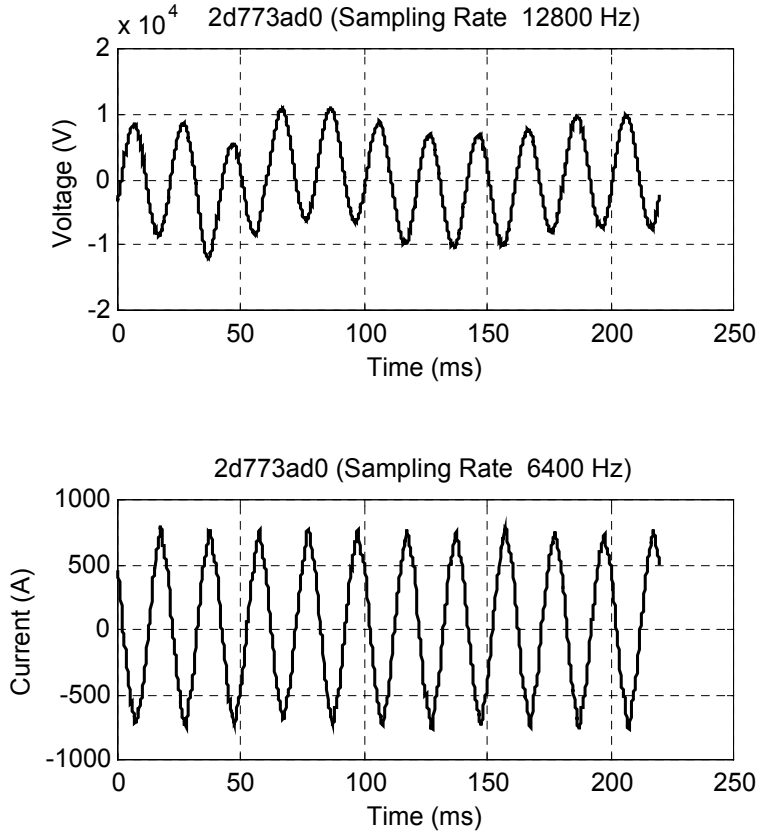

Figure 6.1.11 Voltage fluctuation disturbance (Norway)

The impedance trace is shown in Fig. 6.1.13. An interesting phenomenon is that the impedance point during voltage fluctuation rotates around the original steady state point. Although it far most reach is considerably distant

from the original point, it does not stay for long. If the time delay of impedance relay is more than 0.01s, these sporadic invading points will be ignored by the relay.

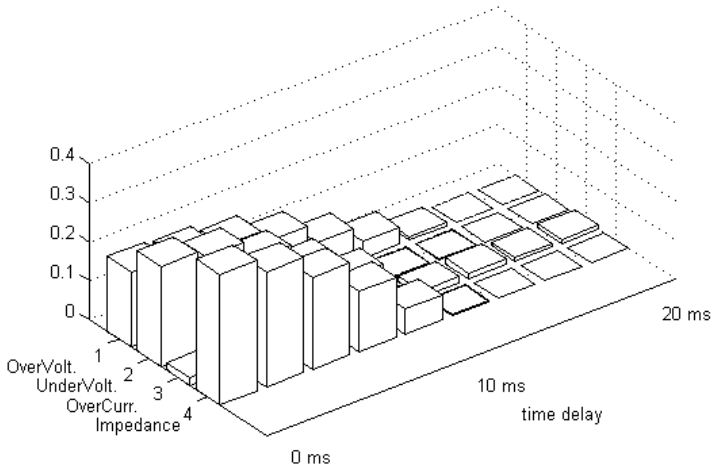

Figure 6.1.12 Impact of voltage fluctuation on relay setting zone

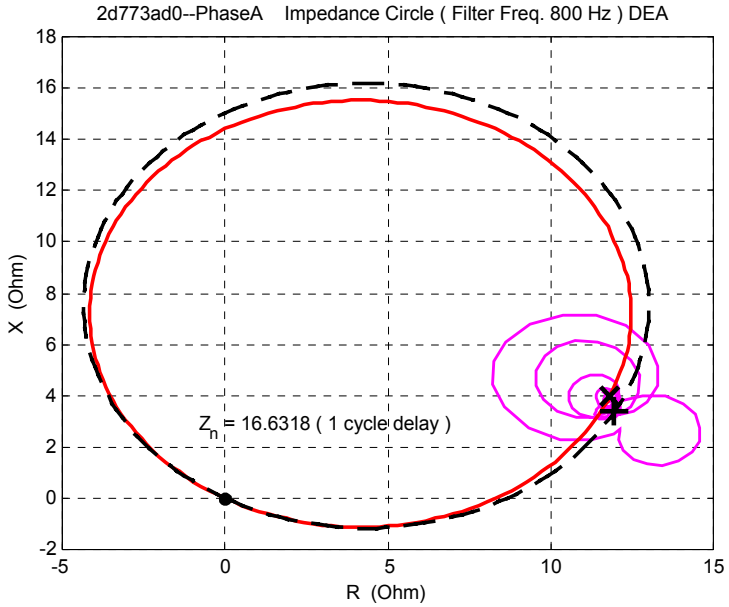

Figure 6.1.13 Impedance variation trace of voltage fluctation

6.2 Design-based Evaluation of Disturbance Impact

In this section, 9 typical disturbance cases are studied. Their impacts on relay filter are illustrated by diagrams, together with possible explanations.

Case 1 Current Transient 1

Fig. 6.2.1 shows a typical current transient recorded in LV system.

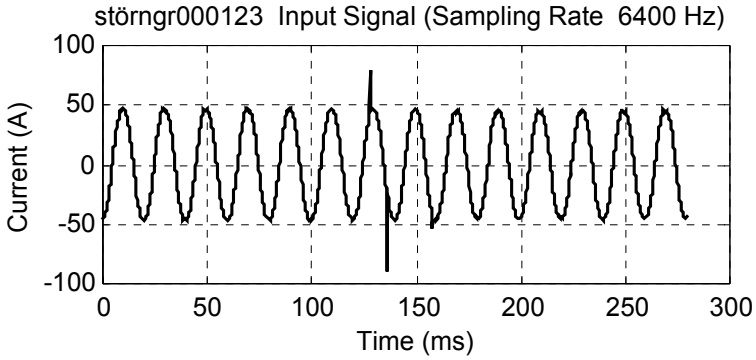

Figure 6.2.1 Current transient 1 (Sweden)

The responses to the current transient by different filters are shown in Fig. 6.2.2. The result is a rather flat plane, which implies that there is no difference on the observation of the input signal by all the filters. In other words, the spikes on the current waveform are ignored by almost all the algorithms. The RMS algorithm is most sensitive to it for delays less than 0.02 s.

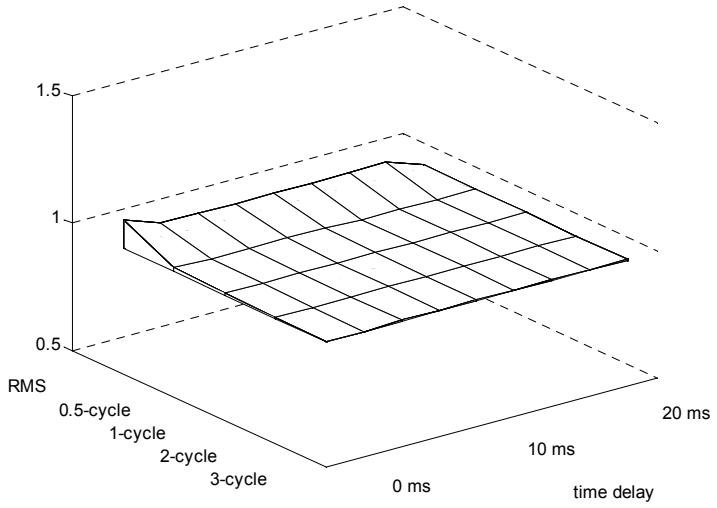

Figure 6.2.2 Impact of current transient 1 on relay performance

Case 2 Current transient 2

This is a current transient with longer duration and obvious phase shift, as shown in Fig. 6.2.3.

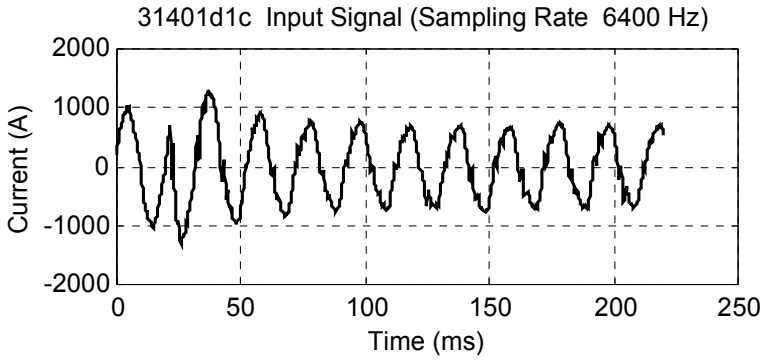

Figure 6.2.3 Current transient 2 (Norway)

Compared with the result in previous case, the impact on relay filter is significant. The responses by various relay filters are different. Such difference is largest when the relay time delay is 0s, which reflects the differences among the peak values on response curves of various filters. The values at 20 ms time delay are almost the same. This means that changing relay type does not bring forth the change of relay performance under such a transient, if the relay time delay is 20 ms.

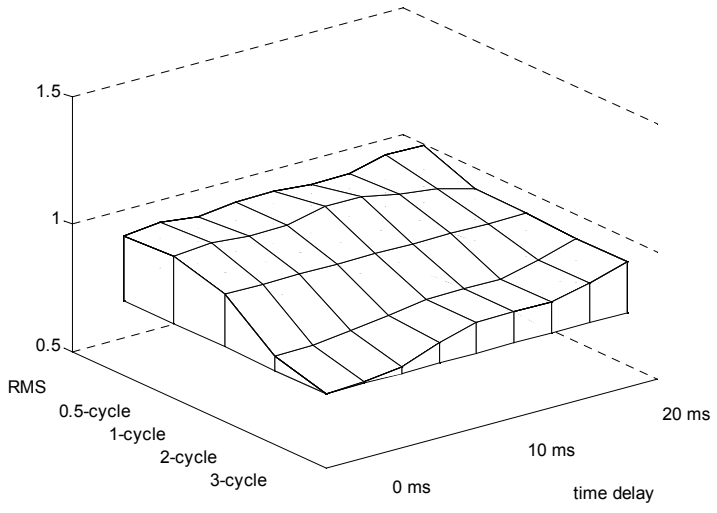

Figure 6.2.4 Impact of current transient 2 on relay performance

Case 3 Current transient 3

This case shows the inrush current for the reclosing of an overhead feeder. It contains severe harmonic distortion, with both odd and even components present.

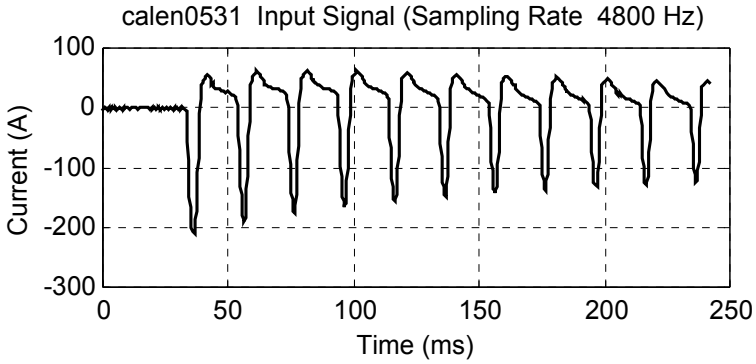

Figure 6.2.5 Current transient 3 (Scotland)

From the result in Fig. 6.2.6, it is observed that the transient has severe impact on relay performance if RMS or 0.5-cycle filter algorithm is selected. The reason is that neither RMS nor 0.5-cycle filter algorithm can remove the even harmonics. As the inrush current is rich in 2^{nd} and 4^{th} harmonics, the relay characteristic curve will be shifted considerably. The differences among the responses of the other 3 filters are much smaller as all of them are capable of rejecting the even harmonics.

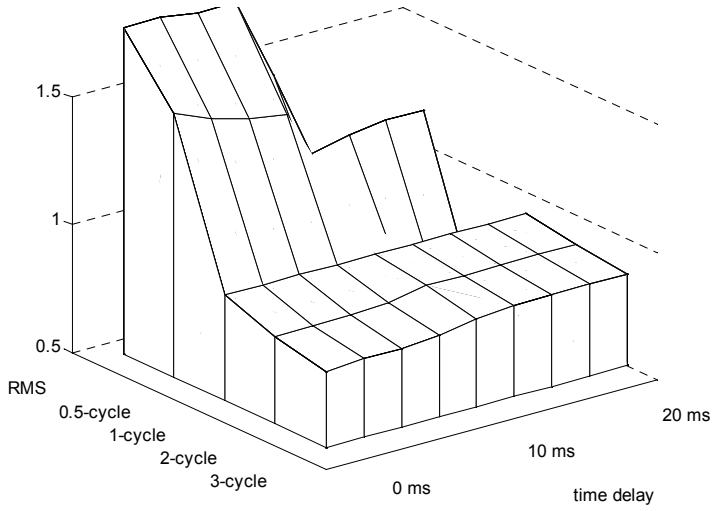

Figure 6.2.6 Impact of current transient 3 on relay performance

Case 4 Current swell

This case shows the current waveform during a voltage dip. In this case the current increases during the dip. In analogy to a "voltage swell", this event will be referred to as a "current swell".

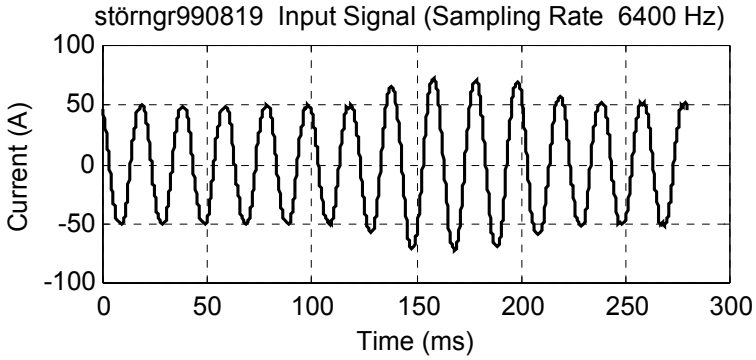

Figure 6.2.7 Current swell (Sweden)

The result in Fig. 6.2.8 indicates that the input signal causes no difference among the responses of various relay filters as well as RMS algorithm.

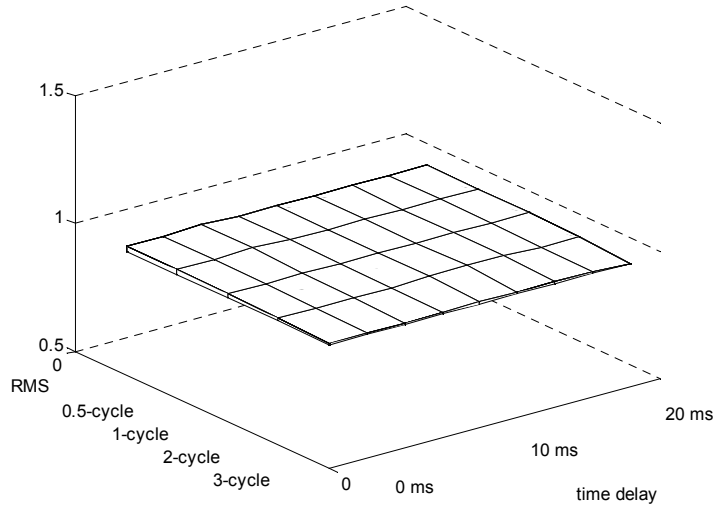

Figure 6.2.8 Impact of current swell on relay performance

Case 5 Dip with Heavy Transformer Saturation

Fig. 6.2.9 demonstrates a current waveform during voltage dip with heavy transformer saturation after the dip. It is observed that the current waveform shows obvious distortion due to this saturation. Its impact on protection is shown in Fig.6.2.10. Compared with the previous case, the impact of this disturbance is more severe.

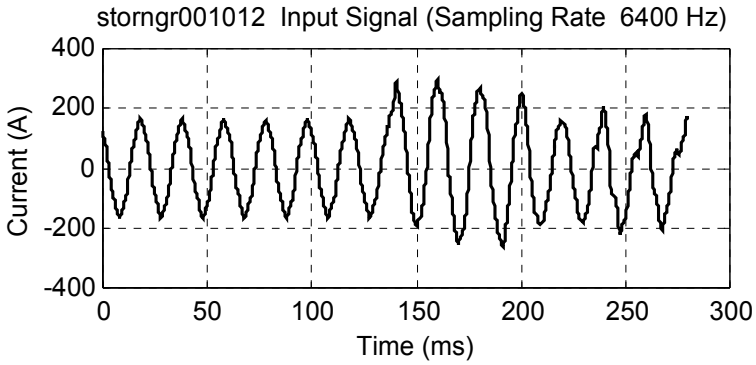

Figure 6.2.9 Transformer saturated current under voltage dip (Sweden)

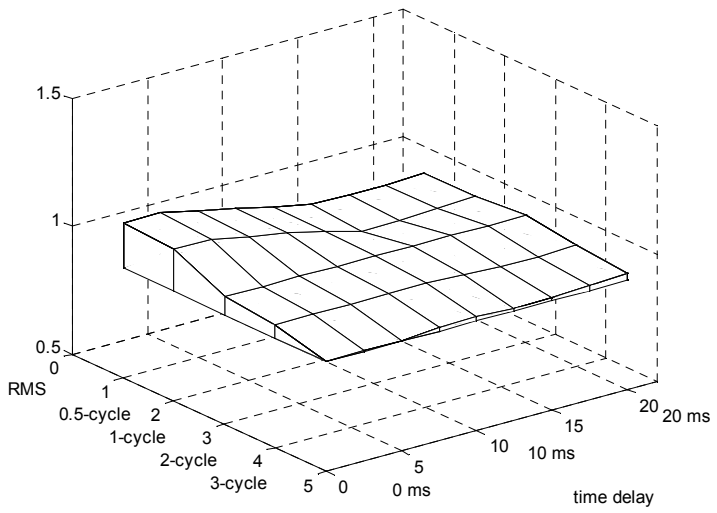

Figure 6.2.10 Impact of transformer saturation under dip on protection

Case 6 Odd Harmonics

Fig. 6.2.11 demonstrates a standard waveform of the current of many electronic devices. The current is rich in 3rd, 5th and 7th harmonics, but little even harmonics.

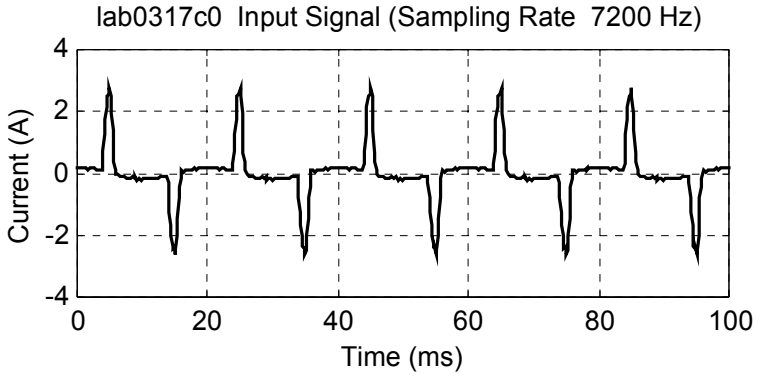

Figure 6.2.11 Odd harmonics (Sweden)

Fig. 6.2.12 shows that such an input signal has no effect on any relay filter but that significantly affects the RMS algorithm. Any relay equipped with a filter will work well. The severe impact on the RMS algorithm, however, implies that other relays such as overload or thermal relay might be affected.

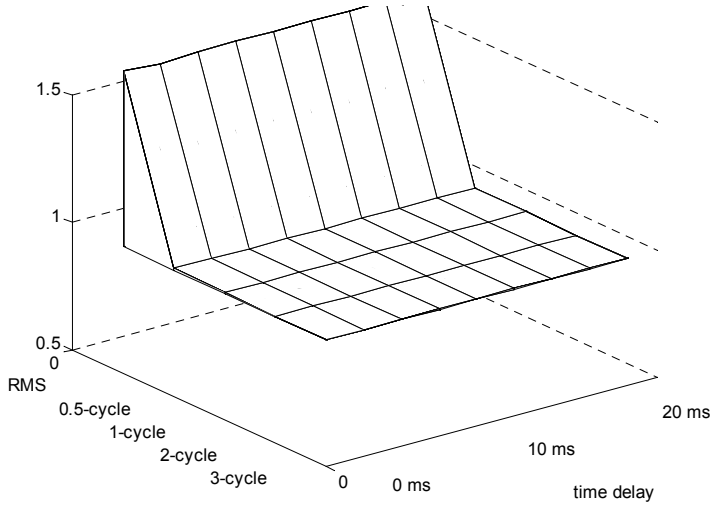

Figure 6.2.12 Impact of odd harmonics on relay performance

Case 7 High frequency harmonics and noise

Fig. 6.2.13 shows a current waveform with a large amount of high frequency harmonics and noise.

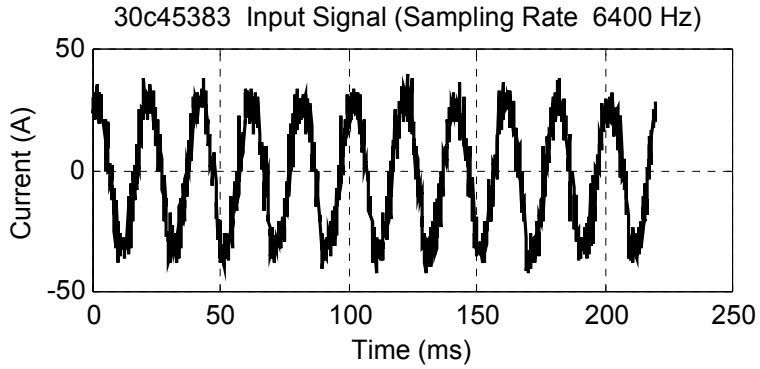

Figure 6.2.13 High frequency harmonics and noise (Norway)

The result in Fig. 6.2.14 indicates that the impact of the input signal on all the filters and RMS algorithms is limited. The impact can be ignored if the time delay is greater than 10 ms.

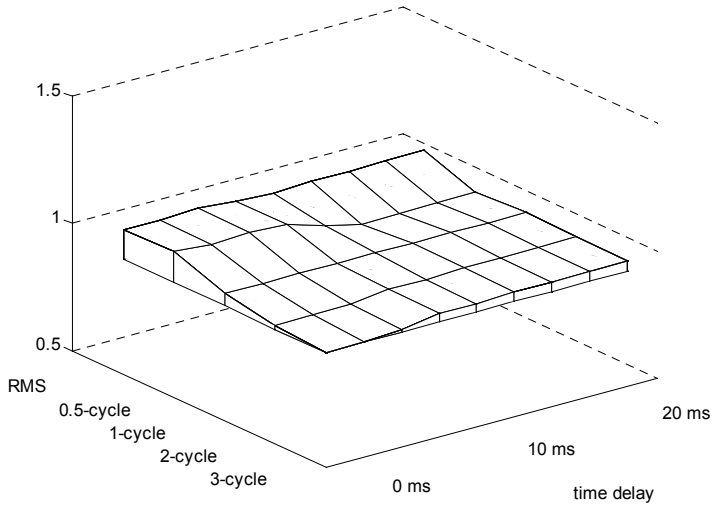

Figure 6.2.14 Impact of harmonics and noise on relay performance

Case 8 Interharmonics

An example of interharmonics is demonstrated in Fig. 6.2.15. It is a phenomenon captured in LV system. It is related to some routine signaling activities in the system.

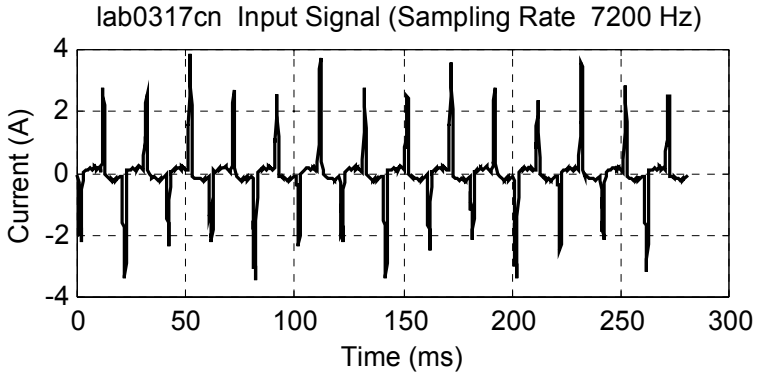

Figure 6.2.15 Interharmonics (Sweden)

The result in Fig. 6.2.16 shows severe impact on relay filter and RMS algorithms. As the signal is rich in 1/3 interharmonics, only the 3-cycle filter can reject them completely. The response by 0.5-cycle filter greatly deviates from those generated by the other filters.

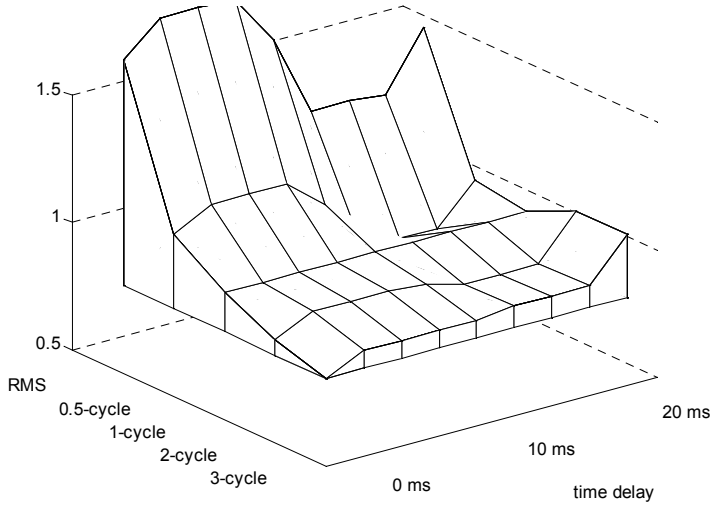

Figure 6.2.16 Impact of interharmonics on relay performance

Case 9 Current of Intermittent Load

Fig. 6.2.17 shows the waveform of an arc furnace current. Arc furnace is a typical intermittent load. Its impact on protection is shown in Fig. 6.2.18. It is observed that the results yielded by 1-cycle, 2-cycle and 3-cycle filters are similar, comparable with case 8. This also implies that the interharmonic effect in this case is less severe than in case 8.

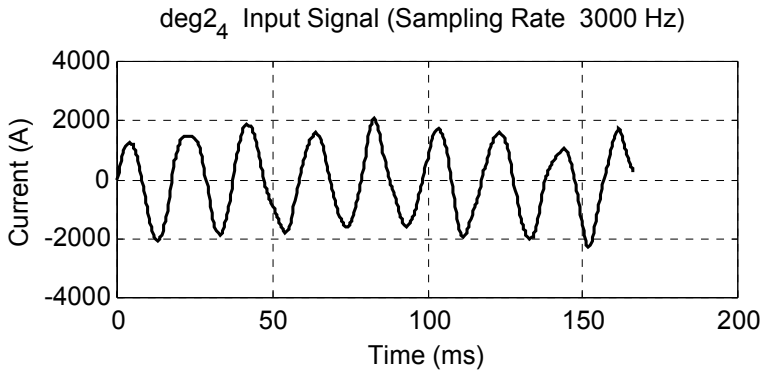

Figure 6.2.17 Current of intermittent load (Sweden)

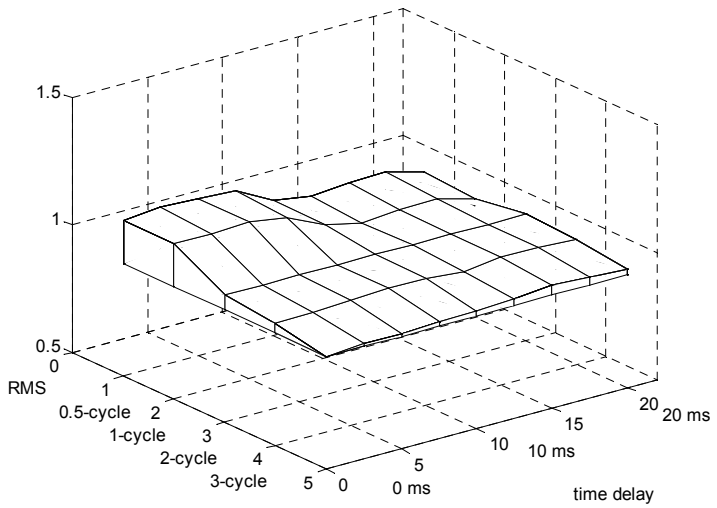

Figure 6.2.18 Impact of intermittent load current on protection

6.3 Comparison Among Cases

The case studies in section 6.1 are focused on variation of disturbances in the power system. Different variations have different impact on relay setting.

From the results it is observed that a voltage dip disturbance is likely to affect more relays with greater severity, when compared with other disturbances. Also of concern is the switching inrush disturbance. The short time transient in either voltage or current has relatively minor impact on relay setting. These conclusions are associated with the fact that dip and inrush disturbances have much longer duration than the others. In most cases, it is not the peak magnitude of the transient but its duartion that decides if the relay is affected.

With the help of impact diagrams as shown in the case studies, the disturbances' effect on relay setting can be ranked based on the disturbance factors illustrated in the impact diagrams. As one disturbance might affect more than one type of relay, further ranking of disturbances for a particular relay type can be made. For example, all the voltage dips can be ranked according to their impact on relay setting selection. Such information is very useful to relay users when determining relay settings.

In section 6.2, the studies are focused on whether the disturbances make different relay filters response differently. From the results it is observed that the most severe disturbances are even harmonics, interharmonics and long transients.

The impact of a disturbance on relay filters can be examined by checking the flatness and smoothness of the surface formed by filter responses. A plain surface means the disturbance signal yields similar relay outputs by different filters, while a surface with great curvature implies much unwanted components or transient in the signal. The disturbances can then be ranked based on the curvatures of the surfaces. Those with higher rank can be applied to test the effectiveness of any existing or new filter algorithm.

Chapter 7 Conclusions

The focus of this work is on the application of power system disturbance data for the testing of power system protection equipment. Towards such a goal, research is carried out not on particular case study, but on seeking a general procedure for processing any possible disturbance before it is applied in protection testing. In other words, the main concern in this work is how to implement such an application of disturbance data on testing .

7.1 Main Contributions in This Work

This work consists of 2 parts: classification of power disturbances and quantification of power disturbances.

7.1.1. Classification of power disturbances

The first part of this work aimed at describing the power quality at the relay terminals. A catalogue of disturbance sources is created from various publications and measurements. A wide range of disturbances is present in the system, most of which have the potential to affect at least some type of protection. Its impact on the protection is very case dependent, therefore a rather large number of potential impacts are described.

7.1.2. Quantification of power disturbances

Quantification of power disturbances, on the other hand, represents an assessment of the severity of disturbance phenomena from the viewpoint of

specific protection relays, algorithms, or protection schemes. The quantification demonstrates the possible detrimental impact of the phenomena on the operation of the protection.. The quantification can be used to rank power disturbances in a database with power quality data.

Both disturbance classification and quantification are indispensable in application of disturbance data for protection testing. They function as different stages in disturbance data processing before these data are applied in practical testing.

7.2 Summary of Conclusions in This Work

7.2.1. Classification of power disturbances

The result of the study after power disturbances at various voltage levels was a rather long list of disturbances with potential impact on protection. Due to the wide range of possible protection methods, especially when including possible future algorithms, almost all disturbances may potentially affect at least one of the methods. The aim of this part of the work was not to assess the impact on specific protection methods but rather to get an overview of what kind of disturbances are present at the relay terminals. The conclusions below should therefore be interpreted in a general sense: they do not necessarily hold for all (existing and future) protection relays, principles, and algorithms.

A first conclusion from the study is that events have a more severe impact on protection than variations. The reason is that events lead to larger changes in voltage and current as well as in many cases a high-frequency transient.

A division was made in dynamic, semi-dynamic, and static effects of disturbances on the protection. Static effects are due to steady-state fundamental component voltage and currents as well as due to waveform distortion. Static effects are of concern for existing, relatively slow, protection principles. They are easy to assess: an increase in current potentially affect an overcurrent relay; a drop in voltage an undervoltage relay; etc.

Dynamic effects are due to high-frequency transients related to switching actions and other sudden changes in the system. They rarely affect existing protection but become very important when considering novel high-speed protection algorithms.

Because transients may also be of a much longer duration (e.g. motor starting and transformer energizing transients) a third class disturbance effect was introduced: semi-dynamic effects. Semi-dynamic effects are due to long-duration transients. They potentially effect both existing protection as novel protection algorithms.

Considering the different types of disturbances, it can be concluded most system events (switching actions, faults) lead to some kind of transient close to the source: travelling waves due to line switching, overcurrents due to a fault, etc. Of more concern for protection testing are system events that lead to severe disturbances in voltage and current at locations further away from the source. The main examples of this are transformer energizing, capacitor energizing, and faults. The disturbances due to these events propagate through the system: the energizing of one transformer may lead to inrush currents for another transformer; capacitor bank energizing may cause a severe current and voltage transient for another capacitor bank; a fault may

lead to a large increase in load current and transformer inrush upon voltage recovery. This propagation of disturbances has to be considered when studying novel high-speed protection algorithms.

7.2.2. Quantification of power disturbances

The quantification of the disturbance impact on protective relays has been made in two different ways: a setting-based quantification and a design-based quantification. Both methods have been applied successfully to a number of recorded events. A simple index, the so-called disturbance factor, is introduced to quantify the possible effect of a given disturbance on a given relay, relay type, or relay algorithm. Both approaches can be used to characterize the severity of a measured or simulated disturbance from a protection viewpoint. The most severe events can then be studied in more detail, e.g. by applying them for testing an actual relay.

The setting-based quantification quantifies the potential risk that the relay tripping zone could be falsely reached due to a disturbance. This method could be applied to verify the setting of individual relays, either during installation or during operation. In the latter case, the closeness to mal-trip could be evaluated. Starting from the viewpoint of relay users, such quantification provides an observation on the possible disturbance impact on relays.

The design-based quantification quantifies the potential impact on relay output performance due to the unwanted components in the disturbance signal. This method could be applied to check the accuracy and speed of any new relay algorithm, i.e. to see if the algorithm can extract the correct fundamental component fast with minor error. Starting from the viewpoint of

relay manufacturers, such quantification provides an observation of the possible disturbance impact on the accuracy of relay algorithms.

The quantification diagrams also provide some intuitive information on the details of a disturbance. By developing criteria based on the impact diagrams, the disturbances can be classified according to their impact severity and duration, based on which databases can be set up for testing of protection relays or algorithms.

7.3 Directions for Further Research

7.3.1. Classification of power disturbances

In disturbance classification, the study can be focused on the propagation of disturbances through the system and from one voltage level to another. This is because the disturbances at a particular location in the are not only due to the local load and operations, but also the effect coming from the other part of the system. The disturbance propagating from one place to another may attenuate or be magnified, or even change appearance in its waveform. To carry out such a study a simulation model will be set up based on a realistic transmission and subtransmission network. A number of measured disturbances will be used to verify and calibrate the simulation model.

7.3.2. Quantification of power disturbances

In disturbance quantification, a disturbance database will be set up for the testing of future high-speed distance protection algorithms. The reason for choosing distance protection is that high-speed relays are much more likely

to appear at transmission voltage levels than in distribution levels. Distance relays are the main force in the protection system for transmission levels.

The methods developed in this work for quantification of the potential disturbance impact will be applied to the high-speed protection algorithms and modified where needed. The disturbance data obtained from measurements and from simulations are processed by the quantification techniques and a selection of the disturbances will be imbedded in the disturbance database. Study of some proposed algorithms for high-speed relays will be carried out to verify the effectiveness of the quantification techniques and make improvement on them.

Appendix Classification of Power System Disturbances

A.1 Events due to System Component Switching

1. Generation unit switching

a. Large unit switching on
b. Large unit switching off
c. Small unit switching on
d. Small unit switching off

— Large generation unit switching on/off

Large unit switching is carried out in HV system.

Figs A.1.1.1 and A.1.1.2 show the situation when a large generating unit is switched on to an existing system. In practice, generating unit is switched onto a system via a transformer.

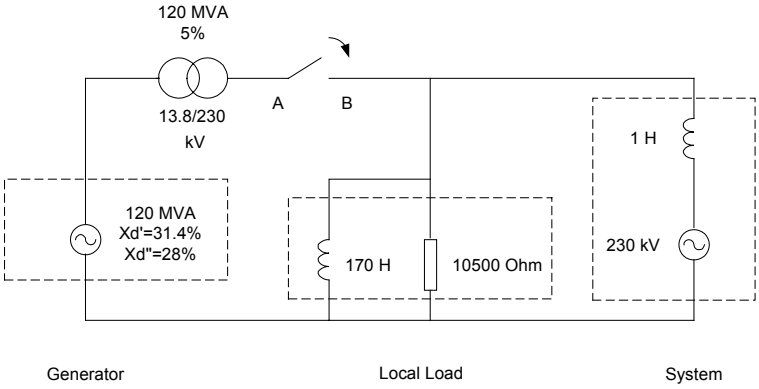

Figure A.1.1.1 Large generation unit switching

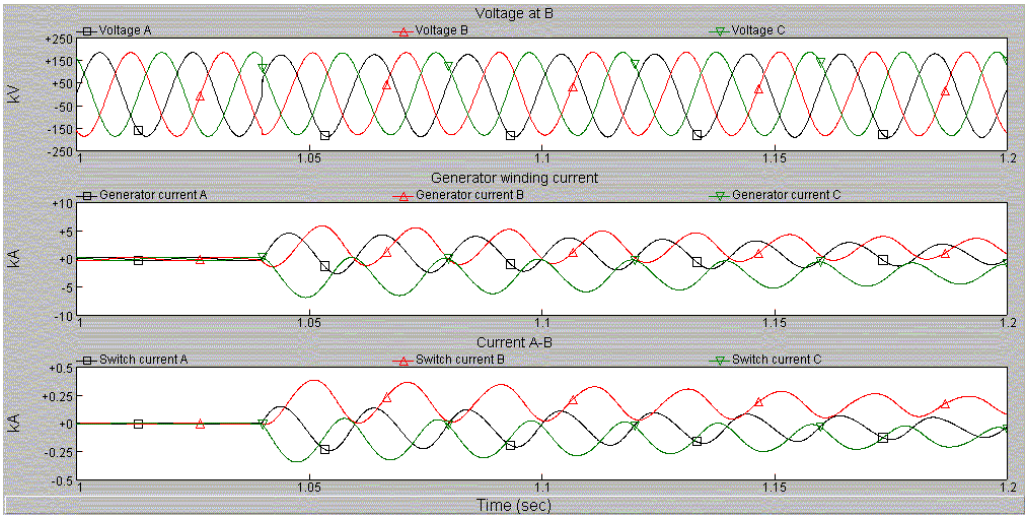

Figure A.1.1.2 Transients during large generation unit switching-on

The transients in current are mainly DC components. There is harmonic distortion due to transformer. Compared with the current, there is little transient in the voltage when the generator-transformer unit is connected to a strong system.

The magnitude of the DC component is dependent on the point on the wave of system voltage when the generator is switched on. A switching near the voltage maximum will lead to high inrush current peak.

The attenuation time constant of the DC component is calculated by the following formula:

$\tau = L / R$

where R and L are the equivalent resistance and inductance respectively.

The equivalent resistance consists of three parts: generator stator resistance, transformer copper loss and system resistance. As the system resistance is very small, so the equivalent value is mainly determined by stator resistance and transformer copper loss resistance. The equivalent inductance consists of two parts: transformer leakage reactance and

system reactance. The system reactance is also very small for a strong system. Therefore the inductance is mainly determined by the transformer leakage reactance.

Normally it takes about 20 cycles or more for generator and switch currents to reach stable status. Compared with the generator stator current, the system injection current from the generator-transformer takes longer time to become stable. This is due to the magnetic core of the transformer that generates harmonics.

Switching off a large generating unit has little effect on voltage and current waveforms in the rest of the system. Fig. A.1.1.3 shows an example of such an operation. Slight voltage steps are observed on the waveforms. Also there exist voltage transients. The transients on voltage waveforms result from phase shift due to generator switching-off.

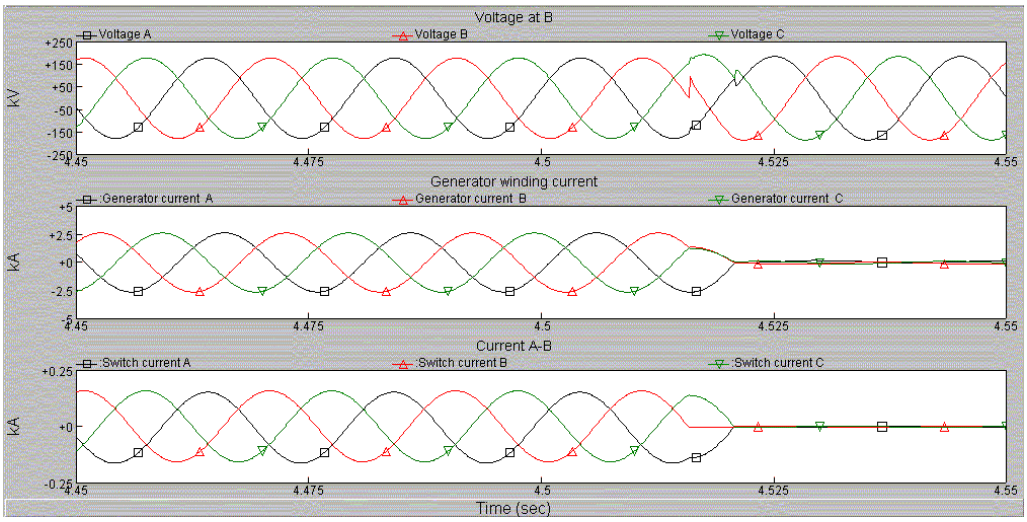

Figure A.1.1.3 Voltage and current waveforms during large generation unit switching-off

— Small generation unit switching on/off

Small unit switching is carried out in MV and LV systems.

There are two types of small generation unit switching: induction generator switching and synchronous generator switching.

An induction generator relies on its attached system for setting up its magnetic field. Normally, such a generation unit is connected to the system directly without a transformer. Figs. A.1.1.4 and A.1.1.5 show an example. Such an operation is mainly carried out in LV system.

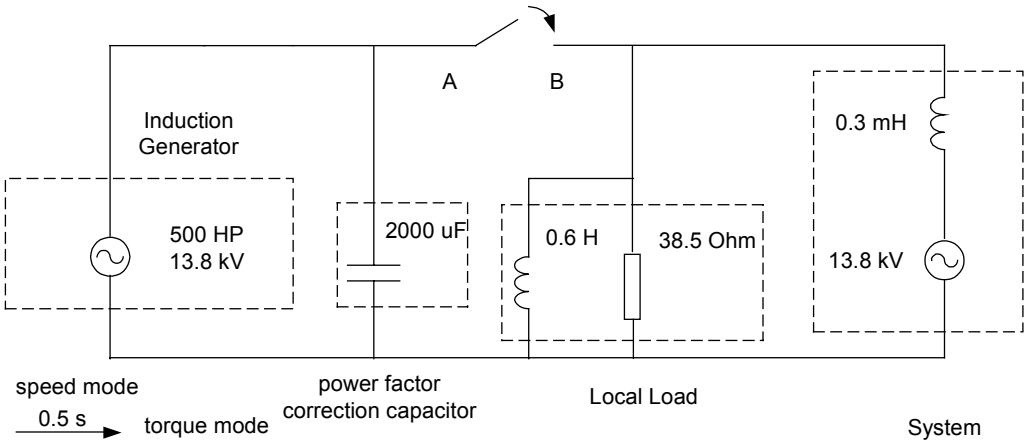

Figure A.1.1.4 Induction generation unit switching-on

From the simulation shown in Fig. A.1.1.5, it is observed that a voltage dip might occur in system voltage, and the inrush current of induction motor generator is high. The voltage dip in system voltage shows a fast drop and a gradual recovery. The in-rush current shows a high magnitude at the moment the generation unit is switched on and then attenuates exponentially. No high frequency transient is observed.

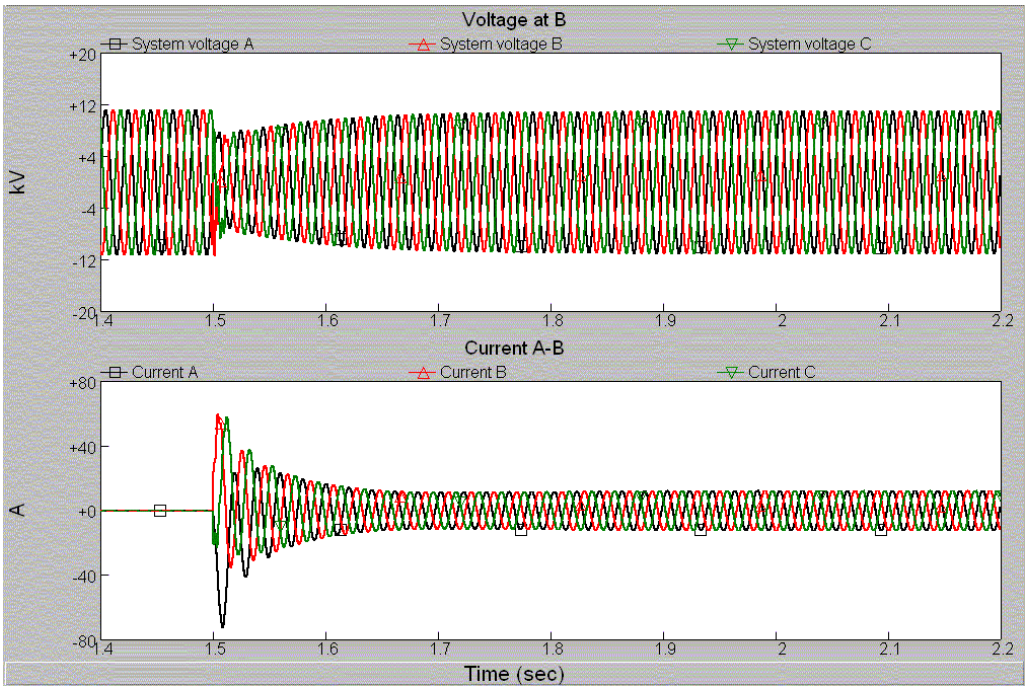

Figure A.1.1.5 Voltage and current waveforms during induction generation unit switching-on

The depth of voltage dip in this case is mainly dependent on the size of induction generator and system. System equivalent impedance plays a key role in determining the depth. The greater the system impedance, the deeper the dip.

The peak value of in-rush induction generator current is also determined by the system impedance. The greater the system impedance, the lower the peak value. The peak value can be several times higher than induction generator's output current when the induction generator is connected to a strong system.

Switching off an induction generator can lead to voltage step in the system, depending on the capacities of motor and system. Also some minor transients can be observed on voltage waveforms. This is shown in Fig. A.1.1.6.

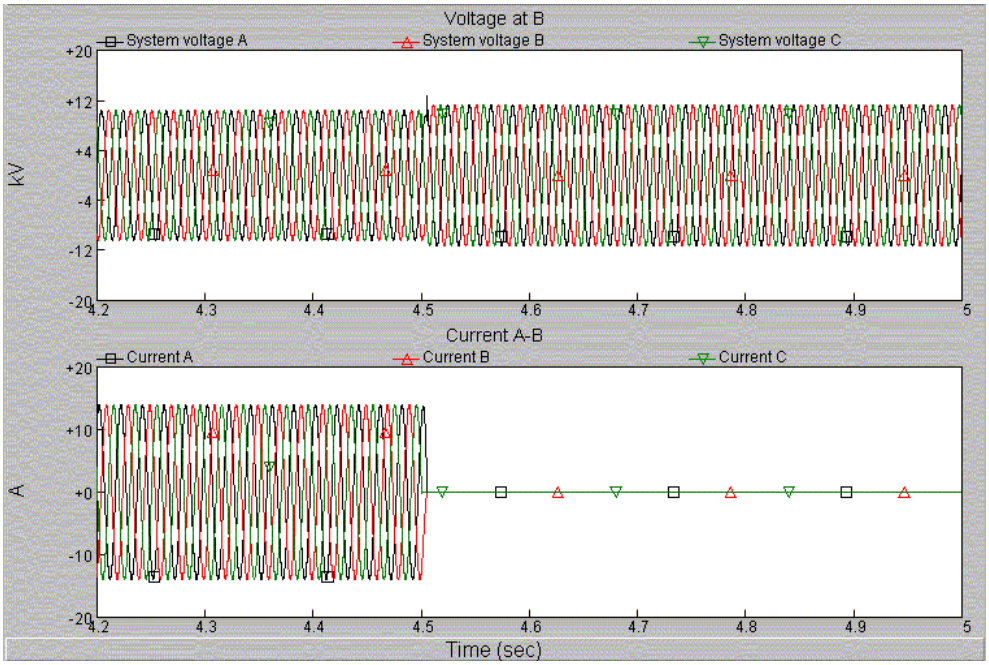

Figure A.1.1.6 Voltage and current waveforms during induction generation unit switching-off

2. Switching of unloaded line/cable

a. Energizing of unloaded line
b. Energizing of unloaded cable
c. De-energizing of unloaded line
d. De-energizing of unloaded cable

Unloaded line/cable switching is carried out in HV system.

When the circuit breaker at the sending terminal of the line/cable is switched on, an electromagnetic wave propagates along the line/cable. This wave will be reflected back at the receiving terminal of line/cable. When it reaches the sending terminal, part of it will be refracted to the source side and the remaining part will be reflected again to the receiving terminal. This process continues until a stable status is reached.

An example diagram of unloaded line switching is shown in Fig. A.1.2.1. The closing of circuit breaker CB causes the travelling waves to propagate along different routes. The reflected wave from C can be superimposed on the source wave. The travelling wave attenuates as the time passes.

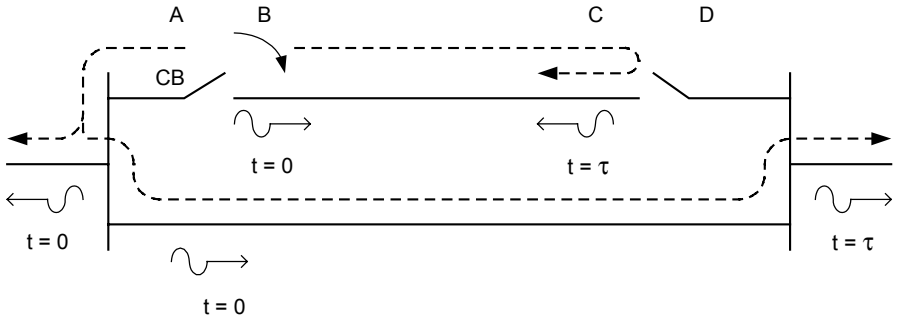

Figure A.1.2.1 Principle of unloaded line switching

The frequency with which the travelling wave goes around is:

$f = 1/(4\tau)$

where τ is the time for the travelling wave to reach the receiving end of the line.

The travelling wave can be distinguished by checking the notches on the voltage waveforms during the first several milliseconds after the circuit breaker is switched. Attenuated in amplitude with increasing time, the 'width' of the notch on the waveforms is equal to 2τ.

— line energizing/de-energizing

I. Line energizing

Depending on the parameters of the transmission line, as well as the structure of system source and loads, the effect of travelling wave on

relevant voltages and currents differs from case to case. By simulating the system diagram in Fig. A.1.2.2, the relevant voltages and currents are studied during unloaded line switching. The transmission line is 100 km long and the voltage level is 230 kV. For transient study, active and reactive loads can be represented by constant shunt resistance and inductance at load busbars.

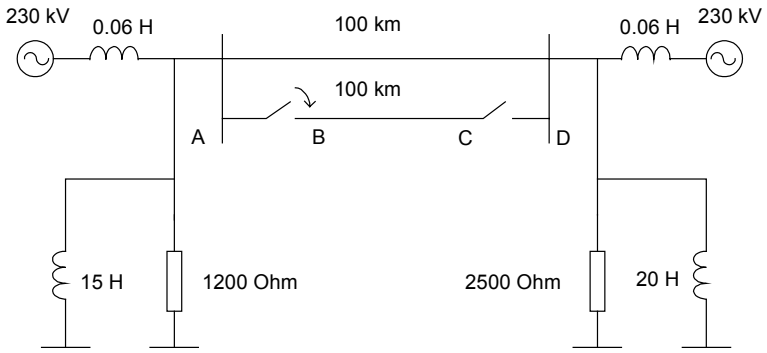

Figure A.1.2.2 System diagram of unloaded line energizing/de-energizing

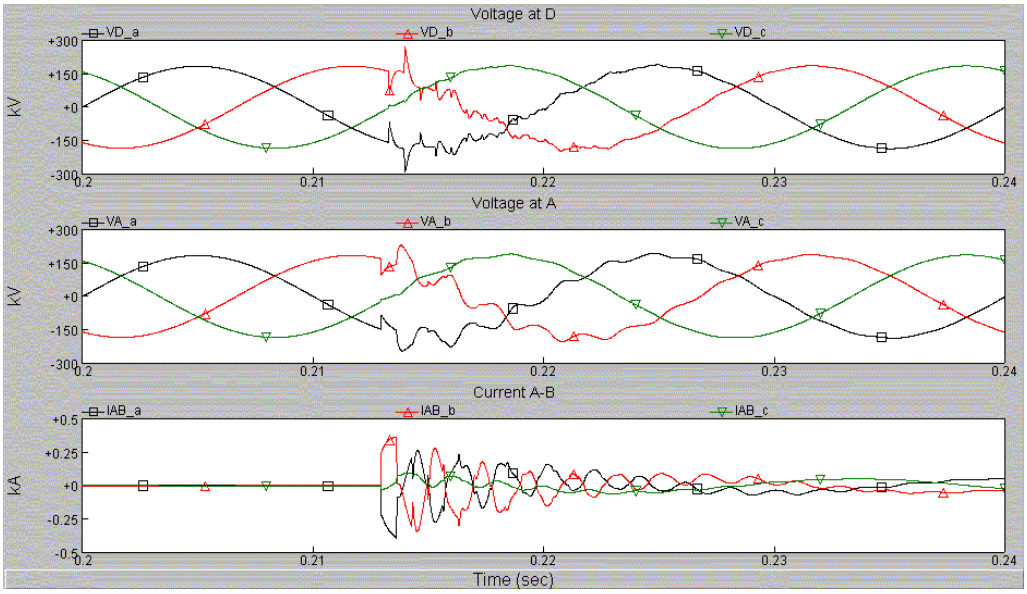

Figure A.1.2.3. Voltages and currents during unloaded line energizing

The following conclusions can be obtained:

- At the terminal of circuit breaker (sending end), the travelling wave is generated the moment when the breaker is switched on. Its period is

equal to 4τ. In this case, it is $4*100/(3*10^5)$ = 1.34 ms. Its magnitude attenuates quickly after the 1st oscillation cycle (1.34 ms).

- At the receiving end of the line, the travelling wave distortion occurs at a delay of τ. Its magnitude also attenuates quickly as in the case of sending end.
- The switching inrush current on the non-loaded transmission line can be very big. It is more than 250 A in this case. For a 230 kV system, the maximum transfer limit is about 440 A.

The peak value of switching inrush current can be calculated by the following formula:

$$I_{max} = \frac{V_{l-l} * \sqrt{2}}{\sqrt{3} * Z_{wave}}$$

where Z_{wave} is the wave impedance of the line to be switched. It is calculated by the following formula:

$$Z_{wave} = \sqrt{\frac{L}{C}}$$

Typical values of the wave impedance of transmission lines are between 200 Ω and 400 Ω. Thus typical values of inrush current can be between 470 A and 939 A for a 230 kV system, and between 1562 A and 3123 A for a 765 kV system.

II. Line de-energizing

De-energizing of transmission line in this case is also simulated. From the simulation results it is observed that the de-energizing operation of an unloaded line has little effect on the relevant voltages.

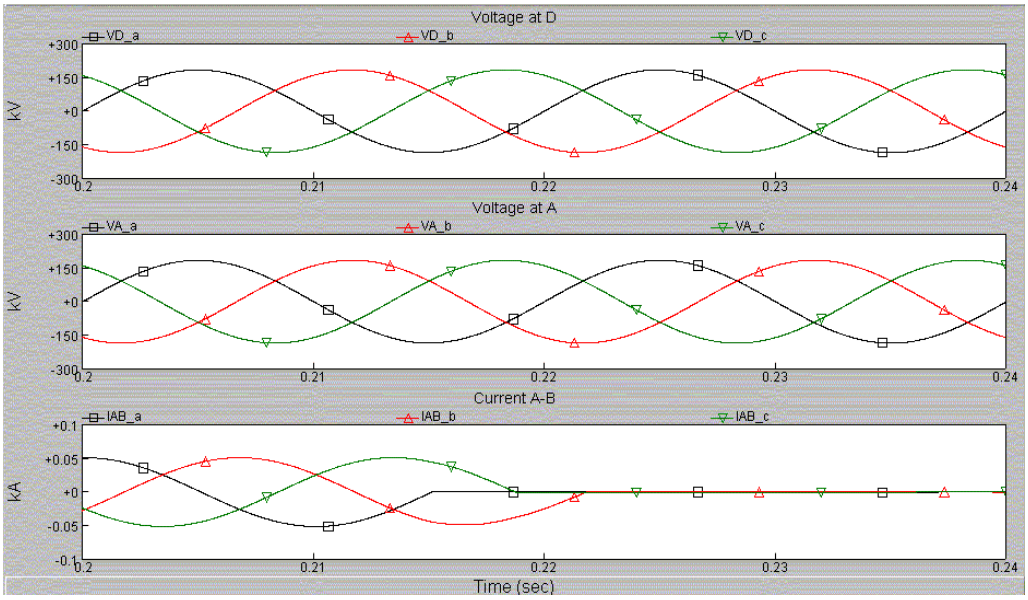

Figure A.1.2.4 Voltages and currents during unloaded line de-energizing

— cable energizing/de-energizing

I. Cable energizing

Unloaded cable switching can be simulated in a similar way as unloaded line switching. Because long cables cause excessive voltage drops and losses, the transmission cable length is normally shorter than overhead transmission line. The system simulated is the same as Fig. A.1.2.2 except that both the loaded and the unloaded cable are 1 km long, at 230 kV. Fig. A.1.2.5 show the voltage and current waveform during unloaded cable energizing.

It is observed that traveling waves with higher oscillation frequency are generated on both the sending terminal and receiving terminal. This is because the cable length is shorter than the line length. So the time for travelling wave to reach another end is shorter, which makes the oscillation frequency higher. Meanwhile the oscillation of traveling wave lasts for

longer time compared with that for long overhead lines. This is because the travelling wave continues losing its energy while propagating. A shorter transportation distance allows the wave to be quickly reflected back and superimpose on the waveform at the original sending point, before its energy is greatly lost. Since cables have lower wave impedance than lines, this results in a high inrush current. As the typical wave impedances for cables are between 100 and 200 Ω, the typical inrush currents are 40-80 A at 10 kV, 270-540 A at 66 kV and 940-1800 A at 230 kV.

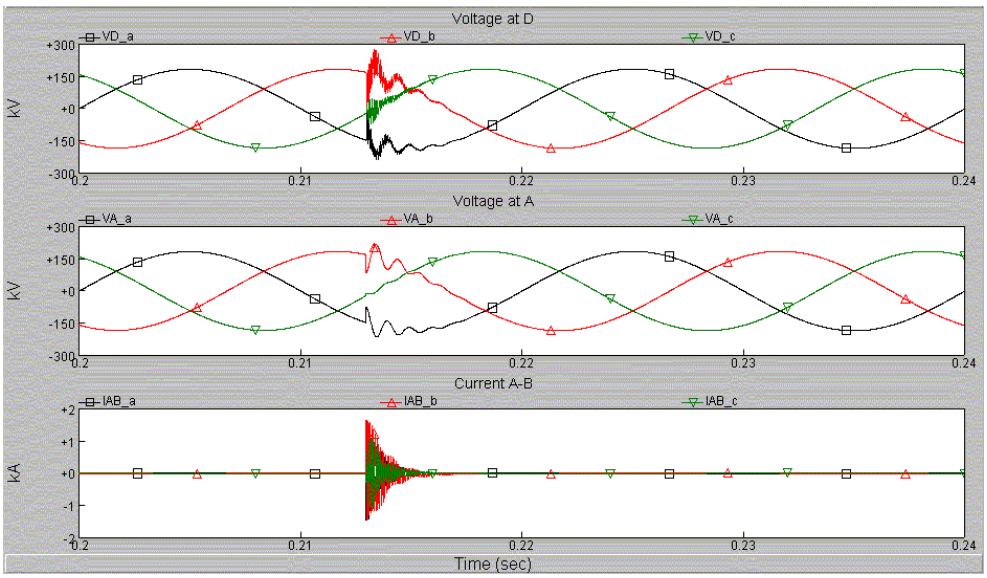

Figure A.1.2.5 Voltages and currents during unloaded cable energizing

Also present in the voltage waveforms is a low-frequency oscillation, which is due to the interaction between system inductance and cable capacitance. The actual waveform is the combination of both high-frequency and low-frequency oscillations.

II. Cable de-energizing

The simulation of cable de-energizing also shows that it does not cause any transients. The only variation is on unloaded cable current. As long as the cable is connected to the power supply, there exists small capacitive

current at a scale of less than 100 A (HV system). When the cable is de-energized, this current disappears.

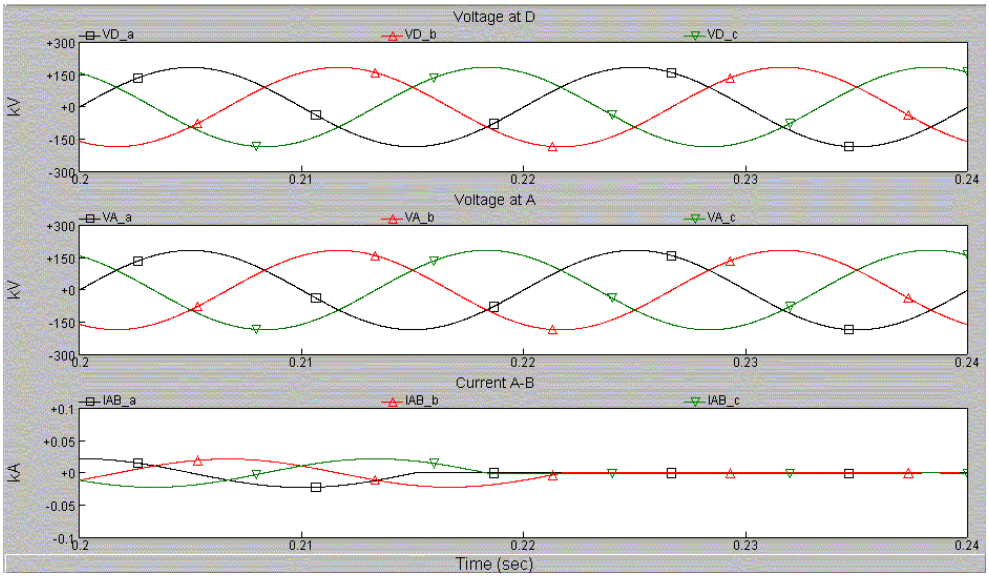

Figure A.1.2.6 Voltage and current during unloaded cable de-energizing

3. Switching of loaded line/cable

a. Energizing of loaded line

b. Energizing of loaded cable

c. De-energizing of loaded line

d. De-energizing of loaded cable

Loaded line/cable switching here refers to manual reclosure after a long interruption. It is carried out in MV and LV radical overhead /underground distribution system. Load here refers to static loads. Dynamic loads, such as transformers and induction motors, are discussed later.

Similar to unloaded line/cable switching, loaded line/cable switching also causes voltage and current transients. However, as the distribution lines/cables are shorter than transmission lines/cables, the generated

transient frequencies will be higher. The amplitudes of transients will also be greater due to the presence of the load to be switched onto the system.

The transients generated during loaded line/cable switching consist of 2 parts: 1. travelling wave; 2. transients due to change of status. When the line/cable is short, the oscillation frequency of travelling wave will be high enough to fall within the frequency range of the transients caused by change of status. Therefore, it is difficult to distinguish the travelling wave from the other transients.

The amplitudes and oscillation frequencies of transients due to loaded line/cable switching are mainly dependent on three factors:

- ratio of source impedance versus load impedance
- transient characteristics of load transformer
- characteristics of load

— line energizing/de-energizing

Fig. A.1.3.1 shows the transient waveforms during loaded line energization. The operation is carried out on a 500m long distribution line at 66kV.

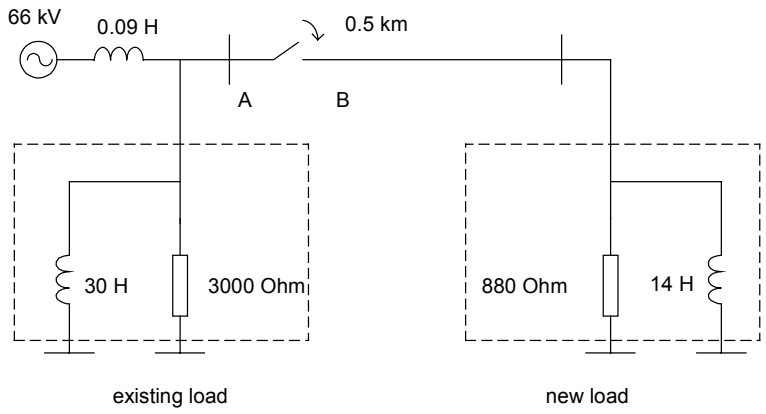

Figure A.1.3.1 System diagram of loaded line energizing/de-energizing

Compared with unloaded line energization, the transients on the waveforms are much less and last for shorter time. No oscillation can be observed as in the case of unloaded line energization. This is because the travelling wave generated by breaker switching is completely absorbed by the attached load and thus won't be reflected back. Also the transient is damped by the resistive part of the attached load.

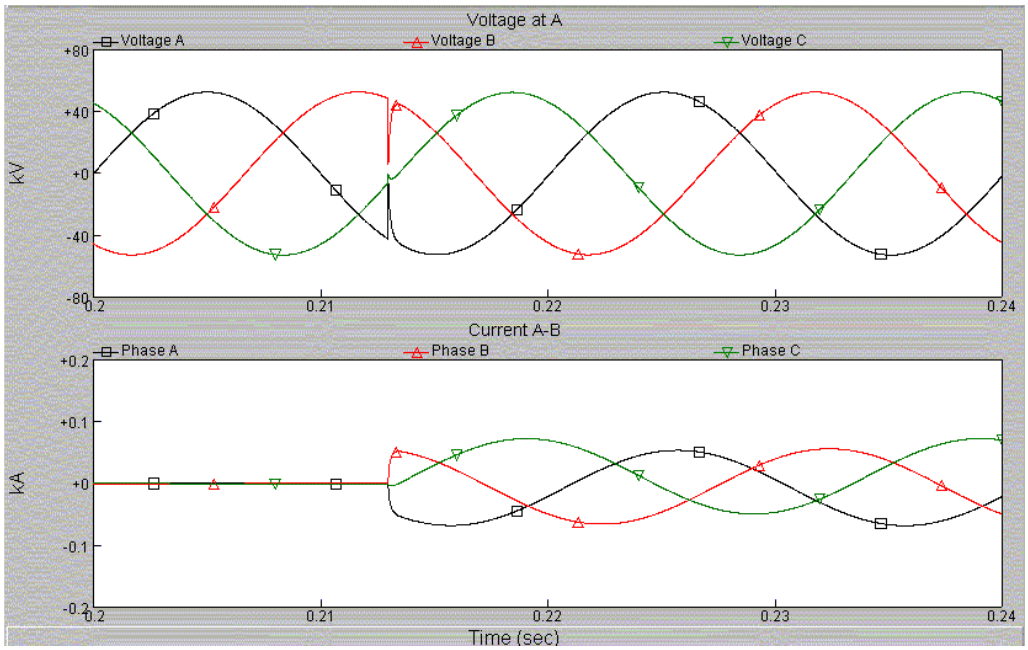

Figure A.1.3.2 Transients during loaded line energizing

The sharp drop on voltage waveform in Fig. A.1.3.2 can be explained by the transients on the line during loaded line energizing, with the help of the diagram in Fig. A.1.3.3.

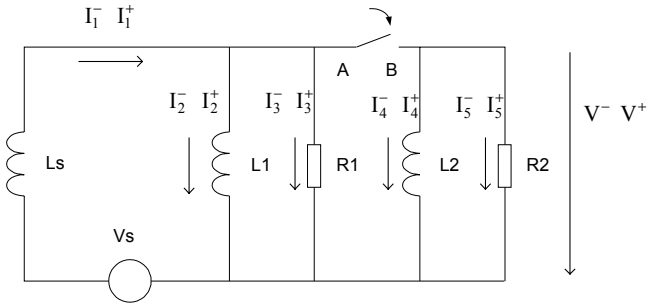

Vs System Source Voltage Ls Source Inductance

L_L Load Inductance R_L Load Resistance

I^- V^- Current or Voltage Just Before Switching

I^+ V^+ Current or Voltage Just After Switching

Figure A.1.3.3 Equivalent circuit of loaded line energizing

From the diagram, the following equations can be obtained for pre-switching status:

$$\begin{cases} I_1^- = I_2^- + I_3^- \\ I_4^- = I_5^- = 0 \\ V^- = R_1 I_3^- \end{cases}$$

while the following equations hold for post-switching status:

$$\begin{cases} I_1^+ = I_2^+ + I_3^+ + I_4^+ + I_5^+ \\ I_1^+ = I_1^- \qquad I_2^+ = I_2^- \\ I_4^+ = I_4^- = 0 \\ V^+ = R_1 I_3^+ = R_2 I_5^+ \end{cases}$$

Based on these equations, the voltage variation can be calculated as:

$$\Delta V = V^+ - V^- = -\frac{R_1}{R_1 + R_2} V^-$$

This explains why the voltage at t=0 is close to zero, as R_1 in this case is much greater than R_2, so that $V^+ \approx 0$.

Switching off the loaded line causes no obvious transients on either voltage or current. However, if the transmission line is directly connected to an upstream transformer, the transformer internal circuit will have effect on voltage waveforms, causing distortion in the 1st cycle. Fig. A.1.3.4 shows such an example.

From Fig. A.1.3.4 it is observed that overvoltage and distortion are generated when the loaded line is switched off. This is due to the energy discharge from both the transformer leakage inductance and the load inductance. The size of the load also affects the magnitude of the overvoltage. The heavier the load, the lower the magnitude. From the diagram it is also obvious that all the voltage waveforms have

discontinuous points at the moments when any phase current becomes zero. This is because the measurement point is connected to the delta side of the transformer. Any change in one phase will affect the status of the others.

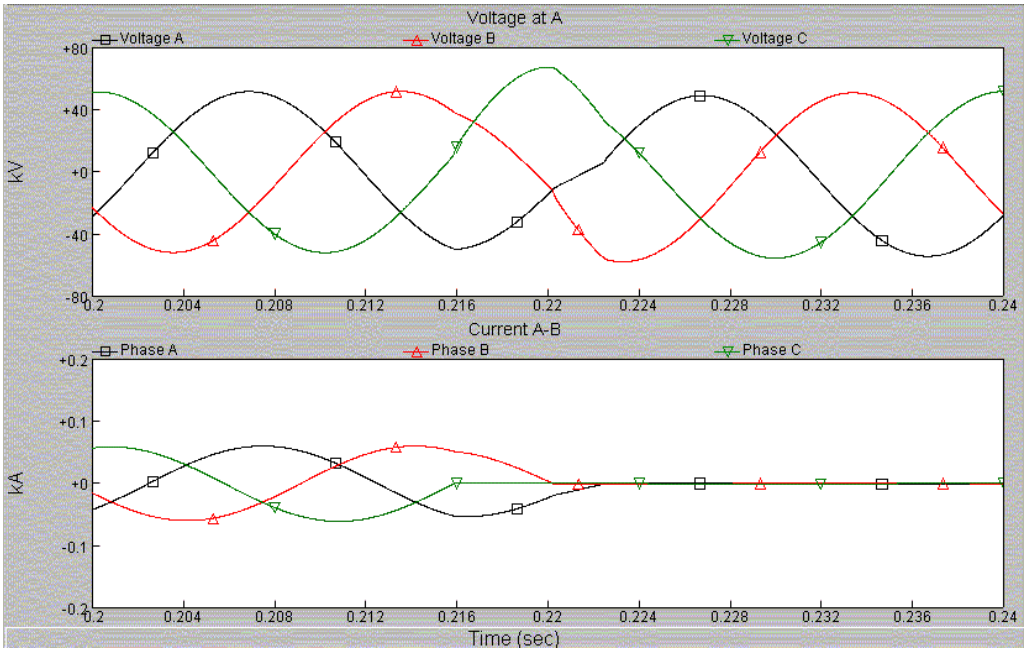

Figure A.1.3.4 Transients during loaded line de-energizing

— loaded cable energizing/de-energizing

Loaded cable energization will yield similar transients both in voltage and current as loaded line energization does. However, the oscillation frequencies of the transients are lower than in case of line energization, when a cable of the same length is applied and the other conditions remain unchanged. Also the overshoot at the beginning of transient is higher compared with the case of loaded line energization.

This is illustrated by comparing the results in Figs. A.1.3.2 and A.1.3.5. In Fig. A.1.3.5, the gap of transient is greater than in Fig. A.1.3.2, which implies higher oscillation frequency and magnitude. The explanation of

such phenomenon lies in the fact that the capacitance per unit length of underground cable is greater than for overhead lines.

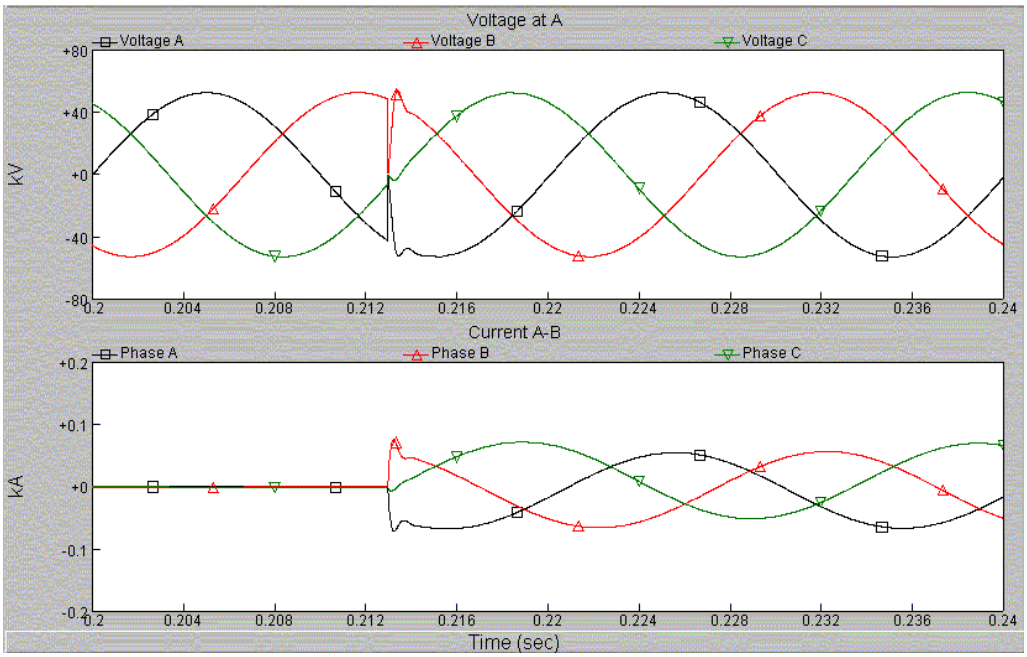

Figure A.1.3.5 Transients during loaded cable energizing

Loaded cable de-energization is similar to loaded line de-energization. Similarly as for loaded line energization, more severe voltage distortion compared with loaded line de-energization can be observed, as shown in Fig. A.1.3.6.

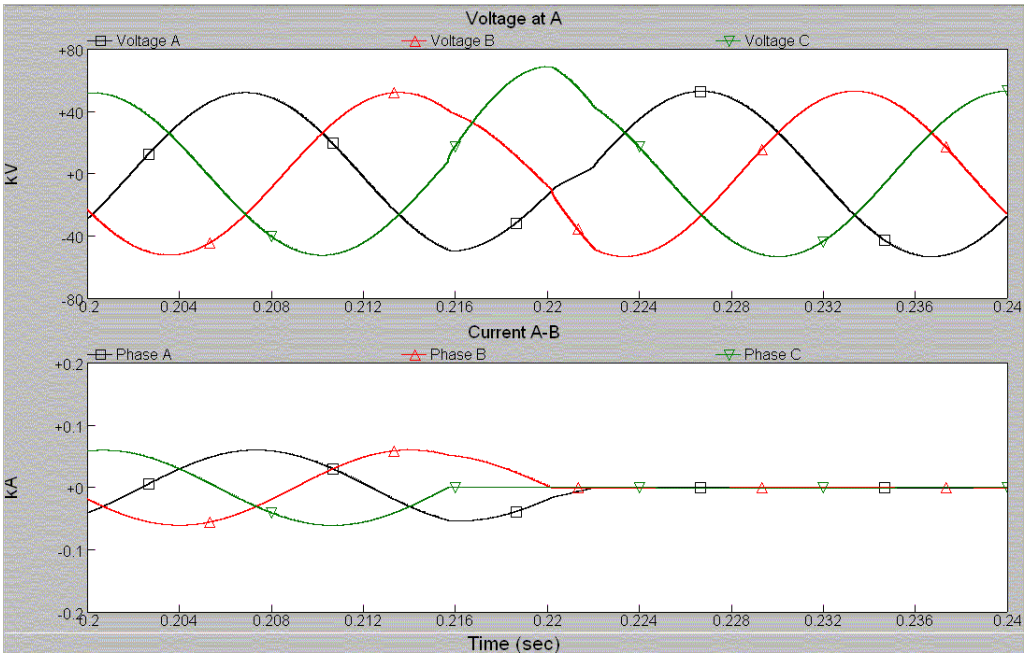

Figure A.1.3.6 Transients during loaded cable de-energizing

4. Transformer energizing

a. Transformer energizing, unloaded
b. Transformer energizing, loaded
c. Transformer de-energizing, loaded
d. Transformer de-energizing, unloaded

This can happen at any voltage level system.

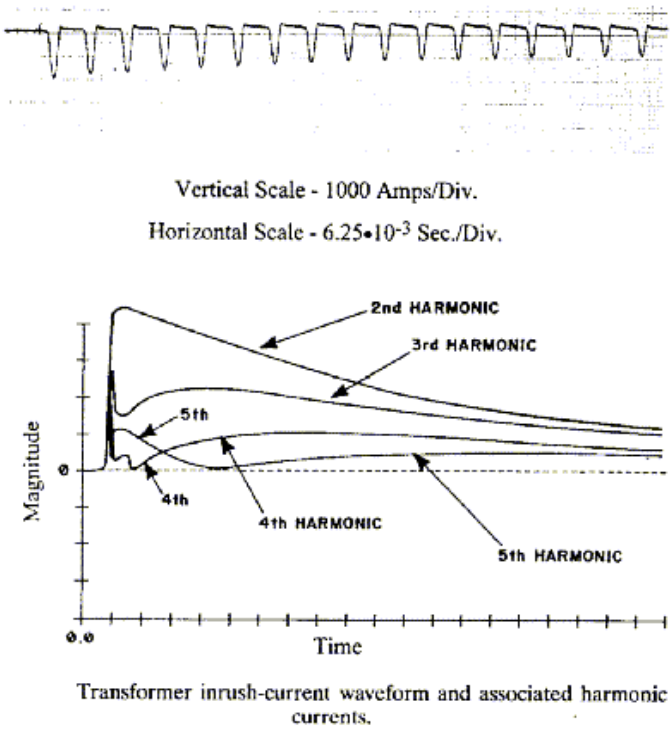

Figure A.1.4.1 Transformer inrush-current waveform and harmonic components[21]

When a transformer is energized, there is a transient inrush of current that is required to establish the magnetic field of the transformer. For the worst-case energization the flux in the core may reach a maximum of twice the normal flux. For flux values much greater than normal, the core will be driven deep into saturation, causing very high-magnitude energization inrush current to flow. The magnitude of this current is

dependent on such factors as supply voltage magnitude at the time of energizing, source impedance, and residual flux in the core, transformer size, and design. This initial energization inrush current could reach values as high as 25 times full-load current and will decay with time until a normal exciting current value is reached. The decay of the inrush current may vary from as short as 20 cycles to as long as minutes for highly inductive circuits [21]. The inrush current contains all orders of harmonics, both odd and even orders.

— transformer energizing/de-energizing, unloaded

Fig. A.1.4.2 shows the diagram for unloaded transformer energizing.

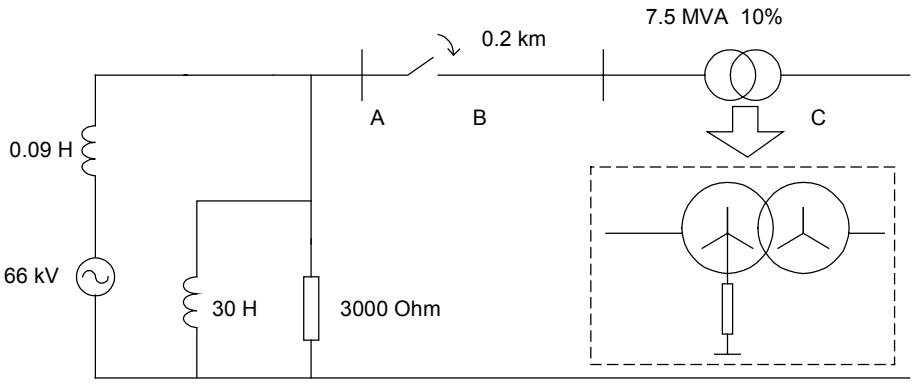

Figure A.1.4.2 System diagram of unloaded transformer energizing/de-energizing

The voltage and current waveforms during unloaded transformer energizing are shown in Fig. A.1.4.3.

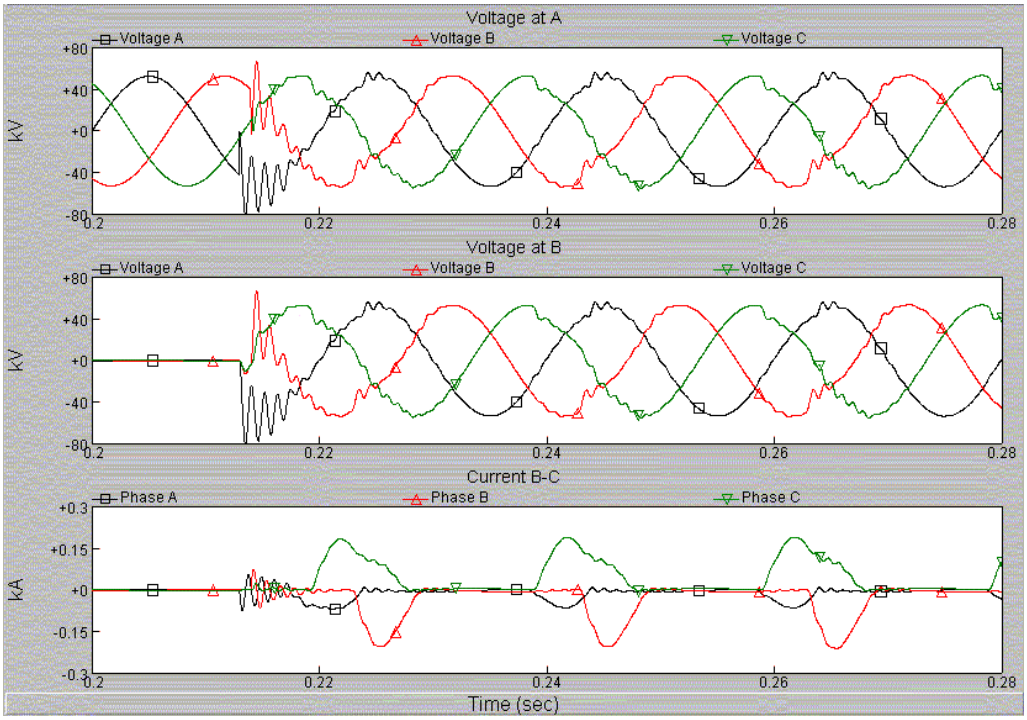

Figure A.1.4.3 Voltage and current waveforms during unloaded transformer energizing

The model used for the transformer is illustrated in Fig. A.1.4.4

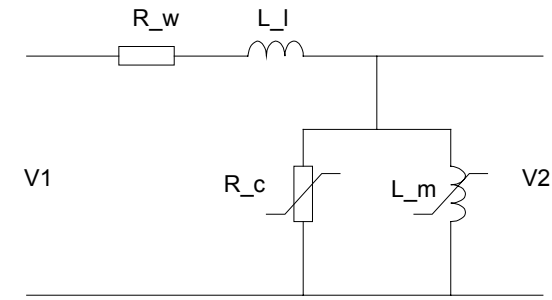

R_w winding resistance L_l winding leakage inductance

R_c core resistance (non-linear) L_m magnetizing inductance(non-linear)

Figure A.1.4.4 Transformer model

In the model, winding resistance and leakage inductance are much smaller than core resistance and magnetizing inductance. The core resistance is a function of voltage and frequency. It represents the eddy current losses and hysteresis losses in the core. The non-linear

characteristics of magnetizing inductance and core resistance makes the excitation current increase steeply when the voltage reaches a knee point.

Taking into consideration the transformer location in the system, the magnitude and oscillation frequency of the high-frequency transients in voltage and current are hardly affected by transformer parameters. They are mainly dependent on system structure and cable/line between transformer and system.

The magnitude of voltage step, in-rush current and harmonic distortion in voltages and currents are closely related to core resistance and magnetizing inductance.

If the transformer energizing occurs after a voltage sag or short interruption, the residual flux will be rather large, which may even worsen the core saturation. Saturation of the transformer core mainly takes place when it is unloaded or lightly loaded. The reason is that the existence of the load affects the time constant of inrush current so that the inrush decays quickly. When there is heavy load, the energy can be absorbed by the load.

When the unloaded transformer is de-energized, ferroresonance might happen, which is usually caused by the core of a transformer going into saturation, with a dramatic change in its effective inductance. This results in resonance in system frequency, or one of its harmonics. This normally happens when single phase breaking operation is carried out in a three-phase system, or when the three phases of a switch or breaker show a large spread in opening time. In this case, an extremely high voltage will appear on the transformer. In case the transformer supplies power to one

of the two parallel lines, and the other parallel line is still energized after transformer de-energization, this can become a sustained phenomenon. Because the resonance frequency is 50 Hz, the resonance is maintained by energy from the source.

Fig. A.1.4.5 shows a simulation example of ferroresonance at 66 kV, in the same system as shown in Fig. A.1.4.2. The circuit breakers on three phases are disconnected at 0.213s, 0.214s and 0.2142s respectively.

The ferroresonance is actually the result of resonance between the equivalent capacitance and the saturated transformer inductance. The equivalent capacitance is mainly dependent on the distributed shunt capacitance of overhead line or underground cable.

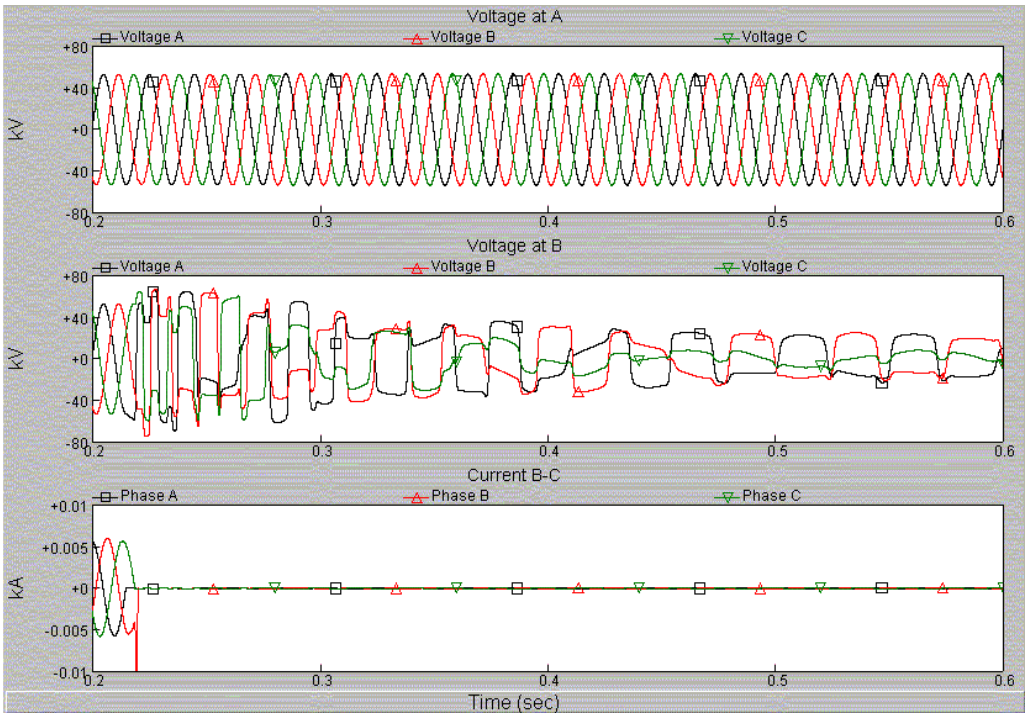

Figure A.1.4.5 Ferroresonance during unloaded transformer de-energizing

— loaded transformer energizing/de-energizing

Loaded transformer energizing can generate similar transients in voltage and current as unloaded transformer energizing. However, as it is a loaded operation, it has the following differences compared with the case of unloaded energizing:

- Lower oscillation frequency. This is because the attached load, which is resistance dominant, can combine with the shunt air core and magnetizing branches to make the equivalent inductance smaller. This leads to a lower oscillation frequency
- Shorter attenuation period. This is due to the existence of resistance at load side, which effectively damps the oscillation.
- Reduced harmonic distortion in voltage and current. The harmonic source of transformer is at the magnetizing branch, which can be represented as a harmonic current source in harmonic load flow study. Adding load resistance reduces the voltage imposed on the magnetizing branch, which in fact lowers the magnitude of the harmonic current source in the load flow study. The existence of load resistance, together with the increased transformer loss reactance under higher frequency, redistributes the harmonic currents in all the branches, making the harmonic current flowing through the system impedance decreased. So the harmonic voltage and current distortion at system side is reduced.

Fig. A.1.4.6 shows the disturbances on voltage and current during loaded transformer de-energizing. The above mentioned features can be observed when comparing the diagram with that in Fig. A.1.4.3.

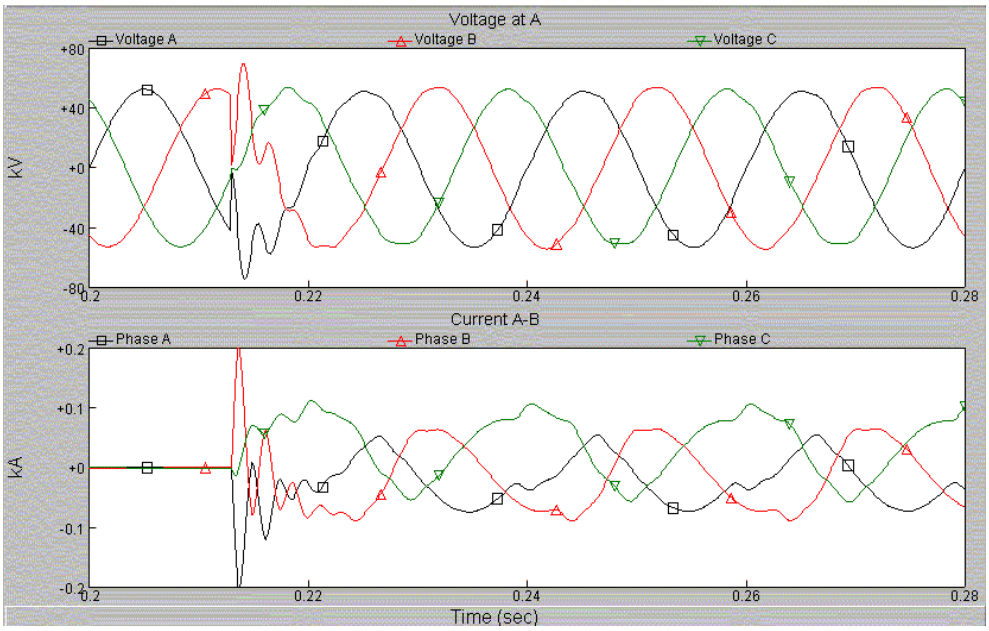

Figure A.1.4.6 Voltage and current waveforms during loaded transformer energizing

Unlike unloaded transformer de-energizing, loaded transformer de-energizing causes no ferroresonance. The attached load resistance functions as damping factor to extinguish the ferroresonance. Only some normal transients can be observed. This is illustrated in Fig. A.1.4.7.

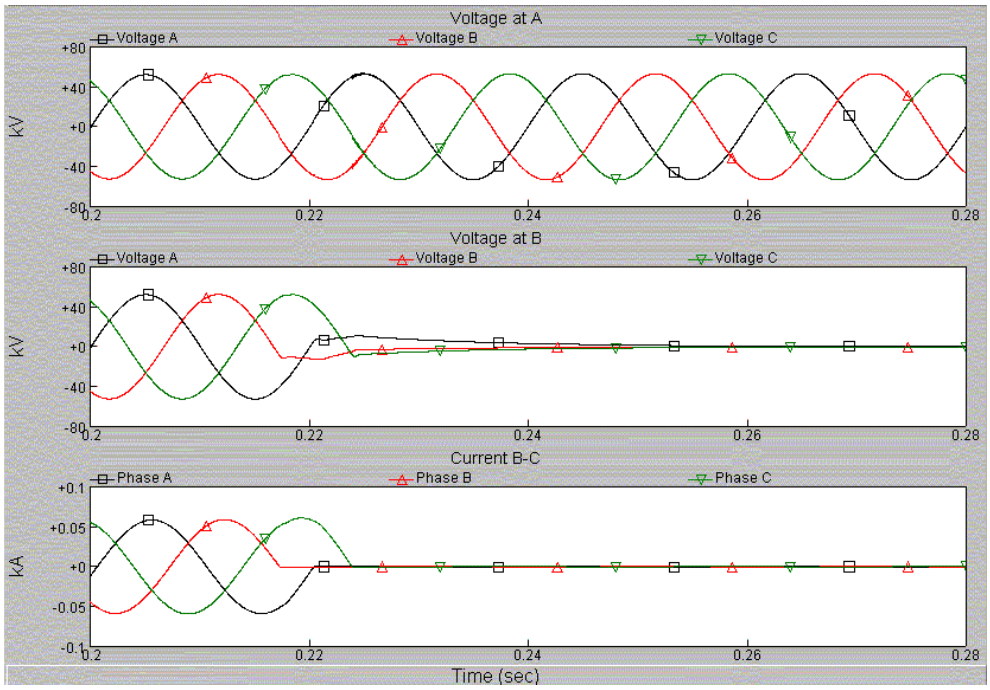

Figure A.1.4.7 Voltage and current waveforms during loaded transformer de-energizing

Transient propagation due to transformer energizing is also a concern. This normally happens during transformer energizing, which causes considerable amount of even harmonics and DC component in the voltage. These disturbances may propagate through transformers to the rest of the system, and be magnified due to resonance effect. Because of this, the load currents at other busbars can be severely distorted, which might have detrimental impact on the locally installed current relays. Fig. A.1.4.8 shows this propagation trend. The current through the load feeder at busbar B can be affected by the disturbance propagated from transformer energizing at busbar A.

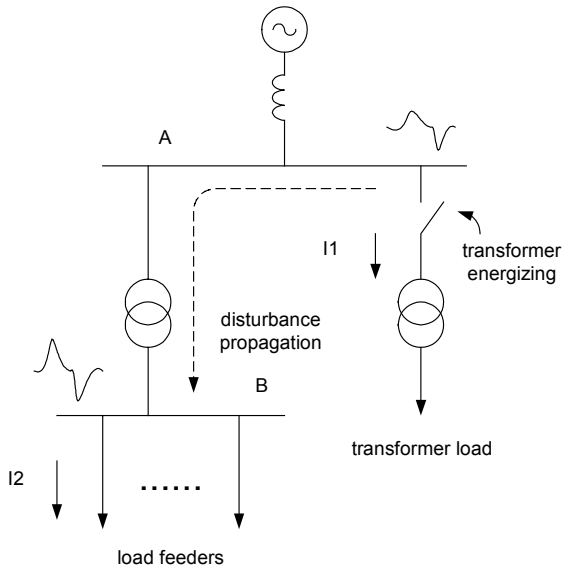

Figure A.1.4.8 Disturbance propagation due to transformer energizing

5. Motor starting

a. Starting of three-phase balanced motors

b. Starting of three-phase unbalanced motors

Motor starting happens in MV and LV systems.

An equivalent model of an induction motor is shown in Fig. A.1.5.1.

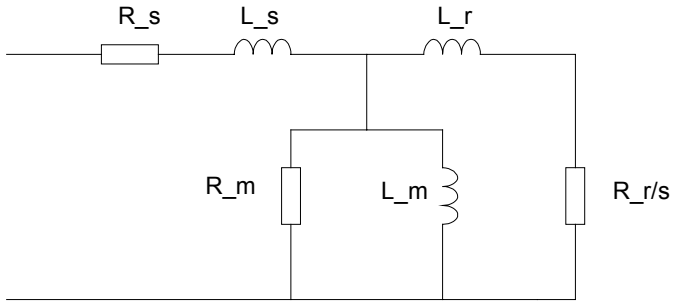

R_s	stator resistance	L_s	stator inductance
R_m	magnetic resistance	L_m	magnetizing inductance
R_r	rotor resistance refered to stator	s	rotor slip
L_r	rotor inductance refered to stator		

Figure A.1.5.1 Equivalent model of induction motor

At the beginning of motor starting, the rotor speed is zero, which means the rotor slip is unity. With the motor develops speed, the slip s becomes smaller and smaller, which increases the resistance of the rotor branch (R_r/s). When the motor reaches its rated speed, the motor current becomes stable. For three phase induction motors, the slip s at full load is of the order of 2% to 5%. Because of this, the starting current at the beginning is much higher than that in normal operation. Typically, the motor will draw 6 to 10 times its full load current during starting.

Motor starting not only causes high starting current, but also leads to a voltage dip. Fig.A.1.5.2 shows an example of such disturbance.

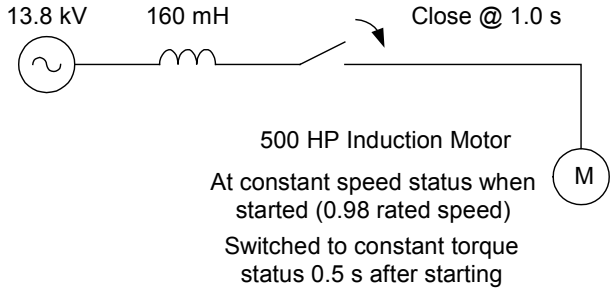

Figure A.1.5.2 Motor starting diagram

The terminal voltage variation and starting current are shown in Fig. A.1.5.3.

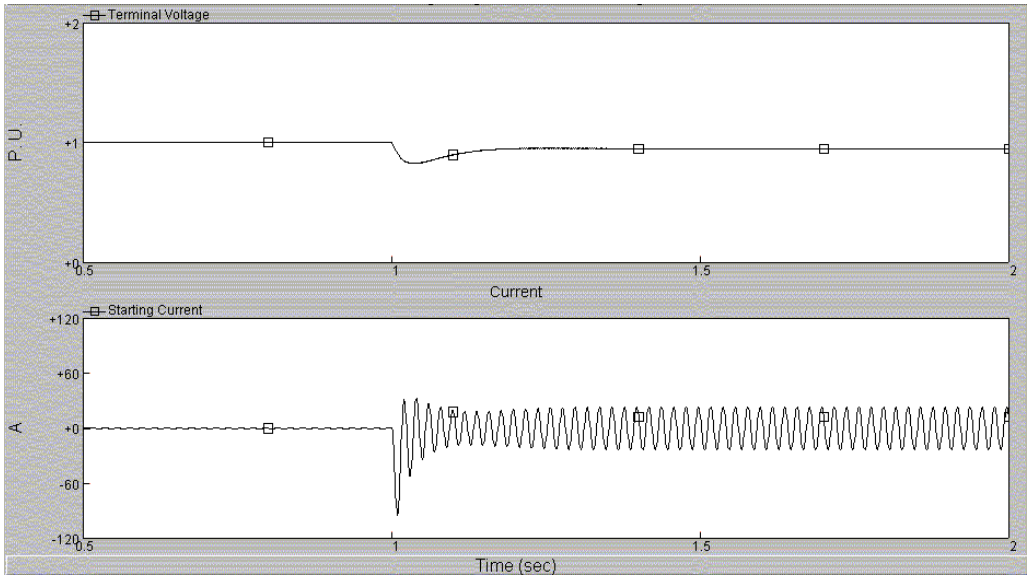

Figure A.1.5.3 Voltage dip due to motor starting

The depth of the voltage dip is dependent on the ratio of motor load and system capacity. The higher the ratio, the greater the depth.

Generally starting time of motor is less than 5 or 6 seconds. But it can be as high as 20 to 30 seconds for motors having loads with high inertia.

Due to rapid variation in load current, repeated motor starting can also result in voltage fluctuations in the system. Like all load switching, motor starting also leads to a change in steady-state voltages and currents.

The starting of a single-phase motor will lead to a current rise and a voltage dip in one or two phases. Large single-phase motors are rarely used in three-phase systems.

6. Capacitor switching

a. Capacitor energizing

b. Capacitor de-energizing

c. Back-to-back capacitor energizing

d. Back-to-back capacitor de-energizing

Capacitor switching used to be restricted to mainly MV and LV distribution systems. Now capacitor switching at HV transmission systems becomes more and more common.

Because capacitor voltage cannot change instantaneously, energization of a capacitor bank results in an immediate drop in system voltage toward zero, followed by a fast voltage recovery (overshoot) and finally an oscillating transient voltage superimposed on the fundamental waveform. The waveforms for voltage and current are shown as in Fig. A.1.6.1.

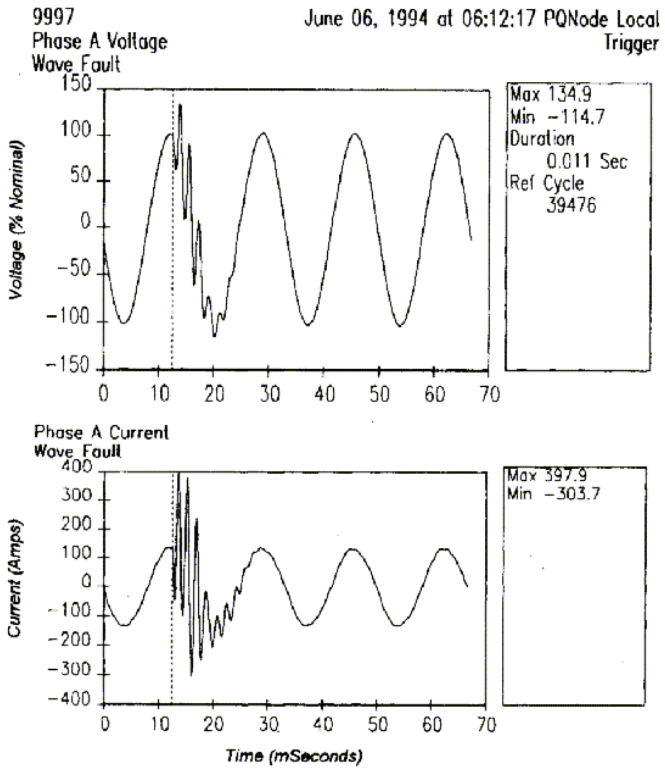

Typical distribution capacitor closing transient voltage and current waveforms.

Figure A.1.6.1 Waveforms for voltage and current during capacitor switching[23]

From Fig. A.1.6.1 it is clear that such an event comes from an upstream capacitor switching, as the fundamental voltage and current remain in phase. A downstream capacitor switching would lead to a leading current after the event.

— Isolated capacitor energizing/de-energizing

The principle of isolated capacitor energization is shown in Fig. A.1.6.2 Isolated capacitor energization means that no other capacitor is connected nearby before the capacitor bank is switched.

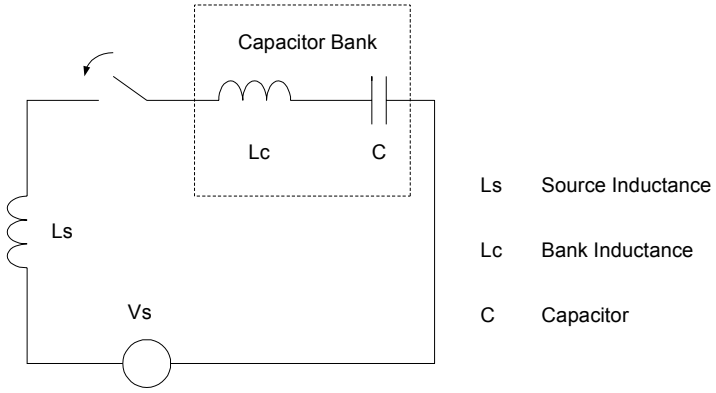

Figure A.1.6.2 Isolated capacitor energization

The maximum peak value of the in-rush current due to isolated capacitor energization can be calculated using the following equation:

$$I_{peak} = \sqrt{2}V_s\sqrt{\frac{C}{L_s + L_c}}$$

where V_s is the RMS value of the pre-switching voltage

The current mentioned above is the maximum peak value that the in-rush current can reach. Depending on the point on the waveform when switching, the actual value might be lower. The inductance attached to the capacitor bank is for the purpose of reducing the magnitude of the in-rush current. In practical situations, the value of C is limited by the value of change in steady state voltage, so the magnitude of in-rush current in isolated capacitor switching is always less than the system short circuit current at the capacitor busbar.

The oscillation frequency of isolated capacitor energization is:

$$f = \frac{1}{2\pi\sqrt{(L_s + L_c)C}}$$

When the capacitor is switched off, the energy stored in the source inductor will be released through arc discharge of the switch, which causes distortion on voltage waveform.

—— Back-to-back capacitor energizing/de-energizing

Back-to-back capacitor energizing/de-energizing refers to the case of multiple capacitor banks connected to the system. A capacitor bank is switched on to the system with other banks already connected, or a capacitor bank is switched off from the system with other banks still connected. Fig. A.1.6.3 shows such a case.

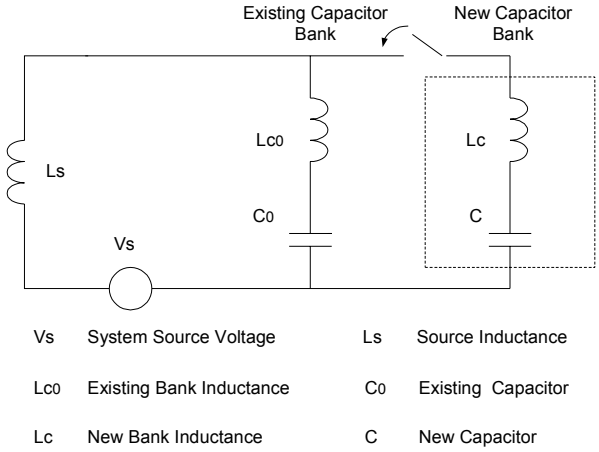

Figure A.1.6.3 Back-to-back capacitor switching

During back-to-back capacitor switching, the in-rush current will mainly flow through the branch of the existing capacitor bank, ignoring the branch for system source. Its equivalent circuit is shown in Fig. A.1.6.4.

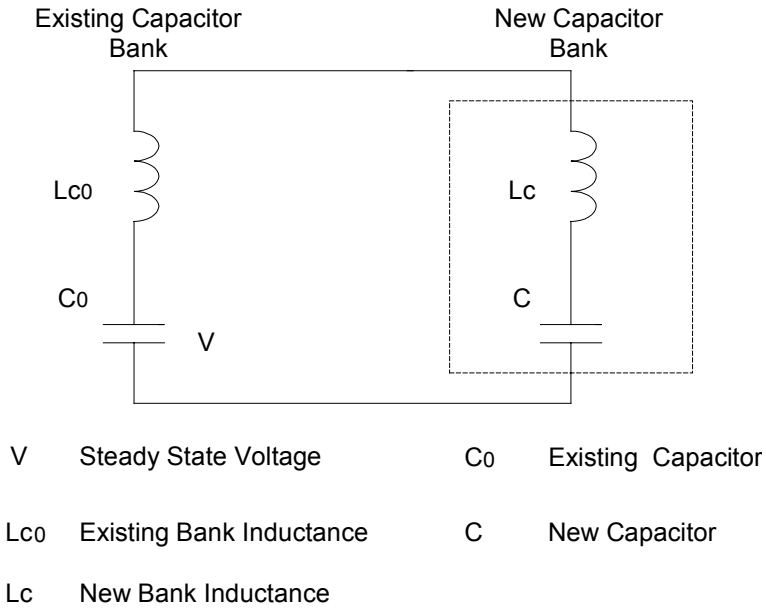

Figure A.1.6.4 Equivalent circuit of back-to-back capacitor switching [24]

The current peak and its oscillation frequency can be calculated using the following formula:

$$I_{peak} = \sqrt{2}V\sqrt{\frac{\frac{C * C_0}{C + C_0}}{L_{c0} + L_c}}$$

and

$$f = \frac{1}{2\pi\sqrt{(L_{C0} + L_C)\frac{C * C_0}{C + C_0}}}$$

Because of the presence of other capacitor banks, the equivalent source inductance is therefore lower than in case of isolated capacitor switching. While the equivalent capacitance is also reduced when introducing the new capacitance, the equivalent inductance drops much more compared with the case for isolated capacitor switching. This is because the capacitor bank inductance is normally much lower when compared with than the system source inductance. So the in-rush current will be greater in amplitude and higher in oscillation frequency. The in-rush current will almost always be greater than the system short circuit current at the multi-bank busbar.

Back-to-back capacitor de-energizing follows the rule as in isolated capacitor de-energizing. Since the existence of other capacitor banks makes the equivalent load size greater, the transient amplitude and oscillation frequency will be greater.

— Impact of capacitor energizing/de-energizing on system

- The transient overvoltage generated during capacitor energizing/de-energizing is a threat to some sensitive electronic equipment such as adjustable-speed drives.
- While the capacitor energizing transient is rarely a concern at the switched capacitor location, significant transient overvoltages can occur at remote capacitors or cables when magnification of the capacitor energizing transient occurs.

Transient frequencies due to utility distribution capacitor switching usually fall in the range of 300-1000 Hz. Transient overvoltages which result are usually not of concern to the utility, since peak magnitudes are below the level in which utility surge protection, such as arrestors, begins to operate. Because of the relatively low frequency, these transients will pass through stepdown transformers to customer loads. Secondary overvoltages can cause voltage magnification or nuisance tripping of adjustable-speed drives [23]. This happens when the following conditions are met:

a. The capacitor switched on the higher voltage system is much larger than the capacitor at the low voltage busbar.
b. The frequency of oscillation which occurs when the high voltage capacitor is energized is close to the resonant frequency formed by the step-down transformer in series with the low voltage capacitor
c. There is little damping from the loads on the low voltage system, e.g. motors in industrial plants

- System harmonic resonance frequency will change after capacitor energizing. There are many inductive and capacitive components in power systems. In a certain power system, there is a resonance frequency, which depends on its construction. When a capacitor bank is switched onto the system, there might be a coupling between the new component and the previous system, which will result in system resonance. System resonance will cause magnification of harmonic current in the system.

The new resonance frequency is dependent on capacitor size and system short circuit capacity. The harmonic order for such a parallel resonance can be estimated by the following equation:

$$H = \sqrt{\frac{MVA_{sc}}{MVA_c}}$$

where MVAsc is the system short circuit capacity at the capacitor switching location

MVAc is the capacitor bank capacity

Further, even synchronized switching, which causes small voltage disturbances, is associated with rather large current disturbances. Fig. A.1.6.5 shows such a case.

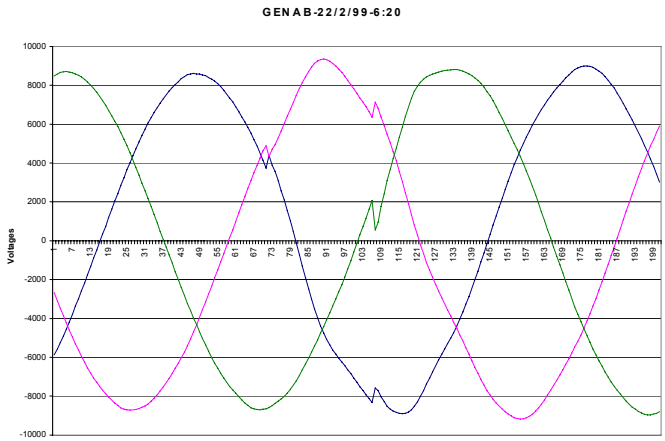

(a)

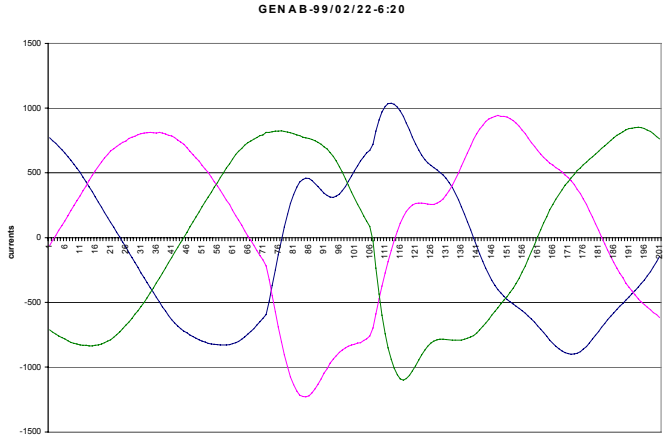

(b)

Figure A.1.6.5 Measured Voltage and current waveforms during synchronized capacitor switching (a) voltage waveforms (b) current waveforms

A.2 Events due to Automatic Devices

1. Transformer tap-changer operation

Transformer tap-changer is a device used to keep voltage within a certain range. Normally it is applied in 2 ways, at HV system and MV/LV system respectively.

At HV systems, it functions to control the distribution of reactive power flow within the transmission system. At MV/LV systems it functions to keep the voltage on the secondary side within tolerances in face of voltage variations on the primary side. A tap changer is essentially a transformer with a variable turn ratio of 1:n. When the loading on a bus changes, the tap changer discretely changes its value n. The following diagram is an example of tap changing versus voltage variation.

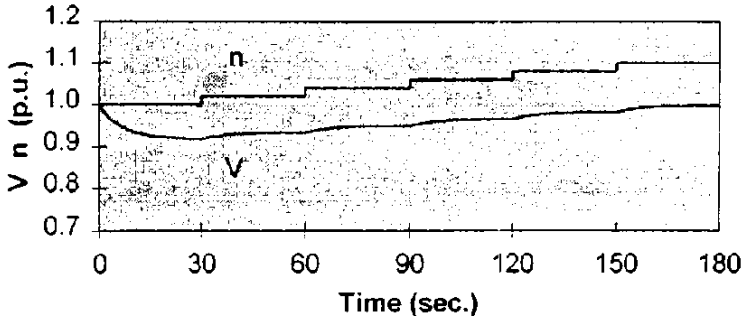

Figure A.2.1.1 An example of tap-changer operation[25]

In practice, tap changer starts to operate some time (30 seconds in Fig. A. 2.1.1) after the voltage drops. The tap changer makes a discrete step (typically about 1%) and then stays at that level for another time interval before the next change is allowed. This process goes on until the voltage recovers to its normal level.

Normally, a transformer has a tapping range of 20%, which is typically divided either in 16 steps (1.23% each) or in 14 steps (1.43% each). With the tap changes its position, the transformer impedance varies also. During operation, one step is applied for each intervention.

As the voltage adjustment for each step is very small, the tap-changer operation can hardly lead to any obvious transient on voltage waveform. Besides, the long interval time for intervention, which is counted in the

scale of second, also provides enough time to smooth any possible transients or harmonics.

A.3 Events due to External Effects

1. Lightning

Lightning is a potent source of impulsive transients. Such a phenomenon mainly appears in HV transmission system as well as in MV/LV overhead distribution systems.

A direct lightning strike to phase generally causes line flashover near the strike point. Not only does this generate an impulsive transient with very high overvoltage, but it also causes a fault with the accompanying voltage dips and interruptions. Depending on the effectiveness of the grounds along the surge current path, some of the lightning striking current may find its way into load apparatus [26].

— Phenomena

The waveforms of lightning surge voltage and current are shown in Figs. A.3.1.1 and A.3.1.2.

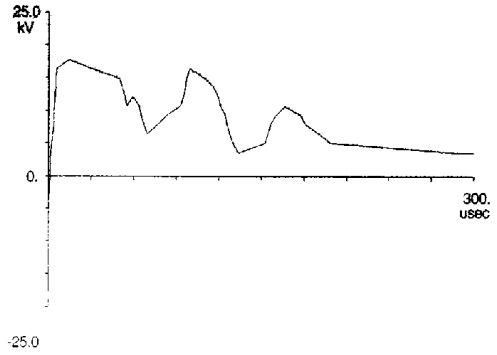

Figure A.3.1.1 Lightning-caused voltage surge at a 10kV metal-oxide distribution arrester[27]

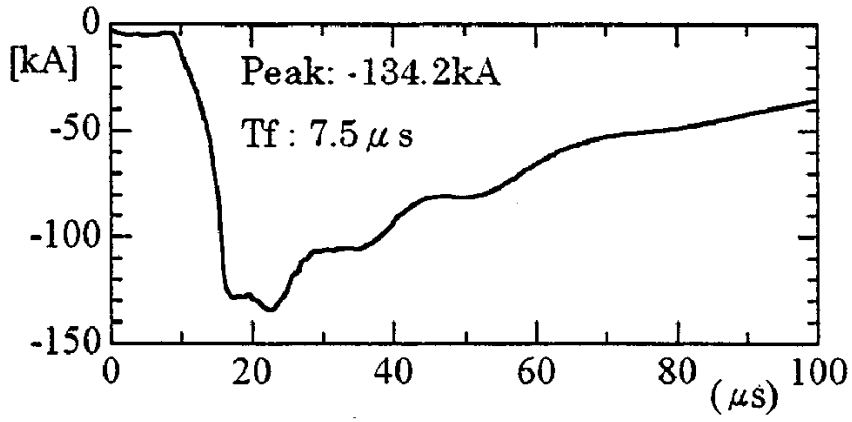

Figure A.3.1.2 Lightning-caused current surge at a 500 kV transmission tower [28]

It can be observed that both voltage and current waveforms have steep front at the very beginning and then attenuate exponentially. The variation happens in a scale of microsecond, much faster than other transients in power systems. The peak surge values are extremely great for both voltage and current. The waveform in Fig. A.3.1.1 reflects the fact that the surge voltage is clamped by varistor-based arrester. The current waveform in Fig. A.3.1.2 is negative because the stroke current flows from ground to cloud.

From Fig. A.3.1.2, it is possible to estimate the peak value of the voltage on a transmission line due to a direct stroke. If 300 Ω is used as the wave impedance, the peak voltage is

V_{peak} = 134.2 *300/2 = 20 (MV)

The reason why the impedance is divided by two in the above equation is that the current propagates both forward and backward along the line, away from the stroke point. The calculated peak voltage is about 50 times the normal peak voltage, so that a flashover/arcing fault will occur. Only

minor lightning strokes lead to transient overvoltages; the rest will lead to faults.

Lightning voltage is determined by lightning current, which propagates through device to the air above it. The peak surge value, steep rise rate and decaying time constant are dependent on the charges accumulated, air condition around the lightning channel and the height where the lightning strikes. In normal case, the greater the height, the lower the peak surge current and the steep rise rate. The current is also affected by the surge impedance of the device. The existence of such impedance can effectively reduce the peak surge current and steep rise rate.

— Propagation of lightning

The lightning voltage can pass through transformer. Fig. A.3.1.3 shows an example of such wave propagation in LV system. Note that this is a very high frequency phenomenon: the horizontal scale is only 5μs.

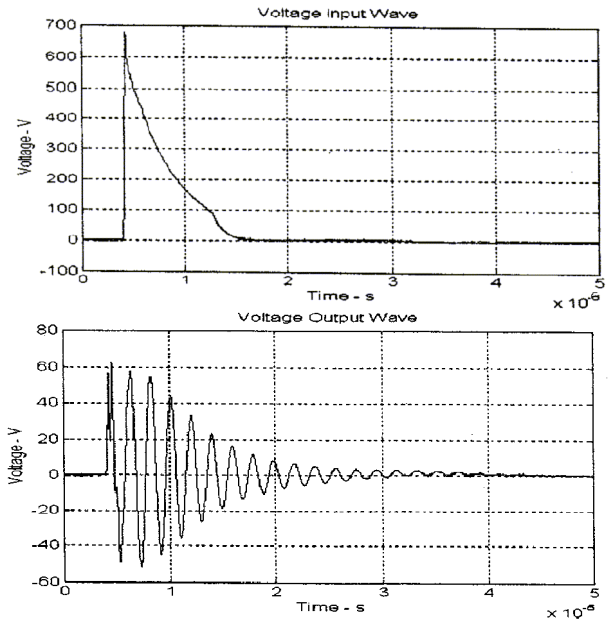

Figure A.3.1.3 Propagation of lightning wave through transformer (Dyn11 type) [29]

The propagation of lightning wave is due to the excitation of transformer stray capacitance and inductance by lightning strokes. The lightning surge has a spectral energy of up to several hundred kHz. If the surge is chopped by a surge arrester, spectral energy up to several MHz can be significant. The stray capacitance and inductance, which cause resonance under extremely high frequency, leads to voltage amplification inside the transformer windings.

Lightning can also cause voltage dips. Fig. A.3.1.5 shows a measured voltage dip due to a lightning stroke. The lightning stroke on the remote transmission overhead lines caused a short circuit fault, which led to voltage dip in our laboratory. Voltage dips due to the same fault where also measured at several voltage levels in the local distribution network.

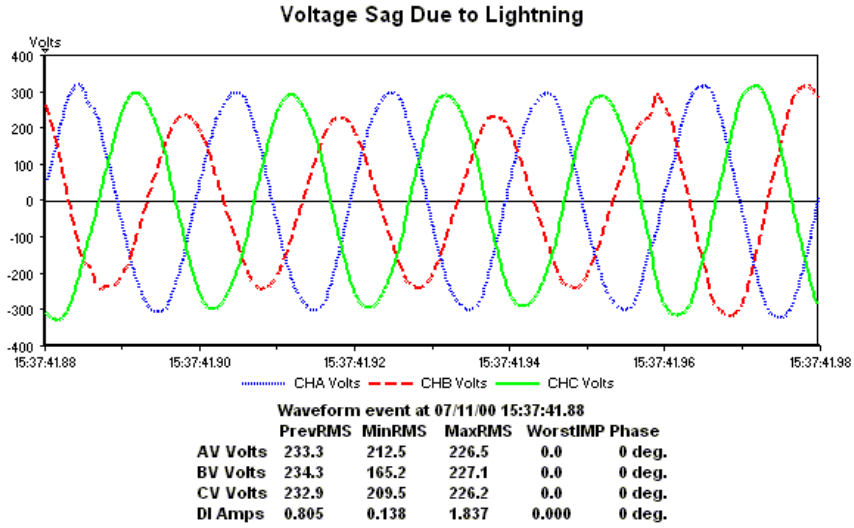

Figure A.3.1.5 Voltage dip due to lightning

A.4 Variations due to System Components

1. Nonlinear generation

Nonlinear generation exists in MV and LV systems.

The Solar power generator is a typical example of nonlinear generation. It is connected to the system via DC/AC converters. Thus it generates harmonics. Besides, the generation output is also changing. But since its output is very small compared with the total power output in the system, this variation will not cause system frequency variations. Typical examples are solar power plant [30][31] and wind power [32]. Figs. A.4.1.1 and A.4.1.2 show the waveforms of these two cases, respectively.

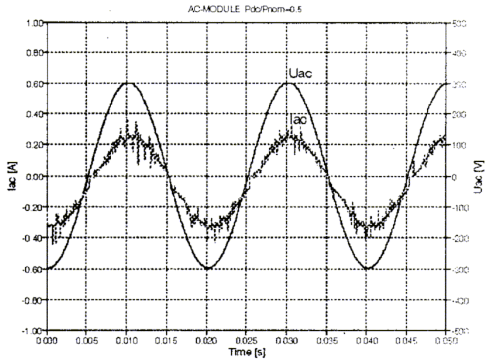

Waveform of current to the grid

Figure A.4.1.1 Voltage and current to the system from solar power plant [33]

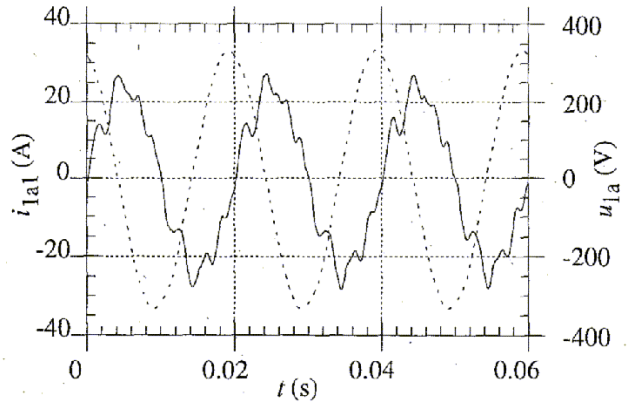

Figure A.4.1.2 Voltage and current to the system from wind power plant [34]

In Fig. A.4.1.1, the high frequency ripple is due to operation of electronic switches in the converters. The voltage and current in Fig. A.4.1.2 are measured at wind speed of 5 m/s. The solid curve is for current, while the dotted line is for voltage. The dominant harmonics are 5^{th} and 7^{th}.

2. HVDC

HVDC exists at HV system. The principle diagram is shown as follows:

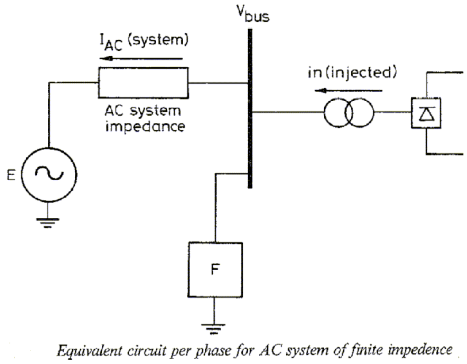

Figure A.4.2.1 HVDC system [35]

Due to the existence of power converters, the injection of harmonics to the system is inevitable. Depending on the type of converter controller, the generated harmonic spectrum varies. If the HVDC is connected to a relatively weak AC system, the voltage and power stability will be tampered. A small disturbance can lead to system voltage unstable.

In practice, 12-pulse or 24-pulse converters are adopted in HVDC systems. The orders of harmonics due to converters are 11^{th}, 13^{th}, 23^{rd}, 25^{th}, …in converter currents. As the converters are not 100% ideal, there will also be some 5^{th}, 7^{th}, 17^{th}, 19^{th}, ….harmonics in the currents. But their magnitudes are much lower compared with those of dominant harmonics.

Measurements of the effect of HVDC links on the harmonic distortion at a Swedish 400 kV substation are presented in [36].

3. Transformer

As bridges between different voltage systems, transformers have effect on all the voltage levels.

Due to the non-linearity of the magnetizing characteristic for transformers the current waveform is distorted and hence contains harmonics. The currents flow through the system impedance and set up harmonic voltages. 3^{rd} and 5^{th} harmonics are dominant in the current in normal operation. However, as the magnetizing branch current of transformer is rather small in normal operation, the harmonics generated by the transformer itself can be negligible.

4. Nonlinear load

Nonlinear load is responsible for steady state voltage/current waveform distortion. Such kind of load mainly exists at MV and LV system.

Waveform distortion can be classified into 4 types: harmonics, interharmonics, DC and noise. In harmonic distortion, consecutive cycles are identical. In interharmonic distortion, consecutive cycles are not identical, but vary with some regularity. In noise distortion, the signal varies in a random way.

The most typical waveform distortion in practice is harmonic distortion, which is mainly due to the application of some power electronic converters that have nonlinear characteristics.

Fig. A.4.4.1(a) shows an example of harmonic distortion due to computer load. Its harmonic spectrum is shown in Fig. A.4.4.1(b).

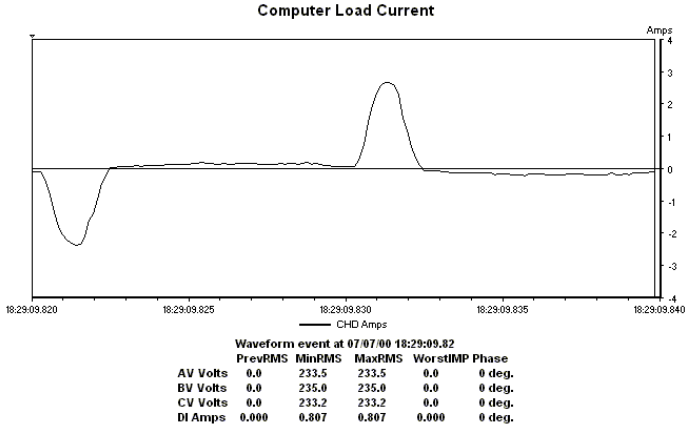

(a)

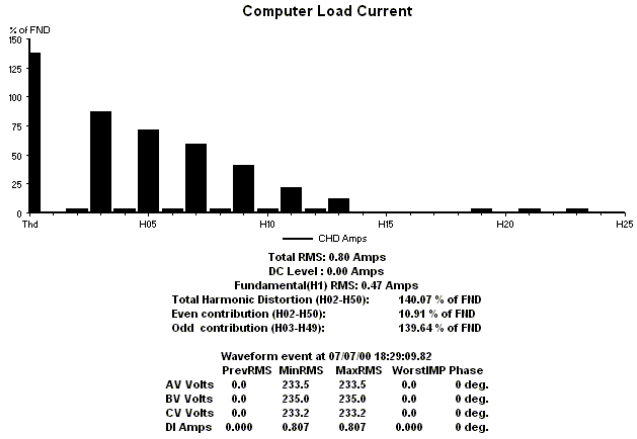

(b)

Figure A.4.4.1 Harmonics due to nonlinear load

An example of interharmonic distortion is shown in Fig. A.4.4.2. The envelope line of current waveform shows a regular fluctuation. Besides the harmonics in the current, a series of interharmonics also exist. The

interharmonics, which are close to 18Hz, 182Hz, 282Hz, 382Hz,… are actually of the orders of 1/3, 11/3, 17/3, 23/3… respectively. There are two sources for interharmonics: 1. Some equipment made of ferromagnetic material under a certain power supply condition; 2. Some signaling sources whose operating frequencies are of interharmonic values.

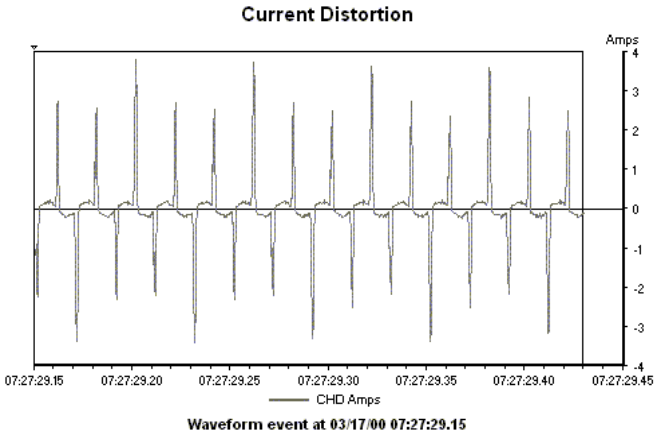

(a)

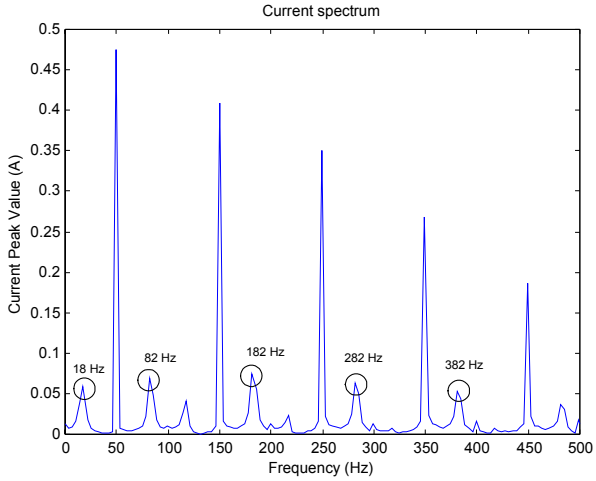

(b)

Figure A.4.4.2 Interharmonics in current and its spectrum

DC components are mainly related to faults or generator operations. They normally extinguish in a short time. Noise exists everywhere. Any equipment can be a source of noise.

5. Intermittent load

Intermittent load exists in any voltage level system.

Some continuous non-symmetrical inrush loads have rapidly varying load current when operating. Such random systematic variation causes voltage flicker as well as harmonic distortion. Since in many cases the load is asymmetrical, voltage unbalance may also happen.

Fig. A.4.5.1 shows the voltage waveforms near an arc furnace load. The diagram shows that the voltage contains both flicker and unbalance characteristics.

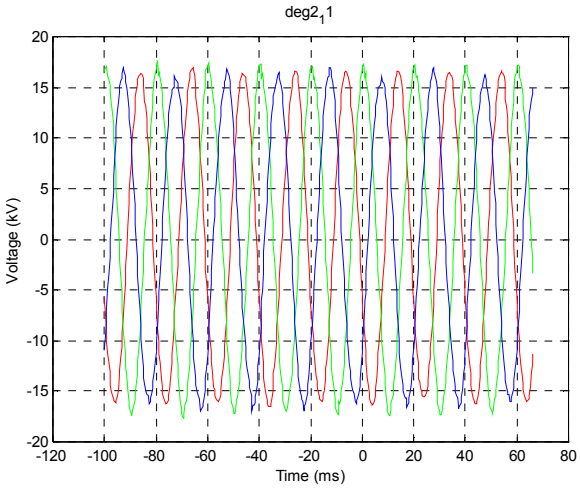

Figure A.4.5.1 Voltage flicker due to intermittent load (arc furnace, STRI)

6. Unbalanced load

Unbalanced load refers to the loads that do not require the same amount of power in all the 3 phases. This happens in any voltage level system.

At LV level almost all load is single-phase (and thus unbalanced). But the load is normally spread equally over the three phases. Of more concern are large single-phase loads connected to MV or HV systems. Typical examples are arc furnaces and traction load.

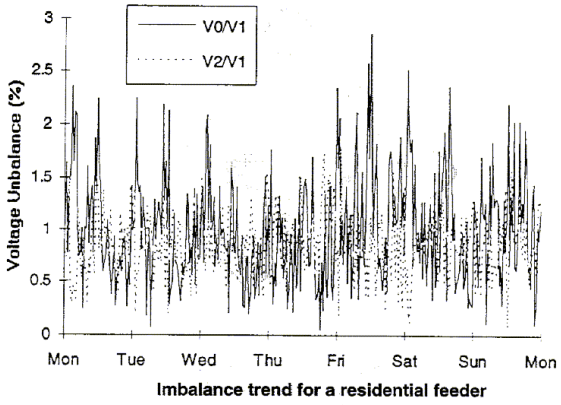

Figure A.4.6.1 Voltage unbalance due to unbalanced load [37]

Such unbalanced loads will cause voltage unbalance.

A.5 Variations due to External Effects

1. Geomagnetical induction

Geomagnetically-induced currents are due to geomagnetic storm. Since it penetrates power system through earthing cable, it mainly appears in HV and LV systems, as well as the earthed MV systems. During a geomagnetic storm, there exists the Earth-Surface-Potential (ESP). ESP is directly proportional to the distance between the neutral grounding points. The ESP causes geomagnetically-induced-current to flow in power systems by creating a voltage potential. The geomagnetically-induced-current enters the system through the grounded-wye power transformer,

and if large enough, results in saturation, thereby producing distorted voltages and currents [38].

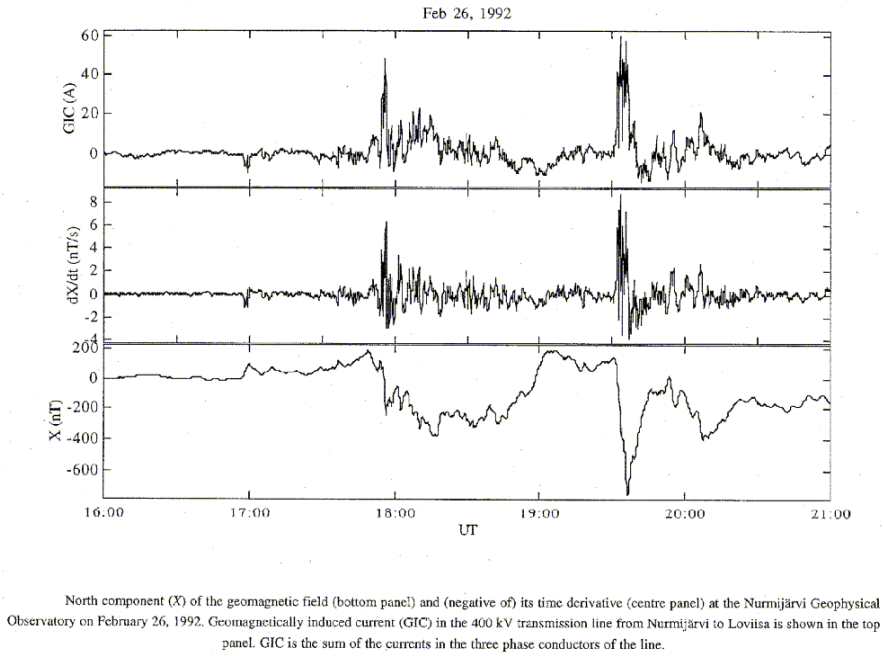

North component (X) of the geomagnetic field (bottom panel) and (negative of) its time derivative (centre panel) at the Nurmijärvi Geophysical Observatory on February 26, 1992. Geomagnetically induced current (GIC) in the 400 kV transmission line from Nurmijärvi to Loviisa is shown in the top panel. GIC is the sum of the currents in the three phase conductors of the line.

Figure A.5.1.1 Geomagnetic induction current [39]

2. Radio-interference

Radio-interference happens in HV systems.

The main effect of radio-interference on power system is harmonic pollution, which is generated due the electromagnetic field generated by high frequency radio signal. This field will have effect on the harmonic power flow in the system.

A summary table, Table A.1, is set up to highlight the sources and the disturbances they generate. In the table, LV stands for low voltage system, i.e. 400 V system; HV stands for high voltage system, i.e. 130 kV and above system; MV stands for medium voltage system, i.e. any system with a voltage class above 400 V and below 130 kV.

When there are more than one disturbance originated from a certain event or variation, the dominant disturbance is highlighted with an asterisk '*' beside 'X'. There might be more than one dominant disturbance for each event or variation.

Table A.1 Disturbance types in various voltage level systems

HV	MV	LV		Sources	Transients	Dip / Swell	Undervolt./ Overvolt.	Waveform Distortion	Flicker/ Fluctuation	Voltage Unbalance
	✔		A_E	Generation Unit Switching, Large	X*			X*		
	✔	✔		Generation Unit Switching, Small	X*	X*	X			
✔				Unloaded Line/Cable Energizing	X*					
	✔	✔		Loaded Line /Cable Energizing	X*					
✔	✔	✔		Transf. Energizing/De-energizing	X*			X*		
	✔	✔		Motor Starting, Balanced	X*	X*			X	
	✔	✔		Motor Starting, Unbalanced	X*	X*			X	X*
✔	✔	✔		Capacitor Energizing	X*		X	X		
✔	✔	✔	B_E	Transf. Tap-changer			X*			
✔	✔	✔	C_E	Lightning	X*	X	X			
	✔	✔	A_V	Nonlinear Generation				X*		
	✔	✔		HVDC				X*		
✔	✔	✔		Transf.				X*		
✔	✔	✔		Nonlinear Load				X*	X	
✔	✔	✔		Intermittent Load				X*	X*	
✔	✔	✔		Unbalanced Load				X*		X*
✔	✔	✔	C_V	GIC	X*			X*		
✔				Radio-interference				X*		

A_E — System events due to switching of system components

B_E — System events due to automatic switching device

C_E — System events due to external influences

A_V — System variations due to system components

C_V — System variations due to external influences

References

[1] IEC 50 (161), 1990, 161-01-05

[2] **Lee**, **T. M.**; **Chan**, **T. W.**, "An investigation on the effects of harmonic contents and phase shift on the performance of RCCB and over-current relays", *Proceedings of the International Power Engineering Conference (IPEC' 97)*, Vol. 2, 1997, Page(s): 775-779.

[3] **Stringer**, **N. T.**, "The effect of DC offset on current-operated relays", *IEEE Transactions on Industry Applications*, Vol. 34 1, Jan.-Feb. 1998, Page(s): 30 -34

[4] **Sanaye-Pasand**, **M.**; **Malik**, **O. P.,** "High speed transmission line directional protection evaluation using field data*", IEEE Transactions on Power Delivery*, Vol. 14 3, Jul. 1999, Page(s): 851 –856.

[5] **Akke**, **M.**; **Thorp**, **J. T.,** "Some improvements in the three-phase differential equation algorithm for fast transmission line protection", *IEEE Transactions on Power Delivery*, Vol. 13 1, Jan. 1998, page(s): 66 – 72.

[6] **Radojevic**, **Z. M.**; **Terzija**, **V. V.**; **Djuric**, **M. B.**, "Multipurpose overhead lines protection algorithm", *IEE Proceedings-Generation, Transmission and Distribution,* Vol. 146 5, Sept. 1999, page(s): 441 – 445.

[7] **Bollen**, **M. H. J.**, "Understanding Power Quality: voltage sags and interruptions", IEEE Press, 2000

[8] **Orr**, **J. A.**; **Emanuel**, **A. E.**, "On the need for strict second harmonic limits", *IEEE Transactions on Power Delivery*, Vol. 15 3, Jul. 2000, page(s): 967-971.

[9] **Bronzeado**, **H. S.**; **Brogan**, **P. B.**; **Yacamini**, **R.**, "Harmonic analysis of transient currents during sympathetic interaction", *IEEE Transactions on Power Systems*, Vol. 11 4, Nov. 1996, page(s): 2051-2056

[10] **Horowitz**, **S. H.**; **Phadke**, **A. G.**, *Power System Relaying*, England: RSP Ltd, 1995

[11] **Phadke**, **A. G.**; **Thorp**, **J. S.**, *Computer relaying for power systems*, England: RSP Ltd, 1998

[12] **Chui**, **C. K.**; **Chen**, **G.**, *Kalman Filtering*, Springer, 1999

[13] **Vitins**, **M.**, "A correlation method for transmission line protection", *IEEE Transactions on Power Apparatus and Systems*, Vol, PAS-97, 1998, page(s): 1607-1617

[14] **Crossley**, **P. A.**; **McLaren**, **P. G.**, "Distance protection based on travelling waves", *IEEE Transactions on Power Apparatus and Systems*, Vol. PAS-102, 1983, page(s): 2971-2983

[15] **Kohlas**, **J.**, "Estimation of fault locations on power lines", *Proceeding of the 3rd IFAC Symposium*, 1973, page(s): 393-402

[16] **Christopoulos**, **C.**; **Thomas**, **D. W. P.**; **Wright**, **A.**, "Scheme based on travelling-waves for the protection of major transmission lines", *IEE Proceedings-Pt. C.*, Vol. 135, 1988, page(s): 63-73

[17] **Bollen**, **M. H. J.**, "On travelling-wave-based protection of high-voltage networks", Ph. D. Thesis, Eindhoven University of Technology, 1989

[18] **Van Dongen**, **A. W. A.**, "Een distantiebeveiligingsalgorithme voor hoogspanningslijnen", Master Thesis, Eindhoven University of Technology, 1988

[19] **Mattavelli**, **P.**; **Felin**, **L.**; **Bordignon**, **P.**; **Perna**, **M.**, "Analysis of interharmonics in DC arc furnace installations", *Proceedings of 8th*

International Conference on Harmonics and Quality of Power, Vol. 2, 1998, page(s): 1092 –1099

[20] **Wang**, **F.**; **Bollen**, **M. H. J.**, "Measurement of 182 Hz interharmonics and their impact on relay operation", *Proceedings of 9th International Conference on Harmonics and Quality of Power*, Vol. 1, 2000, page(s): 55-60

[21] **Witte**, **J. F.**; **DeCesaro**, **F. P.**; **Mendis**, **S. R.**, "Damaging long-term overvoltages on industrial capacitor banks due to transformer energization inrush currents", *IEEE Transactions on Industry Applications*, Vol. 30 4 , July-Aug. 1994, page(s): 1107 –1115

[22] **Shankland**, **L. A.; Feltes**, **J. W.; Burke**, **J. J.,** "The effect of switching surges on 34.5kV system design and equipment", *IEEE Transactions On Power Delivery*, Vol.5 2 April 1990, page(s): 1106-1112

[23] **Grebe**, **T. E.**, "Application of distribution system capacitor banks and their impact on power quality", *IEEE Transactions on Industry applications*, Vol. 32 3, May-June 1996, page(s): 714 -719

[24] **McCoy**, **C. E.**; **Floryancic**, **B. L.**, "Characteristics and Measurements of Capacitor Switching at Medium Voltage Distribution Level", *IEEE Transactions on Industry Applications*, Vol. 30 6, Nov. 1994, page(s): 1480

[25] **Dahlgren**, **R. W.**, "Dynamic mechanisms of power system instability", *Northcon/94 Conference Record*, 1994, page(s): 72 –77

[26] **Dugan**, **R. C.; McGranaghan**, **M. F.; Beaty**, **H. W.;** "Electrical Power Systems Quality", McGraw-Hill 1996

[27] **Barker**, **P. P.**; **Mancao**, **R. T.**, "Lightning research advances with digital surge recordings", *IEEE Computer Applications in Power*, Vol. 5 2 , April 1992, page(s): 11 –16

[28] **Narita**, **T.**; **Yamada**, **T.**; **Mochizuki**, **A.**; **Zaima**, **E.**; **Ishii**, **M.**, "Observation of current waveshapes of lightning strokes on transmission towers", *IEEE Transactions on Power Delivery*, Vol. 15 1, Jan. 2000, page(s): 429 -435

[29] **Kelly**, **R. A.**; **Van Coller**, **J. M.**; **Britten**, **A. C.**, "Response of Eskom's MV/LV distribution networks to lightning transients", *IEEE 4th AFRICON*, Vol. 2, 1996, page(s): 693 -698

[30] **Kempe**, **A.**; **Schonwandt**, **U.**, "EMC of PV-plants with line-commutated inverters", *Conference Record of the Twenty Fifth IEEE Photovoltaic Specialists Conference*, 1996, page(s): 1343 –1346

[31] **Carbone**, **R.**; **Marino**, **P.**; **Testa**, **A.**; **Vasca**, **F.**, "Power factor and harmonic distortion optimization in photovoltaic generating power station", *8th Meditarranean Electrotechnical Conference (MELECON '96)*, 1996, Vol. 2, page(s): 899 -903

[32] **Salman**, **S. K.**; **Jiang**, **F.**; **Rogers**, **W. J. S.**, "Effects of wind power generators on the voltage control of utility distribution networks", *International Conference on Renewable Energy - Clean Power 2001*, 1993, page(s): 196 –201

[33] **de Haan**, **S.W.H.**; **Oldenkamp**, **H.**; **Wildenbeest**, **E. J.**, "Test results of a 130 W AC module; a modular solar AC power station", *Conference Record of the Twenty Fourth. IEEE Photovoltaic Specialists Conference*, 1994, page(s): 925 - 928 vol.1

[34] **Thiringer**, **T.**, "Power quality measurements performed on a low-voltage grid equipped with two wind turbines", *IEEE Transactions on Energy Conversion*, Vol. 11 3, Sept. 1996, page(s): 601 –606

[35] **Yacamini**, **R.**; **Resende**, **J. W.**, "Harmonic generation by HVDC schemes involving converters and static Var compensators", *IEE Proceedings-Generation, Transmission and Distribution*, Vol. 143 1, Jan. 1996, page(s): 66-74

[36] **Lundquist**, **J.**, "On harmonic distortion in power systems", Licentiate Thesis, Chalmers University of Technology, 2001

[37] IEEE recommended practice for monitoring electric power quality

[38] **Kolawole**, **J.**; **Mulukulta**, **S.**; **Glover**, **D.**, "Effect of geomagnetic-induced-current on power grids and communication systems", *Proceedings of the Twenty-Second Annual North American Power Symposium*, 1990, page(s): 251 –262

[39] **Viljanen**, **A.**, "Relation of geomagnetically induced currents and local geomagnetic variations", *IEEE Transactions on Power Delivery*, Vol. 13 4 , Oct. 1998, page(s): 1285 –1290

[40] **Carvalho**, **A.**; **Lacorte**, **M.; Knudsen**, **O.;** "Improved EHV line switching surge control by application of MO-arresters and controlled switching", *Proceedings of International Conference on Energy Management and Power Delivery(EMPD' 95)*, 1995. Vol. 1, page(s): 292 -297 vol.1

[41] **Natarajan**, **R.**; **Misra**, **V. K.**; **Oommen**, **M.**, "Time domain analysis of induction motor starting transients" *Proceedings of the Twenty-First Annual North-American Power Symposium*, 1989, page(s): 120 –128

[42] **Sochulfakova**, **D.**; **Niebur**, **D.**; **Nwankpa**, **C.O.**; **Fischl**, **R.**; **Richardson**, **D.**, "Capacitor switching transients prediction in noisy environments", *Proceedings of American Control Conference*, 1998. Vol. 6, page(s): 3396 -3397

[43] **Wareing**, **J. B.**; **Perrot**, **F.**, "Ferroresonance overvoltages in distribution networks", *IEE Colloquium on Warning! Ferroresonance Can Damage Your Plant (Digest No:1997/349)*, page(s): 5/1 -5/7

[44] **Websper**, **S. P.**; **Johns**, **A. T.**; **Aggarwal**, **R. K.**; **Dunn**, **R. W.**, "An investigation into breaker reclosure strategy for adaptive single pole autoreclosing", *IEE Proceedings-Generation, Transmission and Distribution*, Vol. 142 6, page(s): 601 –607

[45] **Kolcio**, **N.**; **Halladay**, **J. A.**; **Allen**, **G. D.**; **Fromholtz**, **E. N.**, "Transient overvoltages and overcurrents on 12.47 kV distribution lines: field test results", *IEEE Transactions on Power Delivery*, Vol. 7 3, July 1992, page(s): 1359-1370

[46] **Walling**, **R. A.**; **Khan**, **A. N.**, "Characteristics of transformer exciting-current during geomagnetic disturbances*", IEEE Transactions on Power Delivery*, Oct. 1991, Vol. 6 4, page(s): 1707 – 1714

[47] **Tong**, **Y. K.**, "NGC experience on ferroresonance in power transformers and voltage transformers on HV transmission systems", *IEE Colloquium on Warning! Ferroresonance Can Damage Your Plant (Digest No: 1997/349)*, page(s): 4/1 - 4/3

[48] **Venkartasubramanian**, **V.**; **Schättler**, **H.**; **Zaborszky**, **J.**, "Analysis of the tap changer related voltage collapse phenomena for the large electric power system", *Proceedings of the 31st Conference on Decision and Control*, Dec. 1992, pages(s): 2920-2927